The Protective Effects of the Antioxidant Combination of Ferulic Acid with Vitamins C and E against UV-Induced Photodamage in Human Skin Cells

Emma Lewis Bone

Thesis presented for the degree of

Master of Science in Medicine

Department of Human Biology

Faculty of Health Sciences

University of Cape Town

July 2010

Declaration

I, **Emma Lewis Bone**, hereby declare that the work on which this thesis is based is my original work (except where acknowledgements indicate otherwise) and that neither the whole work nor any part of it has been, is being, or is to be submitted for another degree in this or any other university.

I empower the University of Cape Town to reproduce for the purpose of research either the whole or any portion of the contents in any manner whatsoever.

Signed by candidate

23 July 2010

Acknowledgements

I am most grateful to my supervisor Lester for his enthusiasm, patience and insight. Thank you for always keeping a clear mind and calm demeanour when things deviated from the plan.

Appreciation to:

Ms. Ingrid Baumgarten for supplying the primary human fibroblast cultures.

Mr. Ronnie Dreyer for all his help with the FACS.

Dr. Dee Blackhurst for her guidance with the TBARS and conjugated dienes assays, and Prof. David Marais for allowing me access to reagents and equipment in the Lipid Laboratory.

A special thank you to everyone in the Department of Human Biology, especially the following:

Prof. Susan Kidson and Dr. Robea Ballo.

Dr. Sharon Prince and the T-Box Lab, notably Sabina.

Everyone who keeps the department running smoothly: Barbara, Bruce, Charles and Ray.

The Anatomy post-grads: Kundi, Lache and Rip.

Mrs. Toni Wiggins for her kind words and good advice.

Tyrone and the Redox Lab ladies: Britta, Vicky, Rosa and Morea.

Many thanks to the following who provided funding for the duration of this study:

NRF Thuthuka (Lester Davids), NRF Grant holder bursary (Sue Kidson), KW Johnstone (UCT) and UCT (Senior Merit Award).

Lastly a word of thanks to my family and friends:

To my Mom for her constant encouragement and enthusiasm, to my Dad for his humour and my brother, James, for all the entertaining arguments.

To my friends Sarah, Megan, Tarryn, Cathryn, Linda, Penny, Hannes and Mark, thank you for all the good times and laughs provided during the course of this thesis.

Contents

List of Abbreviations

4-HNE	4-hydroxy-2-nonenal
6,4- PP	pyrimidine (6-4) pyrimidone photoproduct
A1	Bcl-2-related protein A1
AAPH	2,2'-Azobis-(-2amidinopropane)
AIF	apoptosis-inducing factor
Apaf-1	apoptotic protease activating factor-1
ARE	antioxidant responsive element
ATP	adenosine triphosphate
Bad	Bcl-2-associated death promoter
Bak	Bcl-2 homologous antagonist/ killer
Bax	Bcl-2-associated X protein
Bcl-2	B-cell lymphoma-2
Bcl-w	Bcl-2-like-protein 2
Bcl-xL	Bcl-extra large
BCA	bicinchoninic acid
BCC	basal cell carcinoma
BH1-4	Bcl-2 homology domains 1-4
BHT	butylated hydroxytoluene
(t) Bid	(truncated) BH3-interacting death domain agonist
Bim	Bcl-2-like protein 11
BrdU	bromodeoxyuridine
BSA	bovine serum albumin
CAD	caspase-3-activated DNase

CAT	catalase
CARD	caspase activation and recruitment domain
c-FLIP	Fas-associated death domain-like IL-1-converting enzyme-inhibitory protein
CPD	cyclobutane pyrimidine dimer
CoQ	co-enzyme Q
CuZn-SOD	copper-zinc-superoxide dismutase
DAPI	4',6-diamidino-2-phenylindole
dATP	deoxyadenosine triphosphate
ddH_2O	double distilled water
DED	death effector domain
DHR 123	dihydrorhodamine 123
DIABLO	direct inhibitor of apoptosis binding protein with low pI
DISC	death-inducing signalling complex
DMEM	Dulbecco's Modified Eagle's Medium
DNA	deoxyribonucleic acid
DPPH	1,1-diphenyl-2-picrylhydrazyl
ECM	extracellular matrix
EC-SOD	extracellular-superoxide dismutase
EDTA	ethylenediaminetetraacetic acid
EGCG	(-)-epigallocatechin-3-gallate
Endo G	endonuclease G
FA	ferulic acid
FACS	fluorescence activated cell sorting
FADD	Fas-associated death domain
FasL/R	fatty acid synthetase ligand/ receptor

FCS	fetal calf serum
FITC	fluoroscein isothiocyanate
FL	fluorescent label
FLICE	Fas-associated death domain-like IL-1-converting enzyme
GPx	glutathione peroxidase
GR	glutathione reductase
GSH	glutathione
GSSG	reduced glutathione
HEPES	4-(2-hydroxyethyl)-1-piperazineethanesulfonic acid
HO	heme oxygenase
HtrA2	high temperature requirement 2A
HPLC	high performance liquid chromatography
IAP	inhibitor of apoptosis
ICAD	inhibitor of caspase-3-activated DNase
KGF	keratinocyte growth factor
LDH	lactate dehydrogenase
LDL	low-density lipoprotein
LL	lower left
LR	lower right
Mcl-1	induced myeloid leukemia cell differentiation protein
MDA	malondialdehyde
MED	minimal erythema dose
MMP-1	matrix metalloproteinase-1
MnSOD	manganese-superoxide dismutase
MOMP	mitochondrial outer membrane permeabilization

MSRA	methionine sulfoxide reductase A
MTT	3-(4,5-Dimethylthiazol-2-yl)-2,5-diphenyltetrazolium bromide
NAD(P)H	nicotinamide adenine dinucleotide phosphate
NMSC	non-melanoma skin cancer
Noxa	Phorbol-12-myristate-13-acetate-induced protein 1 (Noxa- Latin for damage)
PBS	phosphate-buffered saline
PFA	paraformaldehyde
PI	propidium iodide
PUFA	polyunsaturated fatty acid
Puma	p53 upregulated modulator of apoptosis
PS	phosphatidylserine
RIP	receptor-interacting protein
RIPA	radio-immunoprecipitation assay
ROS	reactive oxygen species
SCC	squamous cell carcinoma
SD	standard deviation
SDS	sodium dodecyl sulphate
SDS-PAGE	sodium dodecyl sulphate polyacrylamide gel electrophoresis
Smac	second mitochondrial activator of caspases
SOD	superoxide dismutase
SSB	single-strand breaks
TBA	thiobarbituric acid
TBARS	thiobarbituric acid reactive substances
TBS-T	tris-buffered saline containing tween
TEMED	N,N,N',N'-tetramethylrthylendiamin

Tert-BOOH	*tert*-butyl hydroperoxide
TNF	tumour necrosis factor
TR	thioredoxin reductase
TRADD	TNF receptor-associated death domain
Trx	thioredoxin
UCT	University of Cape Town
UL	upper left
UR	upper right
UV	ultraviolet
UVR	ultraviolet radiation
vEC	vitamins E and C
XO	xanthine oxidase
XTT	2,3-bis-(2-methoxy-4-nitro-5-sulfophenyl)-2H-tetrazolium-5-carboxanilide

List of Figures

Chapter 1: Introduction

Chapter 2: Materials and Methods

Chapter 3: Results and Discussion

List of Tables

Chapter 1: Introduction

Chapter 2: Materials and Methods

Chapter 3: Results and Discussion

Abstract

The skin functions as a biologically active barrier separating the internal milieu from the external environment. It is the body's first line of defense against external trauma and has evolved to detect, integrate and respond to a great variety of stressors including solar radiation. It has been shown that levels of sunlight attained during normal daily activities are mutagenic, and that exposure to the ultraviolet (UV) component of sunlight, specifically the long wavelength UVA (315-400 nm), may lead to photocarcinogenesis and photoaging. UVA-induced skin damage occurs mainly indirectly through oxidative processes initiated by endogenous photosensitization. The increase in intracellular reactive oxygen species (ROS) induced by UVA may overwhelm the cells antioxidant capacity, leading to oxidative stress. As continued oxidative stress may lead to cell death via apoptosis or necrosis, it is hereby hypothesized that the pre-treatment of cells with exogenous antioxidants could be effective in reducing oxidative stress. The combination of ferulic acid, a botanically-derived antioxidant, with vitamins C and E has been shown to provide a photoprotective effect in porcine skin, illustrating that the incorporation of antioxidants into photoprotective agents may be a feasible option for combating UVA-mediated oxidative damage.

This study assessed the ability of 0.8 mM ferulic acid (FA), in combination with vitamins C and E, to reduce the effect of UVA-induced photodamage in human epidermal (HaCaTs) and dermal skin cells (primary human fibroblasts (HFbs) and murine 3T3 cells). Pre-treatment with the FA and vitamins C and E (vEC) combination solution reduced UVA-induced ROS in human fibroblasts while pre-treatment with vEC individually led to a reduction in HaCaTs. As exposure to UVA may also lead to an increase in lipid peroxidation, it was believed that antioxidant pre-exposure may lead to a reduction in ROS and subsequent reduction in lipid peroxidation. The thiobarbituric acid reactive substances (TBARS) and conjugated diene assay were used to measure lipid peroxidation. Pre-treatment with vEC led to an apparent reduction in conjugated diene levels in HaCaTs, but the data did not correlate with the ROS result in the HFbs. As prolonged oxidative stress may result in cell death, this study investigated whether the treatment was able to attenuate

UVA-induced cell death. The cell viability assay showed treatment had no effect on cell death in HaCaTs and 3T3 cells, yet appeared to confer some degree of protection to HFbs. Analysis of the mode of cell death using Annexin V/ propidium iodide staining showed that HaCaTs were predominantly dying by apoptosis. It was determined the human fibroblasts were largely dying by necrosis after 2 h and by apoptosis after 4, 12 and 24 h. Pre-treating the HFbs with vEC alone was able to maintain a level of viability similar to control cells after 24 h. To further understand the mechanisms of apoptotic cell death in HFbs, two apoptosis-associated proteins, anti-apoptotic Bcl-2 and pro-apoptotic Bax, were investigated. Their ratio (Bcl-2:Bax) is indicative of survival, however no significant trends were established and further assays are required to determine conclusive results.

Ferulic acid, in combination with vitamins C and E, has been shown to be effective as a photoprotective agent *in vivo*. The findings of this study have shown that although the antioxidants have little effect in the epidermal keratinocytes, they show great potential in the dermal fibroblasts, which is very important with regards to photoaging. Future studies investigating the effect of the antioxidants on UVA-induced DNA and protein damage will aid in the elucidation of the protective mechanisms portrayed by this dynamic combination.

Chapter 1: Introduction

1.1 Structure of the Skin

The skin is the largest organ in the human body and functions as a biologically active barrier separating internal homeostasis from the external environment [1, 2]. It is the body's first line of defense against external trauma and has evolved to detect, integrate and respond to a great range of stressors, including noxious chemical, physical and biological insults, changes in humidity and solar and thermal radiation [3].

The skin consists of two distinct layers, the epidermis and the dermis, which are separated by a non-cellular basement membrane (figure 1.1). Epidermal-dermal cohesion is vital in preserving the protective function of skin [1, 4].

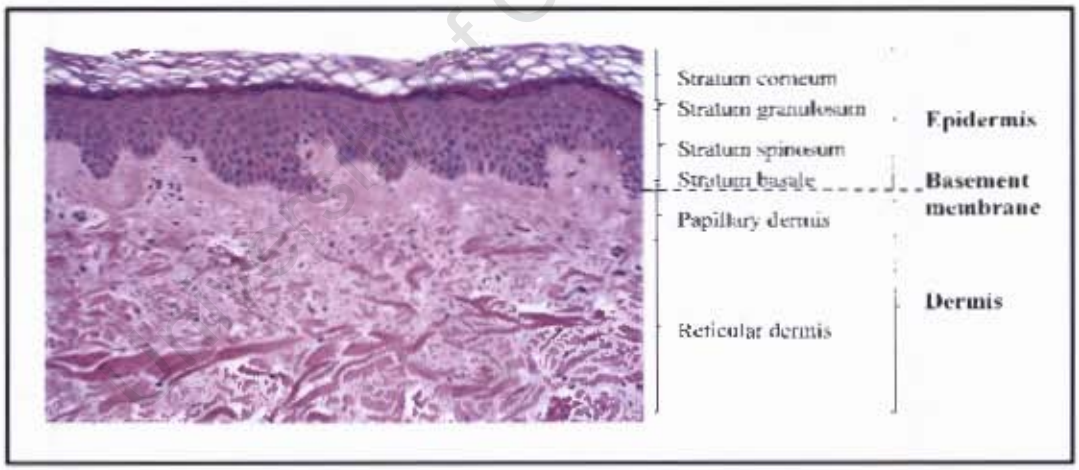

Figure 1.1 Histological representation of the skin, illustrating the specific layers of the epidermis and dermis [5].

1.1.1 The Epidermis

The upper layer of the skin, the epidermis, is a stratified squamous epithelium that regenerates continuously throughout the life of the organism [6]. This continuous self-renewal

is mediated by epidermal stem cells, which reside in the basal layer of the epidermis [6]. The division of these basal stem cells yields a population of daughter cells that are committed to a specific series of events, including cell cycle arrest, outward migration and terminal differentiation [7]. During this journey, keratin-producing keratinocytes undergo a sequence of biochemical and morphological changes that result in the formation of the various epidermal layers [6] (figure 1.2).

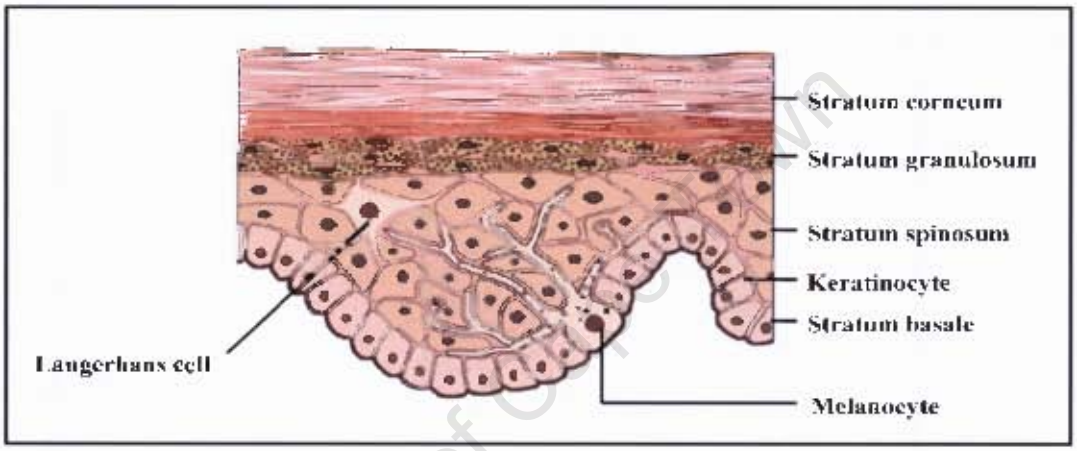

Figure 1.2 Diagrammatic representation of the epidermal layers and resident cell types [8].

The epidermal cell layer bordering the basement membrane is known as the stratum basale, and contains actively proliferating keratinocytes, pigment-producing melanocytes and sensory Merkel cells. In 1963, Fitzpatrick and Breathnach discovered that for every thirty-six viable keratinocytes there was one specifically interacting melanocyte, collectively now referred to as the epidermal-melanin unit [9, 10]. Melanocytes are highly dendritic, neural crest-derived cells. They are responsible for the production of a polymeric pigment called melanin. The synthesis of melanin results from a phylogenetically conserved biochemical pathway called melanogenesis [1]. Melanogenesis takes place in specialized melanocyte-specific organelles called melanosomes. Melanosomes translocate from the perikaryon towards the melanocyte dendrite tips, before they are transferred to neighbouring keratinocytes [11, 12]. Once the melanosomes enter the cytoplasm of the keratinocytes, the

melanin serves as a form of photoprotection against DNA damage by forming a supranuclear melanin cap around the keratinocyte nucleus [13, 14].

The layer above the stratum basale is known as the stratum spinosum (figure 1.2). This 'prickle cell layer' consists of relatively large, polyhedral shaped keratinocytes, as well as bone-marrow derived sentinel cells of the immune system called Langerhans cells. These epidermal antigen presenting cells are also able to express some neuronal markers, as well as neuropeptide receptors, and are key in providing the link between the neuroendocrine and immune systems in the skin [3, 15, 16, 17]. One Langerhans cell is responsible for the immune surveillance of fifty-three surrounding epidermal cells [18]. The next layer, the stratum granulosum, contains keratinocytes that develop a flattened morphology as dividing cells below push them towards the skin surface. The uppermost layer, the stratum corneum, comprises 15-30 sheets of non-viable, but biochemically active cells called corneocytes [1]. This layer is the principal barrier to the percutaneous penetration of exogenous substances, and has well established antimicrobial, chemical and antioxidant defense mechanisms [2, 19].

1.1.2 The Dermis

Dermal tissue is separated from the overlying epidermis by a cutaneous basement membrane (figure 1.1). This specialized membrane plays an important role in normal skin functioning as well as a key part in pathological processes such as wound healing and tumour cell invasion [20]. The dermis itself may be divided into the papillary and reticular dermis, reflecting their respective composition of connective tissue components, cell number, and supply of blood vessels and nerves [1]. Dermal cell populations include fibroblasts, adipocytes, macrophages, mast cells, Langerhans cells, T lymphocytes, dendrocytes, smooth muscle cells and vascular and lymphatic endothelial cells [3].

In vertebrates, connective tissue is functionally designed to provide a structural scaffold for vessels and cells, the principle cell type being fibroblasts [21]. Dermal fibroblasts play an important role in the regulation of tissue structure and cellular microenvironment by the

production of extracellular matrix (ECM) proteins [22], chemokines [23] and matrix metalloproteinases [24], and play major roles in wound healing [1, 21].

The mature epidermis is reliant on the meticulous balance of keratinocyte proliferation and differentiation, which is tightly regulated via a cytokine expression network between keratinocytes and adjacent fibroblasts [25, 26] during both skin development and regeneration [27, 28]. The manner in which keratinocytes and fibroblasts interact is via a double paracrine system [29]. Keratinocytes produce factors such as the cytokine interleukin-1 (IL-1) [30], which in turn induces growth factor expression in fibroblasts [31]. Keratinocyte growth factor (KGF) and other fibroblast-derived mitogens are then responsible for the regulation of keratinocyte proliferation and differentiation [32].

1.2 Skin Cancer and Photoaging

The skin is by design resistant to most external traumas; however over-exposure to certain environmental insults such as ultraviolet (UV) radiation may result in cancer formation [33, 34]. Skin cancer is the most common cancer in South Africa, with approximately 20 000 new cases reported each year [35]. In addition, South Africa has the second highest incidence of skin cancer in the world behind Australia [35].

Skin cancers are clinically classified as melanoma and non-melanoma skin cancer (NMSC), as determined by the original epidermal cell from which the cancer stems. Non-melanoma skin cancer can be further subdivided into basal cell (BCC) and squamous cell carcinoma (SCC). Both BCC and SCC arise from the basal layer of the epidermis, with BCC having a slow progression, and SCC being highly invasive and metastatic [36]. BCC is the most common skin cancer and the most common human malignancy in general [37]. BCCs and SCCs account for approximately 80% and 16% of all skin cancers respectively, while malignant melanomas account for the remaining 4% [38].

The main aetiological cause of skin cancer is exposure to UV radiation, primarily from sunlight [33, 34, 39, 40]. It has been shown that as well as chronic exposure to sunlight, levels of exposure achievable during normal daily activities are mutagenic [41]. In an attempt to protect itself from further UV damage, the skin responds to sun exposure by tanning [42]. The degree of skin pigmentation and the ability to tan are crucial factors in the development of skin cancer, and the risk of NMSC is highest in people who sunburn easily and fail to tan effectively [43]. The predominant acute effects of UV-irradiation on normal human skin include sunburn, inflammation (erythema), tanning and local or systemic immunosuppression. Chronic exposure leads to photoaging, immunosuppression and ultimately photocarcinogenesis [44, 45]. The numerous effects of UV-irradiation are consequential of specific wavelengths that result in different cellular damages and subsequent responses [46, 47].

Exposure of the skin to the UV component of sunlight, specifically the long wavelength UVA, has been shown to initiate two of the key pathways leading to photoaging, namely the induction of matrix metalloproteinases (MMPs) (the enzymes responsible for the degradation of the extracellular matrix) [48] and mutations in mitochondrial DNA [49, 50]. Mutations in mitochondrial DNA have been recognized in degenerative diseases and also found to play a role in skin photoaging [49, 50]. The harmful effect of UVA in generating mitochondrial DNA mutations and inducing MMPs is well documented in human dermal fibroblasts [50, 51].

1.3 Ultraviolet Radiation

Sunlight is composed of a continuous spectrum of electromagnetic radiation that is divided into three main parts based on different wavelengths: ultraviolet (5%), visible (50%) and infrared (45%) (figure 1.3) [52]. The solar UV spectrum occurs between 100-400 nm. It is subdivided into short wave UVC (100-280 nm), medium wave UVB (280-315 nm) and long wave UVA (315-400 nm) (figure 1.3) [53, 54, 55, 56, 57].

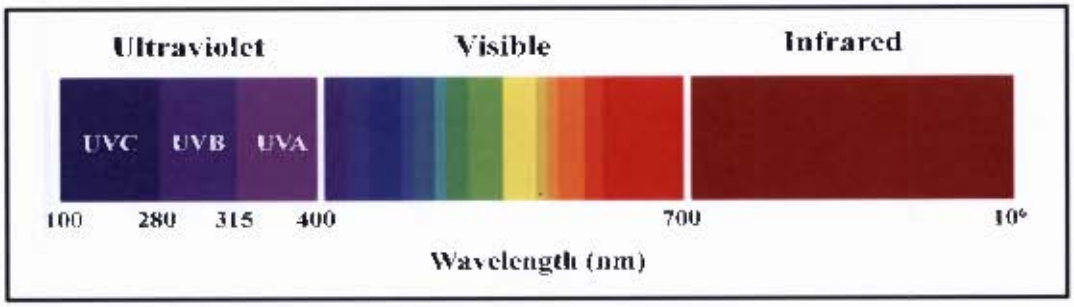

Figure 1.3 The wavelengths constituting the solar light spectrum [58].

The ozone layer efficiently absorbs UV radiation up to approximately 310 nm, thus consuming all UVC and 95% of UVB, whilst UVA is not absorbed at all. The energy carried by each portion of the spectrum is inversely related to its wavelength. UVC is of the highest energy and would be the most damaging to biological tissues; however it is effectively absorbed by stratospheric ozone and is largely irrelevant to human health [57]. Whilst the absorption maximum of DNA is at 260 nm (UVC), it has been determined that 300 nm (within the UVB range) is the most effective wavelength for inducing DNA photoproducts in the basal layer of the epidermis [59].

UVB, which constitutes 5-10% of the UV radiation reaching the earth's surface, is able to directly induce alterations in the structure of nucleic acids by introducing cyclobutane pyrimidine dimers (CPD) [60, 61, 62] and pyrimidine (6-4) pyrimidone photoproducts (6,4-PP) [61, 62]. For many years this high energy wavelength was the primary focus of research aimed at determining the mechanisms underlying skin cancer [62]. More recently however, numerous studies have shown that UVA is also able to induce variety of damages to DNA [63], proteins [64] and lipids [65] with associated detrimental consequences such as skin aging [50] and carcinogenesis [66].

1.3.1 Ultraviolet-A

UVA constitutes more than 90% of the UV radiation reaching the earth's surface, and although this wavelength is considered less energetic than UVB, it has been implicated in

UV-carcinogenesis due to its high penetration properties. Compared to UVB, UVA is about 1000 times more effective in the production of an immediate tanning response, and is considerably more efficient in penetrating the actively dividing cells of the epidermal basal layer, as well as the fibroblasts of the underlying dermis [52, 63, 67, 68]. UVA radiation has been shown to be mutagenic in cultured cells [63], including human fibroblasts [69], and able to induce melanomas [70] and SCCs [71] in mice. In 2006, He *et al.* illustrated that chronic exposure to UVA alone was adequate to induce a malignant phenotype in cultured human keratinocytes [41]. It has also been shown that during normal daily activities, exposure to UVA levels within sunlight sufficiently generates mutations of the tumour suppressor gene *p53* in the basal layer of the epidermis [72].

1.4 UVA-Induced Damage

1.4.1 Indirect Mechanism

At the cellular level, UVA is only weakly absorbed by DNA [73], and the majority of UVA-induced damage occurs indirectly through oxidative processes initiated by endogenous photosensitization. Endogenous photosensitizers are cellular chromophores that include flavins[74], certain sterols[75], aromatic amino acids[76], NAD(P)H, porphyrins, heme [77] and urocanic acid, which occurs at high levels in the stratum corneum [78, 79].

1.4.2 DNA damage

UVA's ability to damage DNA is primarily due to excitation of non-DNA chromophores, leading to increased reactive oxygen species (ROS), which subsequently result in oxidative base damage [61, 80, 81]. ROS can induce numerous covalent modifications to DNA, including single-nucleobase lesions, strand breaks, inter- and intrastrand cross-links and protein-DNA cross-links [82]. It has also been shown that UVA exposure leads to persistent genomic instability in human keratinocytes [83]. Work performed by Peak and Peak (1991) demonstrated that UVA is substantially more effective than shorter wavelength UVR in generating both single strand breaks (SSB) and protein-DNA cross-links [84]. Interestingly the

repair of SSB in cultured human fibroblasts after UVA irradiation appears to be a very rapid process, with 90% being removed within 15 min of exposure [85].

It was initially believed that photodimeric CPDs and 6,4-PPs, which are responsible for single or tandem cytosine to thymine transversions, would not be expected to occur in DNA exposed to UVA. There is evidence to support this theory [86], yet a multitude of studies have shown CPDs to be a major pre-mutagenic lesion in UVA-induced mutagenesis [81, 87, 88, 89, 90, 91, 92, 93, 94, 95, 96]. It has been suggested that UVA induces these CPDs by a photosensitized triplet energy transfer in contrast to the direct excitation of DNA by UVB [81, 92].

1.4.3 Protein Damage

Proteins are major molecular targets for oxidative damage within cells, owing to their high abundance (comprising about 68% of the dry weight of cells) and rapid reaction rates with radicals and excited-state species such as singlet oxygen [97]. ROS cause modifications to amino acids that frequently result in functional changes of structural or enzymatic proteins [98]. The formation of modified proteins as a result of singlet oxygen-mediated photo-oxidation may lead to critical changes in the properties and function of these proteins, induce structural alterations such as protein cross-linking [99] and lead to a change in susceptibility of the oxidised protein to proteolytic enzymes [100]. The oxidation of critical methionine residues (methionine sulfoxide) may lead to the inactivation of certain proteins, and the reduction of this oxidised amino acid appears to be crucial for cell survival in the presence of ROS [101]. The peptide methionine sulfoxide reductase A (MSRA) is a repair enzyme that is able to reduce methionine sulfoxide, and has been found to be upregulated by UVA exposure and represents the only enzyme thus far identified in human skin that is able to repair oxidative protein damage [102].

The detection of carbonyl groups in the skin is commonly used as a marker of ROS mediated protein oxidation [103, 104, 105]. Protein carbonyls may be introduced into proteins through reactions with reactive carbonyl derivatives formed from the reaction of reducing sugars or their oxidation products with lysine residues, or by reactions with aldehydes (4-

hydroxy-2-nonenal (4-HNE) or malondialdehyde (MDA)) during lipid peroxidation [106]. UVA-irradiation of human fibroblasts results in increased protein oxidation, illustrated by a dose-dependent increase in the amount of protein carbonyls [64].

1.4.4 Lipid Damage

Like nucleic acids and proteins, unsaturated lipids are prominent targets of free radical attack in cells that are under photo-oxidative stress. It has been shown that UVA radiation is the most proficient UVR in triggering the peroxidation response [65]. Lipid peroxidation is initiated by free radical (e.g. hydroxyl radical) attack on a fatty acid or fatty acid side chain that has sufficient reactivity to abstract a hydrogen atom from a methylene carbon in the side chain [107] (figure 1.4). The greater the amount of double bonds present in fatty acid side chains the easier the abstraction of a hydrogen atom, making polyunsaturated fatty acids (PUFAs) ideal targets for peroxidation. The removal of a hydrogen atom from one of these bonds yields a carbon-centred lipid radical that subsequently interacts with molecular oxygen to form a peroxyl radical. The resulting peroxyl radical is able to damage membrane proteins, or abstract hydrogen from adjacent fatty acid side chains which results in a chain reaction of lipid peroxidation [107, 108, 109]. The resulting lipid hydroperoxide formed is unstable, and can decompose to various species including MDA, or be reduced to a more stable alcohol form [110] (figure 1.4).

The degree of lipid oxidation can be determined by measuring losses of unsaturated fatty acids, amounts of primary peroxidation products or amounts of secondary products such as carbonyls and hydrocarbon gases [107]. Early peroxidation of unsaturated fatty acids is accompanied by the generation of conjugated diene structures (figure 1.4), which absorb UV light between 230-235 nm, and can be detected spectrophotometrically [107]. MDA (figure 1.4) is used as a convenient biomarker for lipid peroxidation due to its simplistic reaction with thiobarbituric acid (thiobarbituric acid reactive substances (TBARS) assay) to form an intense pink chromogen, which can be measured at an absorbance of 532 nm [107]. It has been shown that UVA-irradiation results in an increase in the amount of MDA in both cultured human keratinocytes [83, 111] and fibroblasts [65]. Exposure to UVA at physiologically

relevant doses is capable of increasing MDA levels via pathways involving iron and singlet oxygen [112]. It has been further shown that lipid peroxidation in human fibroblasts is involved in UVA-induced MMP-1 activation, which plays a role in skin aging and cancer [113].

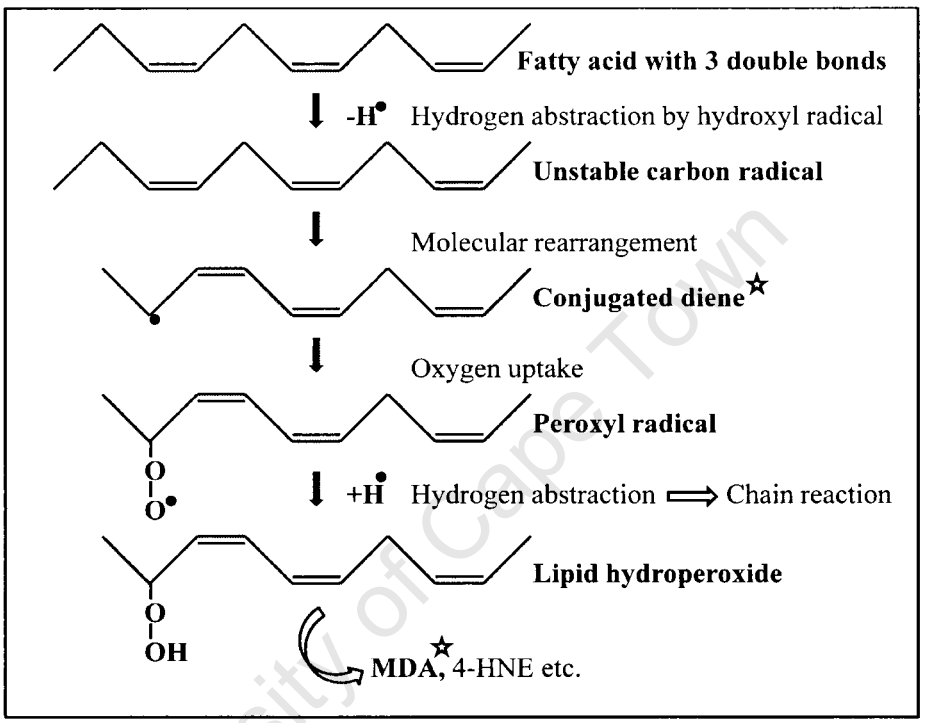

Figure 1.4 Schematic representation of lipid peroxidation in poly-unsaturated fatty acids [114]. Stars indicate the lipid peroxidation products detected in this study.

1.5 Free Radicals and Reactive Oxygen Species

1.5.1 Free Radicals

Free radicals may be defined as 'any species capable of independent existence that contains one of more unpaired electrons' [115]. Radicals may be formed by a non-radical losing or gaining a single electron [115].

Gerschman's free radical theory of oxygen toxicity, which states that the toxicity of oxygen is due to partially reduced forms of oxygen, shed light on the previously vague subject of

oxygen poisoning [116]. The realm of free radicals in biological systems was soon thereafter explored by Denham Harman, who hypothesized that oxygen radicals may be formed as by-products of enzymatic reactions *in vivo* [117]. Harman held free radicals accountable for major cellular damage, mutagenesis and cancer, as well as the degenerative process of biological aging [117, 118]. The science of free radicals in living systems gained renewed momentum after convincing evidence about their importance was proclaimed following the discovery of superoxide dismutase in 1969 [119].

1.5.2 Reactive Oxygen Species

Reactive oxygen species (ROS) are natural by-products of normal cellular metabolism, formed principally through the reduction of molecular oxygen. Molecular oxygen, also known as dioxygen (O_2), in its ground state, contains two unpaired electrons which lead to preferential reduction via a univalent pathway (figure 1.5). The intermediates formed along this pathway include superoxide ($O_2^{\bullet-}$), hydrogen peroxide (H_2O_2) and the highly volatile hydroxyl radical ($HO^{\bullet}$) [80] (figure 1.5).

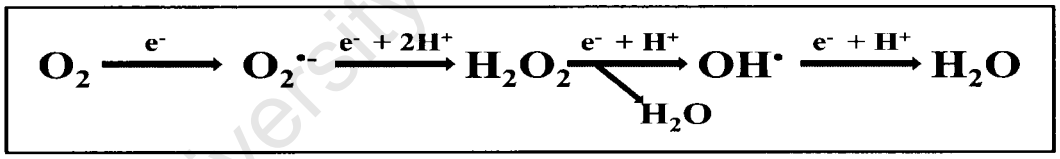

Figure 1.5 Molecular representation of the univalent reduction of oxygen. O_2 (dioxygen), $O_2^{\bullet-}$ (superoxide), H_2O_2 (hydrogen peroxide), $HO^{\bullet}$ (hydroxyl radical) and H_2O (water).

ROS include radical species, such as superoxide and hydroxyl radical, along with non-radical species such as hydrogen peroxide [120] (table 1.1). Most of the ROS produced by cells occur mainly through four endogenous sources: aerobic respiration (mitochondria sequentially reduce oxygen to water) [121, 122], destruction of bacteria or virus-infected cells with an oxidative burst by phagocytic cells [123], peroxisomes (organelles that degrade fatty acids and produce hydrogen peroxide as a by-product) [124] and cytochrome P450 enzymes (the degradation of xenobiotics results in oxidant by-products) [125, 126]. An additional

noteworthy source of ROS comes from the two-step reaction catalysed by the xanthine oxidase (XO), whereby hypoxanthine is converted to xanthine, forming superoxide, and xanthine is converted to uric acid, forming hydrogen peroxide [127, 128]. Exogenous sources that lead to ROS production include x-ray, gamma-ray and UV light irradiation [129].

Table 1.1 Radical and non-radical reactive oxygen species [115].

Free radicals		Non-radicals	
Superoxide	$O_2^{\bullet-}$	Hydrogen peroxide	H_2O_2
Hydroxyl	$HO^{\bullet}$	Hypobromous acid	HOBr
Hydroperoxyl	$HO_2^{\bullet}$	Hypochlorous acid	HOCl
Carbonate	$CO_3^{\bullet-}$	Ozone	O_3
Peroxyl	$RO_2^{\bullet}$	Singlet oxygen	$O_2^1\Delta g$
Alkoxyl	$RO^{\bullet}$	Organic peroxides	ROOH
Carbon dioxide	$CO_2^{\bullet-}$	Peroxynitrite	$ONOO^-$
		Peroxynitrate	O_2NOO^-
		Peroxynitrous acid	ONOOH
		Nitrosoperoxycarbonate	$ONOOCO_2^-$
		Peroxomonocarbonate	$HOOCO_2^-$

In his final paper published in 1934, Professor Fritz Haber (with Joseph Weiss) was the first to propose that the interaction between superoxide and hydrogen peroxide could generate the highly reactive hydroxyl radical [130]. It was quickly recognized that the Haber-Weiss reaction (Eq. 3) may be a mechanism to generate more toxic radicals. The basic reaction (Eq. 3) has a second order rate constant of zero in aqueous solutions and is thus thermodynamically unfavourable in biological systems. Transition metal ions, such as iron, are present at low concentrations in biological systems, and are able to act as catalysts for the reaction (Eq. 1 and 2), possibly accounting for the *in vivo* production of the hydroxyl radical. The iron-catalyzed Haber-Weiss reaction, which makes use of Fenton chemistry, is the principle pathway in generating the most reactive oxygen species, the hydroxyl radical, in biological systems [110].

$$Fe^{3+} + O_2^{\bullet-} \longrightarrow Fe^{2+} + O_2 \quad (1)$$

$$Fe^{2+} + H_2O_2 \longrightarrow Fe^{3+} + HO^- + HO^\bullet \quad (2)$$

The net reaction:

$$O_2^{\bullet-} + H_2O_2 \longrightarrow O_2 + HO^- + HO^\bullet \quad (3)$$

Following UVA-irradiation, the majority of hydrogen peroxide produced in cultured human keratinocytes appears to originate from superoxide, and its subsequent conversion to hydroxyl radicals appears to be a critical step in the UVA-induced generation of strand breaks and alkali-labile sites [131].

1.6 Antioxidant Defense

1.6.1 Redox Homeostasis

ROS have been identified as both deleterious and beneficial molecules within living systems [126]. At low or moderate concentrations, reactive species, such as nitric oxide and superoxide, function in the induction of mitogenic responses and in redox signalling, the latter of which is a regulatory process where the signal is delivered through redox chemistry [132]. Studies have shown that the hydrogen peroxide produced by receptor binding of numerous peptide growth factors is required for certain signal transduction cascades, such as the signalling pathways involving insulin [133] and vascular epithelial growth factor [134]. It has been further shown that the addition of certain antioxidants leads to a suppression of both survival and death signalling, indicating that both of these vital pathways are redox-regulated [135].

1.6.2 Antioxidants

The redox system is vital in maintaining cellular homeostasis. Under physiological conditions, redox regulation is achieved through the generation and elimination of ROS and other reactive species [129]. The steady-state formation of pro-oxidants in cells is balanced by

a similar rate of their expenditure by enzymatic and non-enzymatic antioxidants (table 1.2). An antioxidant is 'any substance that delays, prevents or removes oxidative damage to a target molecule' [115]. When the antioxidant defense mechanisms are overwhelmed by increasing ROS, the pro-oxidant/ antioxidant equilibrium is shifted in favour of the pro-oxidants, resulting in oxidative stress [136].

Table 1.2 Enzymatic and non-enzymatic antioxidants

Enzymatic	Non-enzymatic
Superoxide dismutase (SOD)	Ascorbic acid (vitamin C)
Catalase (Cat)	α-Tocopherol (vitamin E)
Glutathione peroxidase (GPx)	Glutathione (GSH)
Glutathione reductase (GR)	Ubiquinone/ ubiquinol (CoQ)
Thioredoxin reductase (TR)	Thioredoxin (Trx)
Heme oxygenase	

1.6.2.1 Enzymatic Antioxidants

A major enzymatic antioxidant, which is responsible for the dismutation of superoxide to hydrogen peroxide, is superoxide dismutase (SOD) (Eq. 4). Several isoforms of SOD inhabit various cellular compartments. SOD1 (cytosolic or copper-zinc SOD- CuZnSOD) is the major isoform found in the cytoplasm, mitochondrial intermembrane space, nucleus and lysosomes, whereas SOD2 (manganese SOD- MnSOD) and SOD3 (extracellular SOD- EC-SOD) are found in the mitochondria and extracellular matrix respectively [137]. Further conversion of H_2O_2 to $H_2O + O_2$ occurs through the action of catalase (Eq. 5) or through reduction by the seleno-enzyme glutathione peroxidase (GPx) (Eq. 6), whereby GPx catalyzes the oxidation of reduced glutathione (GSH to GSSG). The reduced form of glutathione is restored by glutathione reductase (GR) (Eq. 7) [120].

$$O_2^{\bullet-} + 2H^+ \xrightarrow{SOD} H_2O_2 \quad (4)$$

$$2\,H_2O_2 \xrightarrow{CAT} 2H_2O + O_2 \quad (5)$$

$$2GSH + H_2O_2 \xrightarrow{GPx} GSSG + 2H_2O \quad (6)$$

$$GSSG + NADPH + H^+ \xrightarrow{GR} 2GSH + NADP^+ \quad (7)$$

Superoxide dismutase, catalase and the enzymatic glutathione system are all present in higher concentrations in the epidermis than the dermis, with catalase activity in particular being remarkably higher (720%) in the epidermis [138]. The deleterious effect of UVA-irradiation on keratinocytes is illustrated by the significant decrease in both SOD and catalase activity upon exposure [111]. Like most cellular macromolecules these enzymatic antioxidants are susceptible to oxidative reactive species, and if the oxidative stress is great enough they may be completely inactivated, leading to a further increase in stress [139]. The effects of UVA-treatment on dermal fibroblasts illustrate an inactivation of catalase and a reduction of SOD, with levels of GPx and GR remaining virtually unchanged [140].

1.6.2.1.1 Heme Oxygenase and Iron

In 1989, Keyse and Tyrrell determined that heme oxygenase (HO) was the major 32 kDa stress protein that was found to be induced in human skin fibroblasts by UVA-irradiation [141]. It has since been identified that singlet oxygen is a primary effector in the induction of HO [142]. HO-1 is an inducible form of the enzyme, and is responsible for heme-catabolism, resulting in biliverdin, carbon monoxide and iron [143]. Bilirubin (derived from biliverdin) has strong radical scavenging capabilities [144, 145, 146, 147], while carbon monoxide has been shown to be involved in the photoimmunoprotective effect of UVA [148, 149, 150, 151]. The UVA-induced transcriptional activation of HO-1 eventually (i.e. 1 to 2 days) leads to a HO-1 dependent increase in the iron-storage protein ferritin [152] and a consequent lowering of the pro-oxidant state of the cells [153]. However, there is an initial decrease in the amount of ferritin, before the increase 1 to 2 days later, due to UVA-induced proteolysis which contributes to the free iron in the cell [154]. High levels of free iron are detrimental to cells, in

that singlet oxygen and hydrogen peroxide generated by UVA promote biological damage such as lipid peroxidation in cultured human fibroblasts, via iron-catalyzed oxidative reactions [112, 154, 155]. Human keratinocytes have higher basal levels of the non-inducible form of heme oxygenase (HO-2) than fibroblasts, but little inducible (HO-1) activity [115]. The keratinocytes are the 'first line of defense' against UVA, and may require the added protection of constitutively expressed HO.

Along with members of the heat shock protein and thioredoxin families, HO-1 is considered a vitagene. The term 'vitagene' refers to a subset of genes that are involved in maintaining cellular homeostasis during stressful conditions, such as oxidative stress [156]. Inducers of HO-1 include compounds such as phenolic antioxidants and Michael reaction acceptors, which act via a transcriptional enhancer element known as the antioxidant responsive element (ARE) [157, 158, 159]. Phenolic antioxidants which have shown the ability to induce HO-1 expression include curcumin (in neuronal cultures) and ferulic acid ethyl ester (in human fibroblasts) [156, 160].

1.6.2.2 Non-Enzymatic Antioxidants

1.6.2.2.1 Hydrophilic Antioxidants

Endogenous non-enzymatic antioxidants (table 1.2), recognized to execute thiol-disulfide exchange reactions, play a major role in maintaining redox homeostasis. Glutathione (GSH), the most abundant peptide in cells, possesses a multitude of functions ranging from being a co-factor of various antioxidant enzymes, to directly scavenging hydroxyl radicals and singlet oxygen, and regenerating other antioxidants such as vitamins C and E to their active forms [161]. Thioredoxin, a seleno-protein containing two redox-active cysteines, is an important thiol antioxidant making up the thioredoxin system, consisting of thioredoxin (Trx) and thioredoxin reductase (TR) [162]. Didier *et al.* (2001) demonstrated an increase in intracellular levels of Trx and TR in UVA-irradiated human skin fibroblasts. They further showed that inducible Trx was able to decrease ROS production and protect against UVA-induced apoptosis [163].

Vitamin C is one of the body's major aqueous phase reductants [164]. It is the predominant antioxidant in the skin, with its concentration being 15-fold more than GSH and 200-fold more than vitamin E [165]. This essential water-soluble vitamin comprises two major interconvertible forms, L-ascorbic acid (figure 1.6) and L-dehydroascorbic acid, both present in biological tissues and food [166]. Vitamin C does not absorb UVA and its quenching activity arises solely due to its capacity to scavenge reactive species such as hydroxyl radicals, superoxide and singlet oxygen [115, 167]. By systematic donation of an electron, the resulting ascorbate free radical formed is more stable than most other free radicals, hence its functional significance as a free radical chain terminator. After the loss of a second electron, dehydroascorbate can be regenerated to ascorbate by dehydroascorbic acid reductase or GSH (figure 1.7), or may simply decay [165].

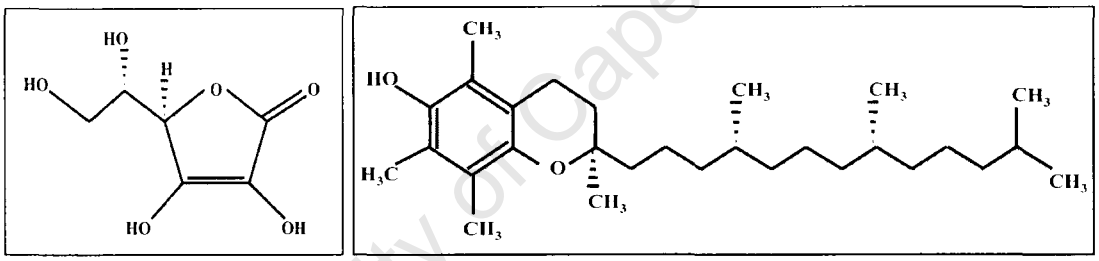

Figure 1.6 Structure of L-ascorbic acid (left) and α-tocopherol (right).

1.6.2.2.2 Hydrophobic Antioxidants

Co-enzyme Q (CoQ) (ubiquinone and ubiquinol) is a lipid-soluble redox molecule that functions mainly as a component of membrane electron transport systems such as the mitochondrial respiratory chain [168]. In the skin the majority of ubiquinone exists in its oxidised form ubiquinone-10 [169], which has been shown to protect primary and HaCaT keratinocytes against UVA-induced oxidative DNA damage, as well as reduce the detrimental photoaging effects of UVA on dermal fibroblasts [170].

Vitamin E is an essential vitamin that, in humans, is rarely deficient due to its broad distribution in food [171]. The term 'vitamin E' collectively refers to the eight naturally

occurring compounds that exhibit vitamin E activity. These include four tocopherols (phytyl side chains) and four tocotrienols (isoprenoid side chains) [169]. The α-, β-, γ- and δ-tocopherols and tocotrienols, which each contain an essential hydroxyl group necessary for antioxidant activity, differ only in the number and position of the methyl groups on the chroman ring. The most potent isoform is RRR-α-tocopherol (figure 1.6), which is responsible for about 90% of the vitamin E activity found within tissues [171]. This lipophilic compound partitions into lipoproteins and cell membranes, where it can confer stability and function as a lipid antioxidant to protect the polyunsaturated membrane lipids from free radical attack. When ROS attack membrane lipids a peroxyl radical may form, which has the ability to generate more peroxyl radicals, which may propagate a chain reaction and threaten the structural integrity of the membrane [172]. The propagation of these chain reactions may be inhibited through the peroxyl scavenging activity of α-tocopherol, which in addition is able to quench the highly reactive singlet oxygen [173]. It has been determined that the concentration of α-tocopherols is 90% higher in the epidermal layer than the dermal layer in human skin [138], which is necessary considering tocopherols in the stratum corneum are highly susceptible to solar stimulated UV irradiation, and both α- and γ-tocopherol levels are dramatically reduced following exposure to UVA and UVB [174].

Non-enzymatic antioxidants work in tissues, including the skin, as a coordinated interactive group of compounds related to chemical structure, location and relative redox potential [175]. For example, when a ROS is generated in a membrane structure and is reduced by α-tocopherol, the oxidised antioxidant can be regenerated by ubiquinol or L-ascorbic acid. The resulting dehydroascorbate can be reduced by GSH, which can subsequently be reduced by the nicotinamide adenine dinucleotide phosphate reduced (NAD(P)H) pool [165] (figure 1.7).

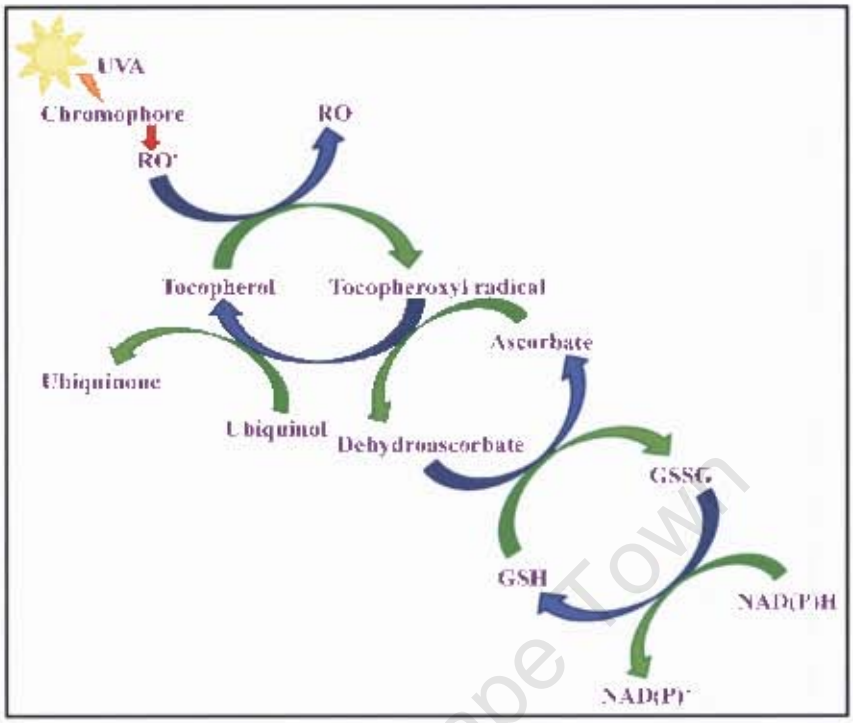

Figure 1.7 Non-enzymatic antioxidant recycling [165]. RO• (reactive oxygen species), RO (reduced reactive oxygen species), GSH (glutathione), GSSG (reduced glutathione), $NAD(P)^+$ (nicotinamide adenine dinucleotide (phosphate)), NAD(P)H (reduced nicotinamide adenine dinucleotide (phosphate)).

1.7 Plant Phenolics and Ferulic Acid

1.7.1 Polyphenolic Phytochemicals

Recently, there has been extensive interest in naturally occurring antioxidants which are capable of reducing ROS-mediated oxidative stress. Oxidative stress is proposed to play a role in several pathological disorders such as cancer and aging, and phenolics in particular are considered potential therapeutic agents [176, 177].

Thousands of compounds possessing a polyphenolic structure (an aromatic ring yielding at least one hydroxyl substituent) have been identified in a variety of plants species [178, 179, 180, 181, 182]. These compounds are secondary metabolites of plants and are typically involved in

maintenance of cell wall shape and integrity, as well as protection against UVR and pathogens [183, 184]. Polyphenols can be subdivided into various groups, including phenolic acids, flavonoids, stilbenes and lignans, based on the number of phenol rings they possess and of the structural components that bind these rings together [185]. Phenolic acids may be distinguished as derivatives of either benzoic or cinnamic acid. The hydroxycinnamic acids are more common than the hydroxybenzoic acids and consist mainly of the structurally related *p*-coumaric, caffeic, ferulic and sinapic acids, which are synthesized via the shikimate pathway from L-phenylalanine or L-tyrosine [185, 186] (figure 1.8). This class of phenylpropanoids have well characterized physiological activities, such as anti-cancer [187], anti-inflammation [187], anti-hepatoxicity [188] and anti-oxidation [184, 189].

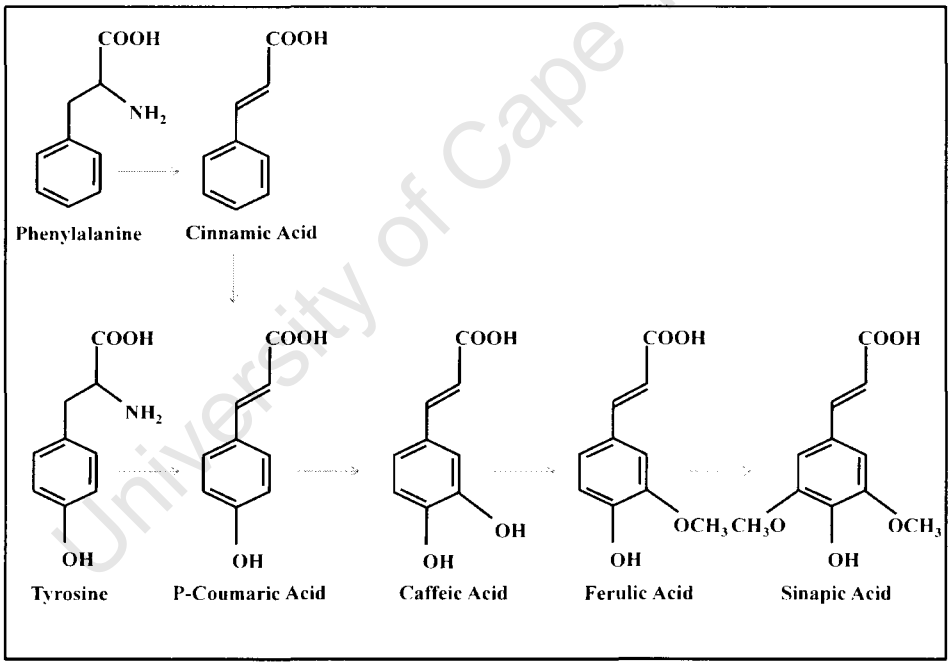

Figure 1.8 Biosynthesis of hyroxycinnamates via the shikimate pathway [186].

The antioxidant activity of polyphenols may be anticipated based on the availability of the phenolic hydrogens as hydrogen-donating radical scavengers. For a polyphenol to be defined as an antioxidant, it must comply with two basic criteria: firstly, it must be able to delay, retard, or prevent the auto-oxidation or free radical-mediated oxidation when in a low

concentration relative to the substrate being oxidised [115]; and secondly, the ensuing radical formed post-scavenging must be stable through intramolecular hydrogen bonding upon further oxidation [190].

1.7.2 Ferulic Acid and Related Compounds

Hydroxycinnamates are found in all compartments of fruit, with the highest concentrations seen in the outer parts of ripe fruit. Caffeic acid, free and esterified, is typically the most profuse phenolic acid accounting for between 75 and 100% of the overall hydroxycinnamic acid content of most fruit [185], whilst ferulic acid (FA) is the most plentiful phenolic acid found in cereal grains, constituting approximately 0.8-2 g/kg (dry weight) of wheat grain and may represent 90% of the total polyphenols [191]. FA has a distinctive bi-functional role in the structuring of cell walls in that it can cross-link heteroxylans in cereal tissues and pectins in beet root tissues [178]. Apart from 10% that exists in the soluble free form, it is primarily found in the *trans* form, esterified to arabinoxylans and hemicelluloses [191]. It may also exist as a dimer in certain cereals, forming bridge structures between hemicelluloses chains [185].

The main mechanism for a phenolic antioxidant is the trapping and stabilizing of radical species such as the lipid peroxyl radical. The elucidation of the anti-oxidation mechanism of FA (3-hydroxy-4-methoxycinnamic acid) has been assessed kinetically [192] and by a structure-activity approach [193]. It is widely accepted that its antioxidant potential may be attributed to its structural characteristics, as its phenolic nucleus and unsaturated side chain can readily form a resonance stabilized phenoxy radical [194]. Any reactive species interacting with FA are highly capable of abstracting a hydrogen atom, forming a phenoxy radical. The resultant radical is highly stable as the unpaired electron may be positioned on the oxygen, or delocalized across the entire molecule. The phenoxy radical generated is unable to initiate or propagate a radical chain reaction and most likely will collide and condense with another ferulate radical to give rise to the dimer curcumin, itself a well reported radical scavenger [195]. Such coupling may generate a variety of compounds, the majority of which still contain hydroxyl moieties capable of radical scavenging [194].

Kanski *et al.* (2001) have demonstrated that FA is able to efficiently attenuate free radical damage in a neuronal cell line more effectively than structurally related vanilic, cinnamic and coumaric acids, through a decrease in ROS formation and lipid and protein oxidation [196]. Ferulic acid has also been shown to reduce lipid peroxidation in microsomes [197] and liposomes [198, 199] and efficiently scavenge nitric oxide [198], 1,1-diphenyl-2-picrylhydrazyl (DPPH) [199, 200, 201], superoxide and hydroxyl radicals [202]. Importantly, FA appears to be a viable option for topical *in vivo* protection against UVA-induced skin damage as it readily permeates through the stratum corneum of excised human skin [198]. A naturally occurring and more hydrophobic form of FA (ferulic acid ethyl ester) has been shown to protect against hydrogen peroxide- induced lipid and protein oxidation in human dermal fibroblasts [156]. Despite these reports, the mechanism of how FA is able to confer protection in skin cells against UVA-mediated oxidative stress still remains to be elucidated.

1.8 Antioxidant Combinations as Photoprotective Agents

The rising incidence of both melanoma and NMSC, and the established role of solar UVR in the aetiology of photocarcinogenicity [203], provides evidence for an urgent need of an improved skin photoprotection system that provides adequate defense against both UVA and UVB [204]. The incorporation of antioxidants into photoprotective agents is a feasible option for combating UV-mediated oxidative damage. Studies are currently being undertaken to isolate potential antioxidants and polyphenolic compounds that could be used to attenuate the deleterious effects of UVA on human skin [205].

The complementary effects of combining vitamins and antioxidants are well established [165, 206, 207, 208, 209, 210]. Vitamin E's ability to scavenge lipid peroxyl radicals and subsequently be reduced by vitamin C to regenerate its active form [211] remains the key reason why this antioxidant pair is often incorporated into topical cosmeceutical formulations [212]. It has been shown that a topical solution containing L-ascorbic acid (15%) and α-tocopherol (1%) provides a four-fold photoprotective effect against UV-irradiation in porcine skin compared to a two-fold protection for either vitamin alone [213]. Interestingly the addition of FA (0.5%) to this combination solution stabilized the formulation and acted synergistically to double

the photoprotection from four to eight-fold [208, 209]. In 2008, Murray *et al.* were able to reproduce this work on human skin, and confirmed that the combination was able to confer significant photoprotection against solar-simulated UV-radiation [210].

Despite this *in vivo* study, *in vitro* studies have not been undertaken to elucidate the effect of the FA with vitamins C and E (vEC) combination treatment on the specific cells of the epidermis and dermis.

1.9 Cell Death Mechanisms

1.9.1 Cell Death

With continued UVA-induced oxidative insult, the primary defensive mechanisms employed by the cell are often not adequate to entirely avoid cellular damage and a second line of defense is required. In an attempt to survive persistent oxidative stress, cells may initiate the process of autophagy. Autophagy pathways, including macroautophagy, microautophagy and chaperone-mediated autophagy, are some of the early cellular responses to early-stage oxidative stress for removal of damaged components before further damage or aggregation occurs [214, 215, 216].

1.9.2 Apoptosis

In 1972 the concept of apoptosis emerged [217], and our knowledge of the mechanisms involved increased considerably through the study of programmed cell death that occurs throughout the development of the nematode *Caenorhabditis elegans* [218]. This structured cell clearance system has distinct morphological features that are distinguishable from senescence or necrosis, such as cell shrinkage, plasma membrane blebbing, chromatin condensation, DNA fragmentation and the formation of apoptotic bodies [217] (table 1.3). Cells undergoing apoptosis are renowned for displaying 'come and eat me' signals to neighbouring phagocytes, and one of these signals is phosphatidylserine (PS) externalisation of the cell membrane. These phospholipids usually exist on the cytoplasmic side of the cell membrane, but they become exposed to the external environment during the course of

apoptosis [219, 220]. This translocation of PS ensures that the apoptotic bodies are swiftly and safely engulfed by phagocytes, avoiding an inflammatory response [217, 220, 221, 222].

Table 1.3 Differences between apoptotic and necrotic cell death [223].

Apoptosis	Necrosis
Individual cells/ small clusters of cells	Neighbouring cells affected
Cell shrinkage and convolution	Cell swelling
Pyknosis and karyorrhexis	Karyolysis, pyknosis and karyorrhexis
Intact cell membrane	Disrupted cell membrane
Cytoplasm contained in apoptotic bodies	Cytoplasm released from cells
No inflammatory response	Inflammatory response

It has been shown in skin reconstructed *in vitro* that UVA is able to induce apoptosis in the superficial dermal fibroblasts without major alterations to the epidermal keratinocytes [224]. This effect suggests differential cell type sensitivity to UVA radiation, which is expected considering the epidermis is the first line of defense and needs to be well equipped to resist damage. Although it must be noted that keratinocytes are not completely resistant to the damaging effects of UV, and that FA vEC pre-treatment of both porcine and human skin has been shown to reduce the number of apoptotic keratinocytes (sunburn cells) compared to untreated skin upon exposure to solar-stimulated UV [208, 209, 210, 225].

1.9.2.1 Caspases

Some of the key proteins in apoptosis belong to a family of cysteine proteases know as the caspases. To date, approximately 14 mammalian caspases have been identified and broadly categorized as initiators (caspases-2, -8, -9, -10), executioners (caspases-3, -6, -7) and inflammatory caspases (-1, -4, -5) [223]. Caspases-11, -12, -13 and -14 are involved in various other apoptotic processes [226, 227, 228, 229]. Initiator caspases have a prominent pro-domain, unlike the executioner caspases that contain either a death effector domain (DED) (caspases-8, -10) or a caspase activation and recruitment domain (CARD) (caspase-2, -9) [230]. Activated caspases cleave a number of assorted substrates in the cytoplasm or nucleus

leading to the many morphologic features of apoptotic cell death [231]. Pre-treatment with the FA vEC combination has been demonstrated to protect against caspase-3 and -7 activation in porcine skin [208, 209].

1.9.2.2 Extrinsic Pathway of Apoptosis

The process of apoptosis may be triggered by extrinsic (death-receptor mediated) or intrinsic (mitochondria mediated) switches (figure 1.10). The extrinsic signalling pathway involves transmembrane receptor-mediated interactions, specifically death receptors that are members of the tumour necrosis factor (TNF) receptor gene superfamily [232]. Members of this family share similar features and are characterized by the presence of cysteine rich domains, that facilitate ligand binding, as well as a critically important 80 amino acid cytoplasmic domain, referred to as the 'death domain' [233]. This death domain is vital in conveying the extracellular death signal to the intracellular signalling pathways. Two examples that best exemplify the extrinsic phase of apoptosis are that of the Fatty acid synthetase ligand (FasL)/ FasR and TNF-α/ TNFR1. The binding of Fas ligand to Fas receptor leads to recruitment of the cytoplasmic adaptor protein Fas-associated death domain (FADD), and the binding of TNF ligand to TNF receptor results in binding of the adaptor protein TNF receptor-associated death domain (TRADD) with additional recruitment of FADD and receptor-interacting protein (RIP) [234, 235]. FADD subsequently associates with procaspase-8 through dimerization of their individual death effector domains (DED), which effectively forms a death-inducing signalling complex (DISC) and leads to the autocatalytic activation of procaspase-8, which is capable of triggering a caspase cascade and subsequent cell death by directly cleaving downstream executioner caspases, such as caspase-3 and -7 [236, 237]. Death receptor-mediated apoptosis can be inhibited by a protein known as FLICE-inhibitory protein (c-FLIP) which binds to FADD and caspase-8, rendering them redundant [238].

1.9.2.3 Intrinsic Pathway of Apoptosis

The mitochondrial pathway is used extensively in response to extracellular cues and internal insults such as DNA damage [239]. This pathway proceeds when pro-apoptotic factors sequestered between the outer and inner mitochondrial membranes are released to the

cytosol as a result of mitochondrial outer membrane permeabilization (MOMP), which triggers a sequence of events that culminates with caspase activation (figure 1.10). If the caspase activation pathway is inhibited, a caspase-independent cell death ensures cellular demise. This process may utilize mechanisms involving ROS, loss of mitochondrial function or released mitochondrial intermembrane apoptogenic factors such as apoptosis-inducing factor (AIF) [240]. MOMP occurs in both caspase-dependent and caspase-independent processes, disrupting mitochondrial function and resulting in subsequent death as energy production diminishes [241].

The B-cell lymphoma-2 (Bcl-2) family of proteins, comprising both anti- and pro-apoptotic members, mediates the cellular 'life-or-death' switch by regulating MOMP [242, 243]. The overexpression of Bcl-2 has been shown to exert a tumourigenic influence by inhibiting cell death, as opposed to promoting cell proliferation like most oncogenes [244]. The Bcl-2 family of proteins is divided into three groups based on the presence of up to four Bcl-2 homology domains (BH1-4): anti-apoptotic members, including Bcl-2, Bcl-xL, Mcl-1 and A1; pro-apoptotic effector members, including Bax and Bak; and lastly the pro-apoptotic members, the BH3-only proteins including Bid, Bim, Bad, Noxa and Puma [245]. Both groups of pro-apoptotic members are required to initiate apoptosis [246, 247]. Commitment to MOMP occurs when the cellular array of anti-apoptotic Bcl-2 proteins are neutralized by BH3-only proteins, as this prevents the anti-apoptotic members from sequestering the pro-apoptotic effector molecules Bax and Bak. A combination of BH3-only proteins is required, as each neutralizes only a subset of anti-apoptotic Bcl-2 proteins (figure 1.9).

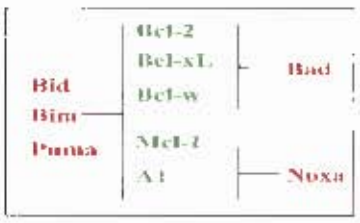

Figure 1.9 Schematic representation of the pro-apoptotic BH3-only proteins (red) and their target anti-apoptotic proteins (green) [243].

BH3-only proteins may be classified as de-repressors (e.g. Bad, Puma and Noxa) or direct activators (e.g. Bid and Bim). De-repressor BH3-only proteins bind anti-apoptotic Bcl-2 proteins and displace direct activator BH3-only members, thus promoting MOMP. De-repressors themselves do not directly activate the effector proteins Bax and Bak. For example, Bid can be released from Bcl-xL by Bad and go on to interact with the effector proteins Bax and Bak [243].

Upon activation of the Bcl-2 effector molecules Bax and Bak, they oligomerize to form homodimers that embed in the outer mitochondrial membrane to promote the release of intermembrane space molecules such as cytochrome *c* [242]. Upon permeabilization these apoptogenic proteins, including second mitochondrial activator of caspases (Smac)/ direct IAP binding protein with low pI (DIABLO), Omi/ high temperature requirement protein 2A (HtrA2), AIF, endonuclease G and cytochrome *c*, are expelled into the cytosol to elicit the execution of cell death by contributing to nuclear degradation [248, 249], promoting caspase activation or by acting as caspase-independent death effectors [250]. A family of proteins capable of suppressing the caspase activity, the inhibitor of apoptosis proteins (IAPs), are negatively regulated by the apoptogenic factors Smac/DIABLO and Omi/Htra2A [251]. When cytochrome *c* is released, it is able to bind to the C-terminal of the adaptor protein apoptotic protease activating factor (Apaf-1), which triggers a dATP-dependent oligomerization of Apaf-1, a process required for activation of the initiator caspase, caspase-9 [252]. Caspase-9 contains a long pro-domain, which allows it to interact with the N-terminal CARD present on Apaf-1. The resultant complex formed is referred to as the apoptosome. Once activated, caspase-9 is free to activate executioner caspases such as caspase-3, -6 and -7, which subsequently affect target molecules such as inhibitor of caspase-3-activated DNase: caspase-3-activated DNase (ICAD: CAD) [253] (figure 1.10).

Cross-talk and integration between the death-receptor and mitochondrial pathways is mediated via the pro-apoptotic Bcl-2 family member Bid. Bid is another substrate of activated caspase-8, and the C-terminal of the truncated form translocates to the mitochondrial membrane and promotes cytochrome *c* release [239]. The two pathways

typically function exclusively, yet under most conditions there is a certain amount of cross-talk [254, 255].

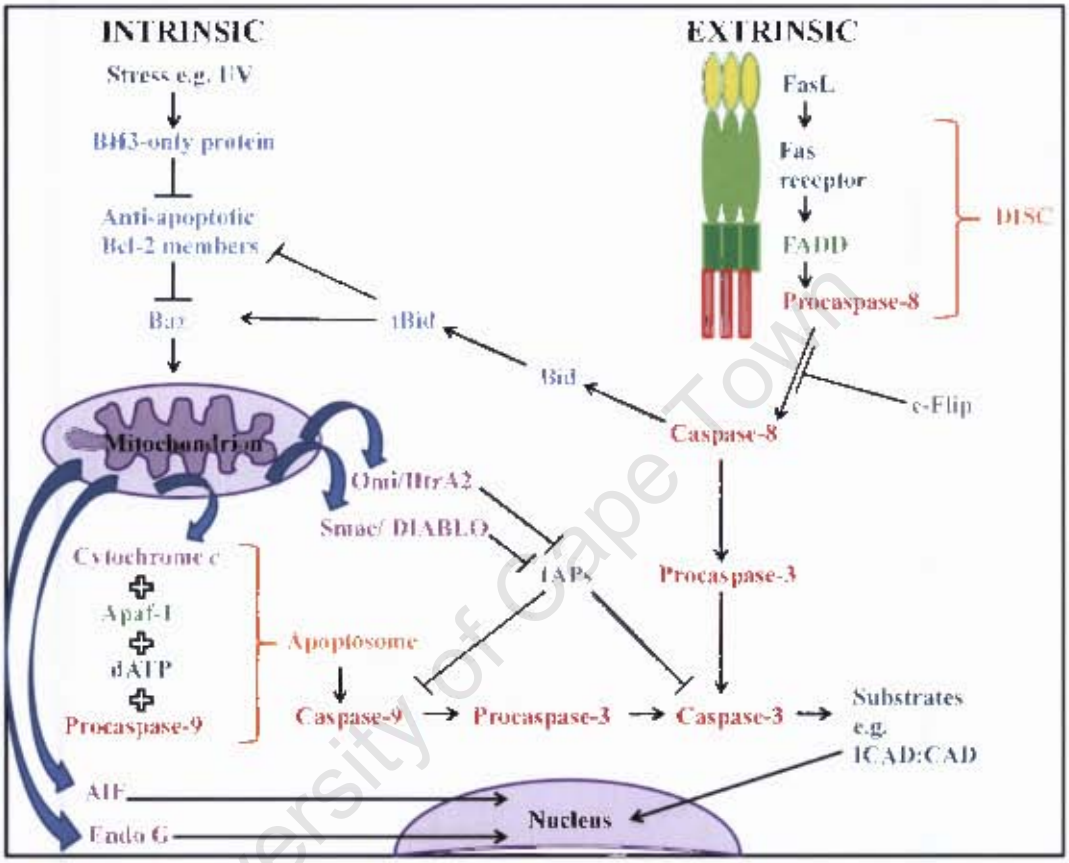

Figure 1.10 Diagram of the intrinsic and extrinsic pathways of apoptosis. UV (ultraviolet), BH3 (Bcl-2 homology domain), Bcl-2 (B-cell lymphoma-2), Bax (Bcl-2 associated X protein), Bid (BH3-interacting death domain agonist), tBid (truncated Bid), Apaf-1 (apoptotic protease activating factor-1), dATP (deoxyadenosine triphosphate), AIF (apoptosis-inducing factor), Endo G (endonuclease G), Omi/ HtrA2 (Omi/ high temperature requirement protein 2A), Smac/ DIABLO (second mitochondrial activator of caspases/ direct IAP binding protein with low pI), IAP (inhibitor of apoptosis protein), FasL (Fatty acid synthetase ligand), FADD (Fas-associated death domain), DISC (death-inducing signalling complex), c-Flip (FLICE-inhibitory protein), ICAD:CAD (inhibitor of caspase-3-activated DNase: caspase-3-activated DNase).

1.9.3 Necrosis

Another mode of cell death is necrosis, which is considered to be a noxious process where the cell passively follows an energy-independent mode of cell death [223]. Although the process of apoptosis and necrosis appear to be two distinct pathways, they appear to overlap via morphologic expressions of a common biochemical network termed the 'apoptosis-necrosis continuum' [256]. An ongoing apoptotic process may be converted to a necrotic process if there is a diminished availability of caspases and intracellular ATP [257, 258]. The nature of the cell death signal, the tissue type and physiological milieu are all factors that determine whether a cell dies by necrosis or apoptosis [256, 259]. Some of the prominent morphological changes that materialize during necrosis include cell swelling, vacuolation, damage to organelles and ultimately loss of cell membrane integrity (table 1.3) [217, 260].

It has been shown that the mode of UVA-induced cell death in human fibroblasts shifts from apoptosis to necrosis at high doses of UVA [159], whereas human keratinocytes are able to resist both modes of death [256]. It is thought that cell-type specific susceptibility to UVA-induced necrotic cell death in skin cells is directly correlative to the intracellular labile iron pool [261]. The differential response of epidermal keratinocytes and dermal fibroblasts to UVA may partially be explained by the keratinocytes having a lower basal and UVA-inducible labile iron level than the fibroblasts [261]. Also, unlike the fibroblasts, there is no significant decrease in UVA-mediated ATP depletion in keratinocytes [261], which is a hallmark of necrotic cell death [262].

Project Objective and Aims

Objective

The broad project objective is to elucidate the protective effects of ferulic acid, in combination with vitamins C and E, on UVA-irradiated human keratinocytes and fibroblasts.

Aims

Aim 1: Determine the optimal concentration of ferulic acid for human keratinocytes (HaCaT cells) and human/ mouse fibroblasts (primary human fibroblasts and murine 3T3 cells).

Aim 2: Quantify the amount of ROS produced following UVA-irradiation and subsequently determine the lipid peroxidation status in human keratinocytes (HaCaT cells) and fibroblasts (primary human fibroblasts).

Aim 3: To establish whether treatment was able to attenuate cell death, and if not, identify the mode of cell death in human keratinocytes (HaCaT cells) and fibroblasts (primary human fibroblasts). Proteins specific to the mode of cell death in fibroblasts would then be assessed.

Hypothesis

The pre-treatment of human epidermal keratinocytes and dermal fibroblasts with the antioxidant combination of ferulic acid, vitamin C and vitamin E will confer protection against UVA-mediated photodamage.

Chapter 2: Materials and Methods

2.1 Cell Culture

2.1.1 General Maintenance

A spontaneously transformed human keratinocyte cell line (HaCaT, a gift from Dr. N. Fusenig, Heidelberg, Germany) represented epidermal cells, while primary human dermal fibroblasts (courtesy of Ms. Ingrid Baumgarten, Department of Chemical Pathology, UCT) and an immortalized mouse embryonic fibroblast cell line (NIH/3T3 cells, ATCC number CRL1658) represented dermal cells in all experiments. (Murine 3T3s were initially incorporated into this study as the availability of primary human fibroblasts was uncertain. Human fibroblasts were the preferential dermal representative, and once they became frequently available the 3T3s were excluded from experiments.)

All cells were aseptically maintained in Dulbecco's Modified Eagle's Medium (DMEM) (Highveld Biological Pty. Ltd., Johannesburg, South Africa), supplemented with 10% (v/v) heat inactivated Fetal Bovine Serum (Highveld Biological Pty. Ltd., Johannesburg, South Africa) and 1% penicillin (100 U) (Sigma, Schnelldorf, Germany)/ streptomycin (100 µg/ml) (Sigma, Schnelldorf, Germany), at 37°C in a humidified 5% CO_2 atmosphere.

Cells were checked daily for any morphological changes, and tested for mycoplasma contamination fortnightly (Appendix B). To passage cells, media was removed and cells were rinsed once with 1X phosphate-buffered saline (1X PBS) (Appendix A), before being incubated in a trypsin (0.05%)/ ethylenediaminetetraacetic acid (EDTA) (0.02%) solution (Appendix A) for 5 min at 37°C. HaCaT cells received treatment with 0.05% EDTA (Appendix A) for 10 min at 37°C prior to trypsinization. All primary human fibroblasts used never exceeded passage 9 for all experiments.

2.1.2 Phase Contrast Microscopy

Cell were seeded onto coverslips (22x22 mm, Marienfeld, Lauda-Konigshofen, Germany) in 35 mm^2 dishes, and grown until approximately 90% confluent. Cells were treated according to the experimental setup (Chapter 2, Subsection 2.2.2). Following irradiation complete DMEM was added and cells were allowed to recover for 30 min. Medium was removed and cells were rinsed with 1X PBS before being placed in a 4% paraformaldehyde solution (Appendix A) for 15 min. The coverslips were rinsed with 1X PBS and mounted onto a slide (Marienfeld, Lauda-Konigshofen, Germany) using mounting fluid (Appendix A). Slides were viewed on the Zeiss Axiovert 200M fluorescent microscope, and images were taken using a monochrome Zeiss high resolution camera (Axiocam HR). Images were analysed using Zeiss Axiovision software (version 4.8).

2.2 Experimental Design

2.2.1 Irradiation Conditions

In all experiments cells were irradiated with 22.3 J/cm^2 UVA, provided by F15W/T8 PUVA lamps (Waldmann, Germany), determined by the following formula (where I is a measure of irradiance and T is time):

$$T\ (min) = \frac{Dose\ (mJ/cm^2)/0.06}{I\ (\mu W/\ cm^2)}$$

The wavelength emitted was between 315-400 nm (UVA), with an emission maximum of 365 nm. This formula was used to calculate the total time needed to deliver a dosage that was equivalent to 30 min in the midday South African sun. A time of 2 h 12 min, equivalent to 22.3 J/cm^2, was determined.

2.2.2 Experimental setup

The standard experimental setup included all the following controls (figure 2.1):

I. control (vehicle[1] only)
II. control- sham[2] (vehicle only)
III. FA only- sham
IV. FA + vEC[3]- sham
V. FA + vEC + UVA
VI. FA only + UVA
VII. vEC only + UVA
VIII. UVA only

[1.] Vehicle was <1% absolute ethanol for all samples

[2.] Sham irradiation involved placing the experimental dishes under aluminium foil to prevent any resultant changes due to the UV exposure.

[3.] 35 μM Vitamin E (1% (v/v)) and 50 μM Vitamin C (10% (v/v)) (Appendix A) were used in all experiments.

The treatment regime is summarised in figure 2.1. Briefly all cells were incubated with the various treatments for 18 h at 37°C in a 5% CO_2 atmosphere, before being rinsed once with 1X PBS and exposed to UVA. Cells were either harvested immediately or allowed to recover in complete DMEM for 2, 4, 12 or 24 h at 37°C in a 5% CO_2 atmosphere, before being analysed.

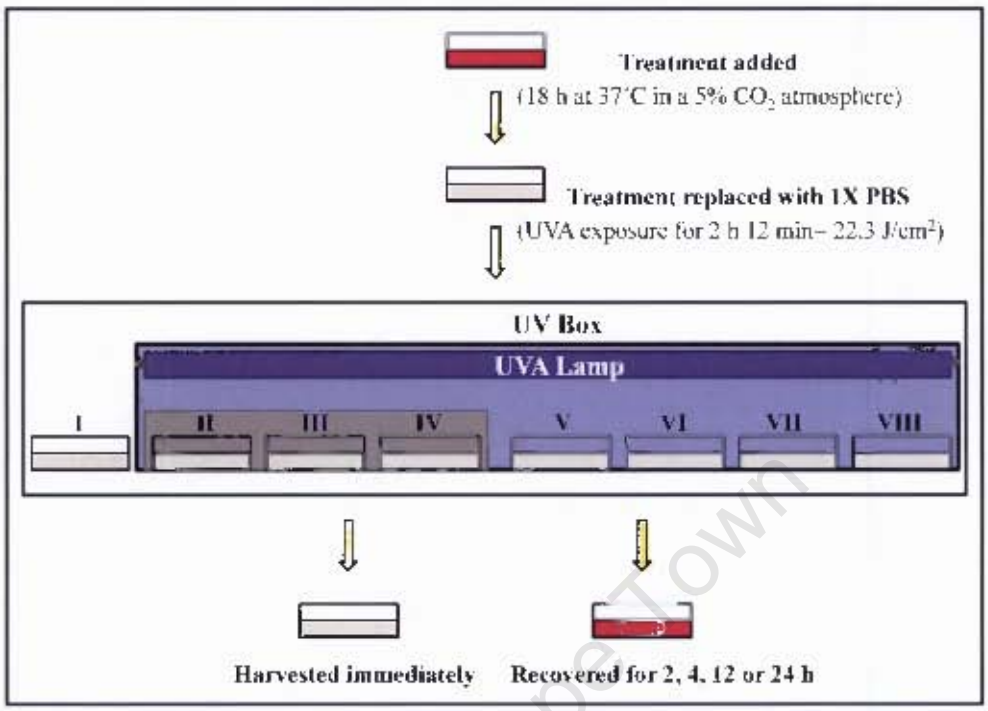

Figure 2.1 Experimental design. Cells were incubated with the various treatments for 18 h at 37°C in a 5% CO_2 atmosphere before being exposed to 22.3 J/cm^2 of UVA. Specific sham irradiated controls were maintained throughout all experiments. Cells were either harvested immediately or allowed to recover in complete DMEM for specified time points.

2.3 Cell Viability Assay

Cell viability was assessed using the XTT assay (XTT Cell Proliferation Kit II, Roche, Germany). The principle of the assay is based on the ability of metabolically active cells to reduce the yellow XTT tetrazolium salt to an orange-coloured, water-soluble formazan product. The amount of product is directly proportional to mitochondrial metabolism (i.e. cell viability) and can be quantified by assessing the absorbance at 450 nm.

2.3.1 Cell Preparation

Cells were cultured in 100 mm^2 dishes until approximately 90% confluent. They were then trypsinized and seeded into 96-well tissue culture plates (Cellstar®, Greiner Bio-One, Frickenhausen, Germany) at the following densities: $3x10^4$ cells/ well for primary

fibroblasts; $2.5x10^4$ cells/ well for 3T3 cells; and $5x10^4$ cells/ well for HaCaT cells. Cell numbers were determined through manual counting by means of a haemocytometer (Neubauer improved bright-line, Marienfeld, Lauda-Konigshofen, Germany) (Appendix B) and allowed to adhere to the wells for 24 h.

2.3.2 Determining the Optimal Concentration of FA

To determine the optimal concentration of FA (Appendix A for stock solution) that generated the least amount of cytotoxicity, cells were treated with the following concentrations: 0.2 mM, 0.4 mM, 0.8 mM, 1.5 mM or 3 mM in complete medium. The final volume in all wells was 200 µl, and cells were incubated for 18 h at 37°C in a 5% CO_2 atmosphere. The XTT reagent was prepared (Appendix A) and 50 µl was added directly to each well and incubated for 4 h at 37°C. Following incubation the absorbance was measured at 450 nm using a multi-well reader (VERSAmax™ tunable microplate reader, Molecular Devices, Sunnyvale, CA, USA; Software: Softmax Pro version 4.3.1) and results were calculated by determining the percentage viability relative to the control (vehicle only).

2.3.3 Cell Viability Following UVA exposure

To determine the effects of the various treatments on cell viability, cells were allowed to adhere for 24 h, before being exposed to treatment. Cells were incubated with the various treatments for 18 h at 37°C before being exposed to 22.3 J/cm^2 UVA. Post-irradiation cells were incubated with XTT reagent for 4 h at 37°C. The absorbance was then measured at 450 nm using a multi-well reader and results were calculated by determining the percentage viability relative to the control (vehicle only).

2.4 Flow Cytometry

Flow cytometry, which made use of a fluorescence-activated cell sorting (FACS) system, was used to quantify intracellular ROS and to determine the mode of cell death. The instrument used for this study was the Becton Dickinson FACS Calibur (Division of Immunology, UCT), which made use of a blue (488 nm) argon laser. Individual cells are

suspended in a narrow stream of fluid and passed through one or more laser beams that cause light to scatter and fluorescent dyes to emit light at different frequencies. Briefly, this system identifies cells by analysing forward and side scatter while fluorescent labelling is used to investigate cell structure and function. Fluorescence signals are accumulated in one to several channels relating to different laser excitation and fluorescence emission wavelength. In this study, forward and side scatter were measured in linear mode, while the fluorescent channels were measured using a logarithmic amplification scale. Green emitted fluorescence (Dihydrorhodamine 123 and Annexin V-FITC) was measured in fluorescence channel FL1 (530 nm), while red emitted fluorescence (propidium iodide) was measured in fluorescence channel FL3 (675 nm). All data generated were analysed using CellQuest Pro software (version 5.2.1).

2.4.1 ROS Assay

In order to quantify the amount of intracellular ROS produced, Dihydrorhodamine 123 (DHR 123) (Molecular Probes®, Eugene, OR, USA) (Appendix A for stock solution), a fluorogenic substrate, which becomes oxidised from non-fluorescent, uncharged DHR 123 to fluorescent, cationic rhodamine 123, was used.

Cells were seeded onto 35 mm^2 dishes and allowed to adhere overnight. Medium was changed every alternate day until the cells reached 90% confluence. Cells were then exposed to treatment according to the experimental treatment regime (Chapter 2, subsection 2.2.2), to a final volume of 2 ml. Following irradiation, 1 ml of fresh complete medium containing DHR 123 (0.1 mg/ml) was added to each dish, and cells were incubated for 30 min at 37°C. After the incubation period, media was collected and any non-adherent cells were harvested through centrifugation at 2500 rpm for 5 min (Hermle Z233 MK-2, HERMLE Labortechnik GmbH, Wehingen, Germany) at room temperature. The adherent cells were washed once with 1X PBS, removed by trypsinization and pooled with the non-adherent cells. Eppendorf tubes containing entire cell populations were centrifuged at 3500 rpm for 5 min at room temperature, the supernatants discarded and the cells washed once with 1X PBS. Cells were resuspended in 500 µl of fresh 1X PBS, transferred to 5 ml FACS tubes (BD Falcon tubes,

BD Biosciences, Becton Dickinson International, Erembodegem, Belgium) and analysed immediately by flow cytometry.

The fluorescent DHR 123 was detected in FL1 and the results from 10000 events were plotted in a histogram. The mean fluorescence of the entire population (M1) was determined and analysed as a percentage relative to the control. An example of the histogram output can be seen in figure 2.2.

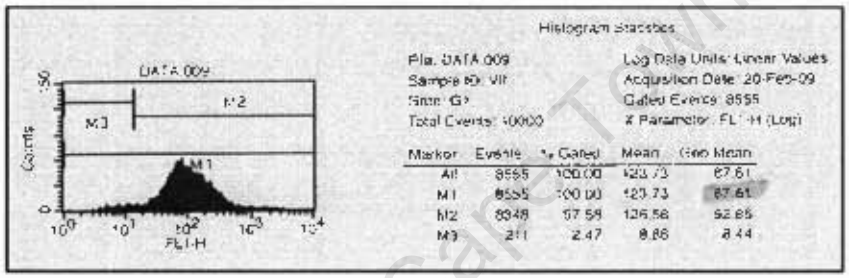

Figure 2.2 Dihydrorhodamine 123 was detected in the fluorescent channel FL1 (530 nm). The mean of the entire cell population (M1) was used to determine an increase or decrease in intracellular ROS. Plots were generated using CellQuest Pro software.

2.4.2 Mode of Cell Death Assay

Cell membrane phosphatidylserine (PS) translocation is a marker of early apoptosis and can be visualised through the use of the Ca^{2+}-dependent phospolipid binding protein Annexin V. When Annexin V is conjugated to the fluorogenic substrate fluorescein isothiocyanate (FITC), early apoptosis is able to be detected.

Propidium iodide (PI) is a vital dye that stains DNA and is excluded by viable or early apoptotic cells with intact plasma membranes. Thus it is only able to penetrate dying or dead cells where the membrane integrity has been compromised and is used as a marker for late apoptosis/ necrosis.

To analyse cell death, cells were seeded into 35 mm^2 dishes and grown to approximately 90% confluence. Treatment was conducted according to the experimental setup, and cells were allowed to recover for the stipulated time points (Chapter 2, subsection 2.2.2). Following the recovery periods, suspended and adherent cells were pooled, washed once with cold 1X PBS and resuspended in 100 µl cold 1X binding buffer. Cells were incubated with 5 µl Annexin V and 10 µl PI (50 µg/ml) (Appendix A) for 15 min at room temperature in the dark before a further 400 µl 1X binding buffer was added to the cells. The samples were transferred to 5 ml FACS tubes and immediately underwent flow cytometric analysis.

Annexin V was detected in FL1 and plotted on the x-axis, while PI was detected in FL3 and plotted on the y-axis. The cells populations were displayed in quadrants, such that the lower left (LL) quadrant represented the viable population (Annexin V and PI negative), the lower right (LR) represented early apoptotic cells (Annexin V positive), the upper right (UR) represented late apoptotic cells (Annexin V and PI positive) and the upper left (UL) quadrant represented necrotic cells (Annexin V negative and PI positive). The data was expressed as percentages of cells (per 10000 events read) present in each quadrant. An example of the dot plots generated by the CellQuest Pro software is shown in figure 2.3.

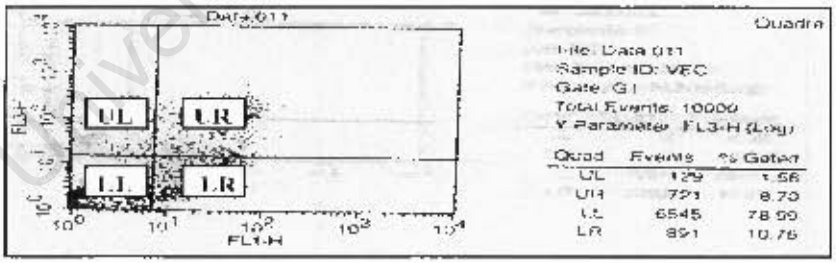

Figure 2.3 Dot plot generated from FACS analysis of cells stained with Annexin V and propidium iodide. Annexin V was detected in FL1 (530 nm) and propidium iodide in FL3 (675 nm). Plots were generated using CellQuest Pro software.

2.5 Lipid Peroxidation Analyses

2.5.1 Cell Preparation

Cells were seeded in 100 mm^2 dishes and grown to approximately 90% confluence. Treatment was added according to the experimental setup (Chapter 2, subsection 2.2.2). Cells were collected immediately following irradiation, by centrifuging any suspended cells at 2500 rpm for 5 min at room temperature, and by directly scraping cells from the dishes using a rubber policeman. Cells were then re-suspended in 1ml 1X PBS placed into a 50 ml falcon tube on ice and sonicated (MSE Soniprep 150, Wolf Laboratories Limited, Pocklington, York, UK) for two 15 sec pulses at 12 amplitude microns.

2.5.2 Folch Extraction

Lipids were extracted from sonicated cells according to the Folch extraction protocol [263]. Briefly, methanol (2500 µl) was added to 1 ml of sonicated cells (in 1X PBS) and vortexed for 10 sec, followed by the addition of 1250 µl of chloroform. The mixture was vortexed for 10 sec and centrifuged at 3000 rpm for 15 min (Eppendorf Centrifuge 5810R, Hamburg, Germany). The supernatant was transferred to a new borosilicate glass tube (Kimble/ Kontes, Vineland, NJ, USA), lipids were re-extracted from the remaining cell pellet and the supernatants combined. A 1:1 ratio of 0.9% saline (Appendix A) was added to the chloroform, mixed by inversion, and centrifuged at 3000 rpm for 15 min. The infranate was transferred, using a drawn-out pipette, to a new borosilicate tube before being dried down by nitrogen gassing (approximately 45 min). The borosilicate tube used in the final step was weighed before and after the lipid had been added, in order to determine the percentage of lipid peroxides relative to the total amount of lipid.

2.5.3 TBARS Assay

The TBARS assay was performed according to Asakawa and Matsushita (1980) [264]. Briefly, dried lipids were re-suspended in 25 µl of chloroform, while water and chloroform were used as controls. To 25 µl of sample, 25 µl $FeCl_3$ (0.27%) (Appendix A), 25 µl of butylated hydroxytoluene (BHT) (0.22% in ethanol) (Appendix A), 375 µl glycine buffer (0.2 M

glycine.HCl) (Appendix A) and 375 µl thiobarbituric acid (TBA) (Appendix A) was added, vortexed vigorously and heated at 100°C for 20 min. After heating, 250 µl glacial acetic acid was added, followed by 500 µl chloroform. Samples were vortexed vigorously and centrifuged at 3000 rpm for 15 min. The supernatant (300 µl) was placed in duplicate in a 96-well plate and absorbance was measured at 532 nm.

The molar extinction co-efficient for 300 µl supernatant (1.40 X $10^5 M^{-1}.cm^{-1}$) was used to calculate the amount of TBARS per total lipid (µmol/mg) using the following formula (where A is absorbance):

$$\frac{A532\text{-blank}}{0.14\ (\mu mol)} \div \text{lipid (mg)}$$

2.5.4 Conjugated Diene Assay

Samples were prepared as above (sections 5.2.1 and 5.2.2). Dried lipids were re-suspended in 1 ml cyclohexane and vortexed for 1 min. Samples (300 µl) were placed in triplicate in a 96-well plate and absorbance was measured at 234 nm.

The molar extinction co-efficient for 1 ml of cyclohexane (2.95 X $10^4 M^{-1}.cm^{-1}$) was used to calculate the amount of conjugated dienes per total lipid (µmol/mg) using the following formula (where A is absorbance):

$$\frac{A234\text{-blank}}{0.0295\ (\mu mol)} \div \text{lipid (mg)}$$

2.6 Protein Expression

2.6.1 Cell Preparation

Cells were seeded in 100 mm^2 dishes and grown to approximately 90% confluence. Treatment was added according to the experimental setup, and cells were allowed to recover for the stipulated time points (Chapter 2, subsection 2.2.2).

2.6.2 Protein Extraction

At the specified times (Chapter 2, subsection 2.2.2) dishes were washed twice with cold 1X PBS and lysed in 150 µl cold complete RIPA extraction buffer (Appendix A). In all cases cells that had lifted during treatment were collected (by centrifugation at 2500 rpm for 5 min at room temperature) and pooled with their respective dishes. Cell lysates were collected and placed at -80°C for 1 h to decrease DNA contamination. Samples were centrifuged at 12000 rpm for 20 min at 4°C. The supernatant was divided into two aliquots (to minimise freeze/ thawing) and were stored at -80°C until use. For the duration of the experiments samples were freeze/ thawed a maximum of three times each.

2.6.3 Protein Quantification

Total protein was quantified using the BCA Protein Assay kit (Thermo Scientific, Pierce, Rockford, IL, USA). This kit is based on the purple-coloured, water-soluble reaction product that is generated by the chelation of two bicinchonicic acid (BCA) with one cuprous ion. The protein concentrations are determined by measuring absorbance at 562 nm and plotting the unknown values against a standard curve generated by known concentrations.

Fresh protein standards were prepared for all protein quantifications. A bovine serum albumin (BSA) working stock (2 mg/ml) was made up in 0.9% saline (Appendix A) and placed in duplicate in a 96-well plate on ice, representing standards concentrations of 0-2000 µg/ml. These readings would later be used to generate a standard curve from which the unknown concentrations of protein could be determined.

To quantify the extracted protein, 5 µl of sample was placed in duplicate in a 96-well plate on ice. Samples were diluted 5X by adding 20 µl of incomplete RIPA reagent. Working reagent was prepared (Appendix A) and 200 µl was added to each well, followed by 30 min incubation at 37°C. Following incubation, absorbance was measured at 562 nm using a multiwell-plate reader. The absorbance values were then read off the standard curve, generated from the BSA standard readings, to obtain accurate protein concentrations reported as µg/ml.

2.6.4 Western Blotting

For western blot analyses, quantified samples were prepared for sodium-dodecyl-sulphate polyacrylamide gel electrophoresis (SDS-PAGE). A 15% resolving layer was overlaid with a 5% stacking layer (Appendix A), in an Enduro Vertical Electrophoresis System (Labnet, Labnet International, Inc., Woodbridge, NJ, USA). Protein samples were diluted to a final concentration of 40 µg using incomplete RIPA buffer. Loading dye (Appendix A) was added (5 µl) and samples were denatured for 2 min at 100°C. Five micro litres of protein marker (peqGOLD protein marker IV, PEQLAB Biotechnologie GmbH, Erlangen, Germany) was loaded into the first well to serve as a molecular weight control and approximately 25 µl of sample was loaded into individual wells before the apparatus was submerged in fresh tank buffer (Appendix A). Proteins were electrophoresed at 80-100 V.

Following electrophoresis, proteins were transferred to a nitrocellulose membrane (Amersham Hybond-ECL, GE Healthcare) at 100 V for 1 h in fresh, cold transfer buffer (Appendix A). Membranes were then briefly washed in TBS-T (Appendix A), before being blocked in 5% fat-free milk (Appendix A) for 1 h at room temperature. Membranes were subsequently incubated with primary antibodies overnight at 4°C. Table 2.1 lists the antibodies and their respective concentrations.

Table 2.1 Concentrations of primary and secondary antibodies used in this study.

Primary antibody	Concentration	Secondary antibody	Concentration
Bcl-2 (Cat: Bcl-2 (100): sc-509 mouse monoclonal, Santa Cruz Biotechnology, Inc., Santa Cruz, CA, USA)	1:200 in 5% fat-free milk	Goat anti-mouse (Horseradish peroxidase conjugated Cat: 170-6516, Bio-Rad, Hercules, CA, USA)	1:1500 in 5% fat-free milk
Bax (Cat : Bax (B-9): sc-7480 mouse monoclonal, Santa Cruz Biotechnology, Inc., Santa Cruz, CA, USA)	1:200 in 5% fat-free milk	Goat anti-mouse (Horseradish peroxidase conjugated Cat: 170-6516, Bio-Rad, Hercules, CA, USA)	1:1500 in 5% fat-free milk
p38 (Cat: p-38 MAP Kinase: MO800 rabbit polyclonal, Sigma, Schnelldorf, Germany)	1:5000 in TBS-T	Goat anti-rabbit (Horseradish peroxidase conjugated Cat: 170-6515, Bio-Rad, Hercules, CA, USA)	1:5000 in 5% fat-free milk

Following overnight incubation, membranes were washed twice for 10 min in TBS-T, before being incubated with their respective secondary antibody in 5% fat-free milk for 1 h at room temperature. Membranes were rinsed twice for 10 min in TBS-T, prior to the addition of the chemiluminescent substrate (SuperSignal® West Pico Chemiluminescent Substrate, Thermo Scientific) for 1 min, and then exposed to medical x-ray film (CP-BU new film, AGFA) for various exposure times. Films were developed (AGFA Developer) (Appendix A) and fixed (Ilford Rapid Fixer) (Appendix A), for 2 min each, before being rinsed in fresh water.

2.6.5 Densitometry

To quantify protein expression, densitometric analysis (semi-quantitative) was performed by scanning films into the computer (CanonScan 8000F), and utilising functions in the Image J software program (version 1.42q). Values obtained for each lane were divided by the protein loading control (p38) in order to standardise results.

2.7 Data Analysis

Data are shown as means ± SD. Differences between test and control conditions were assessed by performing unpaired, two-tailed t-Tests (Microsoft Office Excel 2007) and differences with value of $p < 0.05$ were considered as significant.

Chapter 3: Results and Discussion

The results presented in this chapter are aligned with the aims stipulated in Chapter 1. The first aim was to determine the optimal concentration of FA for keratinocytes and fibroblasts. Once this was established, the effect of the FA vEC combination on UVA-induced ROS and the resulting consequence on lipid peroxidation was investigated. The next aim examined whether the FA vEC combination could protect UVA-exposed cells from cell death, and if not determine the mode of cell death employed. Once the mode of cell death was specified, the expression of related proteins was examined. The table below illustrates how the cell types will be represented throughout Chapter 3 (table 3.1).

Table 3.1 Representation of cell types throughout this study.

Cell Type	Name Seen in Text	Colour Representation
Human keratinocytes	**HaCaTs**	Blue
Primary human dermal fibroblasts	**HFbs**	Purple
Murine fibroblasts	**3T3s**	

3.1 Aim 1

3.1.1 Determining the Optimal Concentration of FA

The first aim was to identify the optimal concentration of FA for human keratinocytes (HaCaT cells) and human/ mouse fibroblasts (primary human dermal fibroblasts and 3T3 cells). This was determined through the use of a cell viability assay (Chapter 2, subsection 2.3.2).

The addition of FA to HaCaTs resulted in a significant dose-dependent increase from 100% viability (vehicle only) to 179.77±32.13% with the addition of 3 mM FA ($p<0.05$) (figure 3.1). The doubling time of normal HaCaTs has been shown to be 42 h [265], and as the XTT assay measures viability over a total of 24 h, this increase may be explained by either i) the fact FA directly increased the proliferation rate, or ii) based on the XTT assay being a

marker of mitochondrial activity, it could have increased the metabolic activity of the cells. These findings were in contrast to previous studies that examined other plant polyphenols such as (-)-epigallocatechin-3-gallate (EGCG) [266], apigenin [267] and curcumin [268], which all demonstrated an anti-proliferative effect in human keratinocytes [269]. Despite 0.8 mM diverging from the control (0.8 mM FA: 130.38±4.63% vs. Control: 100%) (figure 3.1), with the ultimate future aim of using FA in a full-thickness skin model, and additional previous work performed in our laboratory on the protective effects of 0.8 mM FA vEC combination on melanocytes, this concentration was selected for the HaCaTs.

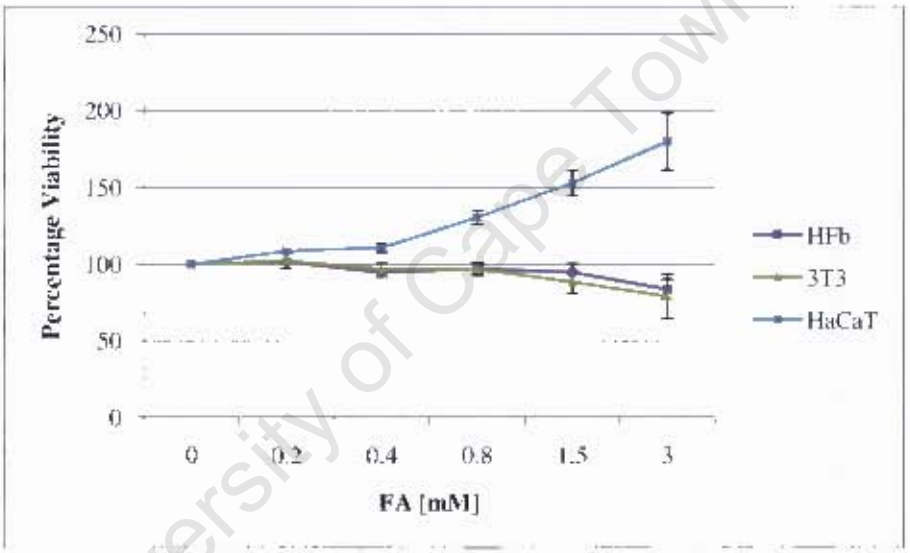

Figure 3.1 Graphic representation of the cell viability assay to determine the optimal concentration of ferulic acid in human keratinocytes (HaCaT cells), human fibroblasts (HFbs) and murine fibroblasts (3T3 cells). Values are expressed as a percentage of the control and data are presented as mean ± SD, n=3.

With regards to the HFbs, the addition of FA displayed no potential proliferative effect, considering the doubling time is 17 to 24 h [270, 271]. Furthermore, in contrast to the HaCaTs, the addition of 3 mM FA led to a slight reduction in cell viability (figure 3.1). Previous studies have shown the addition of certain antioxidants are able to exhibit a proliferative effect in HFbs, as was seen in work performed by Pinnell *et al.* (1994) through the addition

of 0.1 mM vitamin C [272]. The addition of 0.8 mM FA to both 3T3 and human fibroblasts resulted in no significant decrease in cell viability, and thus, in keeping with the HaCaTs, 0.8 mM was selected as a standard concentration for all future experiments.

Whilst 0.8 mM FA proved the optimal concentration for this study (figure 3.1), FA concentrations utilised in other studies range widely. Trombino *et al.* (2004) illustrated that low concentrations of FA (0-50 μM) exhibited a wide range of antioxidant activities in 3T3 cells and microsomal membranes [197], whilst other studies have shown the concentrations of FA required for 50% inhibition (IC_{50}) of the DPPH radical, superoxide and hydroxyl radicals in solution are approximately 45.3 μM, 5312.3 μM and 502.1 μM respectively [202]. For the purposes of this study, FA was to be used in combination with vitamins C and E, although the mechanism of FA's stabilizing effect on these vitamins remains unknown [209]. What is known, is that the redox potential of FA is considerably higher than vitamins C and E (0.595 vs. 0.282 and 0.48 respectively) [273] and it is not believed to directly protect them, but to preferentially interact with pro-oxidative intermediates or serve as a sacrificial substrate [209]. These studies lend further support to the use of 0.8 mM FA, the maximum concentration with the minimum amount of damage.

3.1.2 Effect of Treatment on Cell Morphology

To determine if the various treatments were having an effect on cell morphology, both HaCaTs and HFbs were studied 30 min post irradiation by phase contrast microscopy. In the HaCaTs there was little notable difference between control, FA vEC treated and UV-only cells (figure 3.2). The HaCaTs maintained their characteristic polyhedral shape [274], and did not display any noticeable form of cell surface blebbing or shrinkage at low and higher magnifications (figure 3.2).

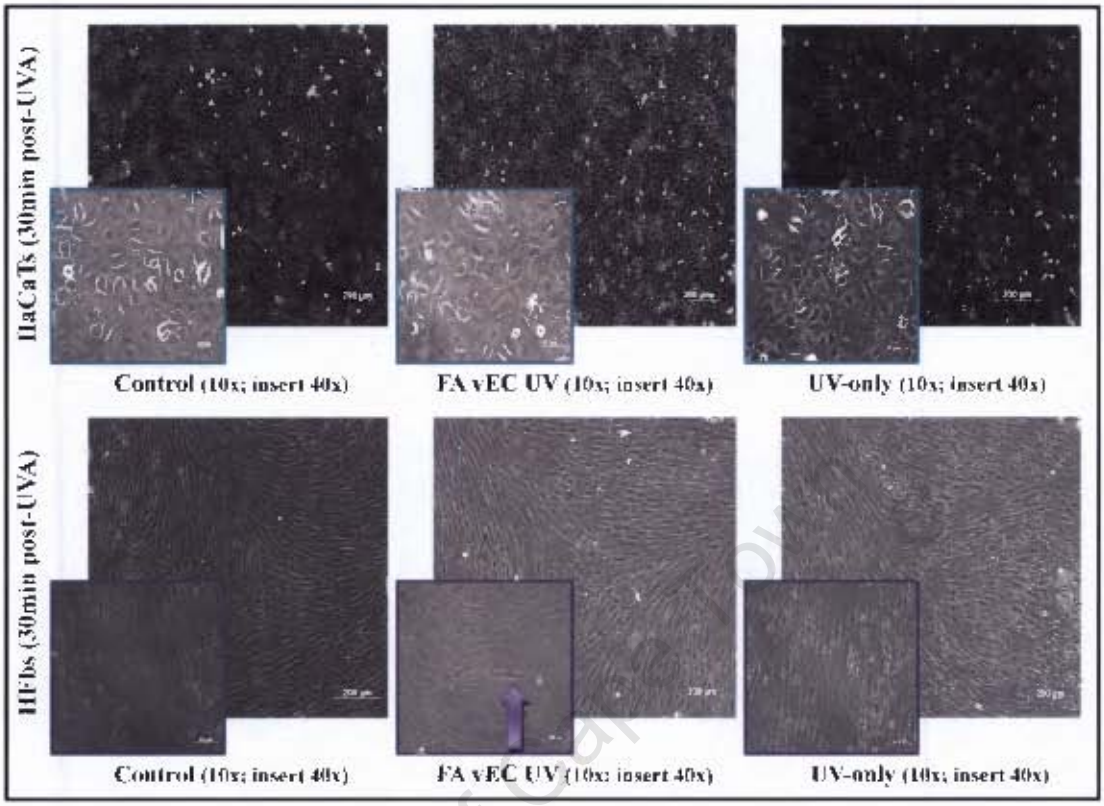

Figure 3.2 Phase contrast images depicting the morphological changes induced by UVA radiation. HaCaTs and HFbs 30 min post-UVA irradiation (main image: 10x, scale bar: 200 μm; insert: 40x, scale bar: 50 μm).

In contrast, the UV-only HFbs displayed some cell shrinkage and rounding when compared to the control cells (figure 3.2). The UV-only cells appeared less elongated and differed from the ordered, spindle-shaped fibroblasts seen in the control and FA vEC pre-treated cells (arrow, figure 3.2). Pre-treatment with the FA vEC combination appeared to maintain cell morphology similar to control cells.

As questions have been raised about whether basal, endogenous cellular antioxidant levels differ with age in fibroblasts, it was pertinent to consider this point in this study. However, a recent report unequivocally showed that the age of the fibroblast donor does not affect the basal antioxidant activity or cell survival after UVA-induced stress [275] thus making our

source of fibroblasts (young donors), a feasible model. Noteworthy however are the findings of Kim *et al.* (2005) who showed the doubling time of fibroblasts (from a 10 yr old donor) were drastically affected by passage number, with fibroblasts at passage 8 have a doubling time of <24 h and fibroblasts at passage 28 have a doubling time of >55 h [270]. In light of these findings, our primary cultures were only ever grown to passage 9.

3.2 Aim 2

The second aim was to quantify the amount of intracellular ROS produced following UVA-irradiation and subsequently determine the lipid peroxidation status, in human keratinocytes (HaCaT cells) and fibroblasts (primary human dermal fibroblasts).

3.2.1 Quantification of Intracellular ROS

The fluorescent probe DHR 123 was used to quantify UVA-induced ROS production, and results were determined by FACS analysis (figure 3.3).

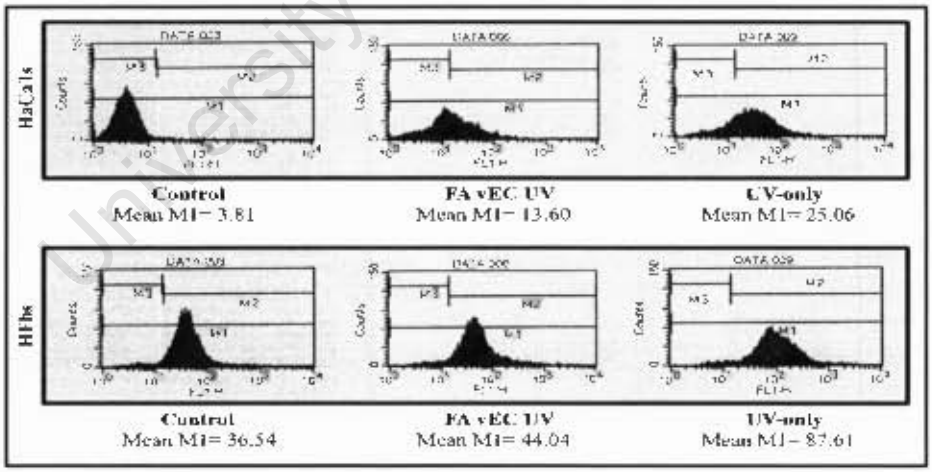

Figure 3.3 Representation of histograms generated from intracellular ROS analysis, using DHR 123, following UVA exposure in HaCaTs and HFbs. The mean fluorescence (M1) is determined from 10000 cells in each treatment group. This figure represents HaCaTs and HFbs 24 h post-irradiation, sample groups shown include control, FA vEC treated and UV-only cells.

In this study, exposure of HaCaTs to 22.3 J/cm^2 UVA led to a significant increase in the amount of intracellular ROS compared to the control (UV-only: 19.01±7.79 vs. Control: 6.33±1.88, $p<0.05$) (figure 3.4). This result correlates to work performed by Shorrocks *et al.* (2007), who demonstrated that high doses of UVA (1000 and 2000 J/cm^2) was able to generate an increase in intracellular ROS in HaCaTs [83]. The apparent reduction in ROS observed in HaCaTs pre-treated with the FA vEC combination appears to be solely due to the antioxidant activities of the vitamins. This finding correlates with work done by Pinnell *et al.* (2003) who showed that while the individual vitamins were able to confer photoprotection, the combination was far superior [213]. They reported the combination of vitamin C (15%) and vitamin E (1%) was able to decrease sunburn cell formation (apoptotic keratinocytes), and provide a four-fold photoprotective effect, in porcine skin exposed to solar-stimulated radiation [213]. However, Pinnell *et al.* (2004, 2005) showed the addition of 0.5% FA to their vEC solution was able to double the photoprotective effect [208, 209], which is not the effect observed in this *in vitro* study (figure 3.4). Although FA displays radical scavenging effects in antioxidant assay systems, where it is able to efficiently scavenge DPPH [199, 200, 201], superoxide and hydroxyl radicals [202], it appeared to have no effect on intracellular ROS levels in HaCaTs, compared to UV-only cells. This may be explained by FA reacting differently in HaCaT cells compared to *in vivo* [208, 209] or antioxidant assay systems [200, 202].

In HFbs, 22.3 J/cm^2 UVA appeared to lead to an increase in intracellular ROS in UV-only cells compared to control cells (UV-only: 68.82±59.89 vs. Control: 27.39±7.08) (figure 3.4). This observation was in accordance with a previous study by Polte and Tyrrell (2004) that showed the high UVA dose of 2500 J/cm^2 led to an increase in intracellular peroxides in human dermal fibroblasts [113]. Whilst the dose used by Polte and Tyrrell (2004) was exceptionally high, a lower dose of 10 J/cm^2 UVA has also been shown to adversely affect human dermal fibroblasts by increasing singlet oxygen [276]. Oplander *et al.* (2008) further demonstrated that whilst exposure to 25 J/cm^2 UVA was able to increase intracellular superoxide in primary human dermal fibroblasts, the addition of 1 mM vitamin C was able to completely abrogate this effect [277]. The present study examined the effect of 22.3 J/cm^2 UVA on primary human dermal fibroblasts, and although a lower concentration of vitamin

C was used (50 μM), the synergistic interaction with vitamin E and FA [209] lead to an apparent decrease in intracellular ROS compared to the UV-only cells (FA vEC: 21.99±15.9 vs. UV-only: 68.82±59.89) (figure 3.4).

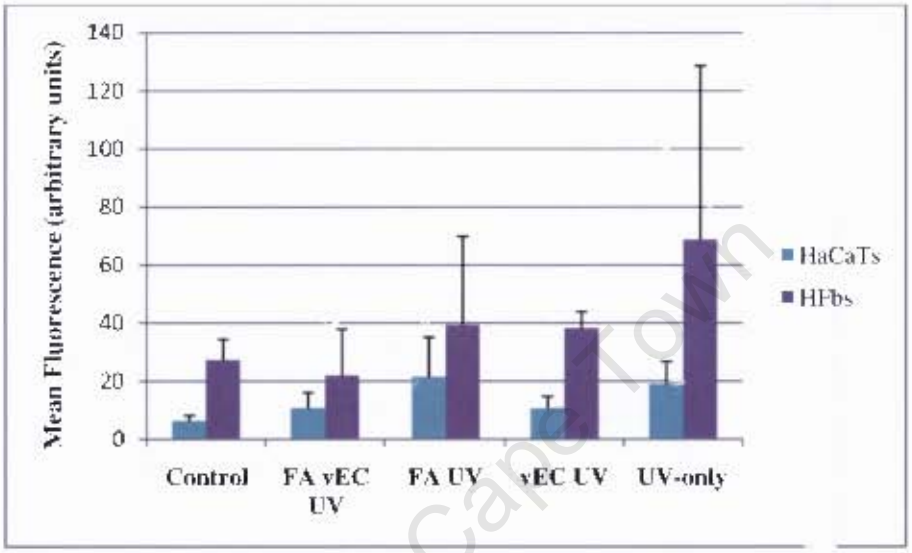

Figure 3.4 Graphic representation of the mean fluorescence of UVA-induced ROS in HaCaTs and HFbs. Data are presented as mean ± SD, n=4.

Polte and Tyrrell (2004) examined the involvement of lipid peroxidation in UVA-induced MMP-1 expression in human fibroblasts [113]. Their sham irradiation control for UVA-induced ROS was in accordance with the data in this study, in that the sham irradiated samples illustrated a slight increase in ROS (figure 3.4). This may be a result of an increase in temperature, or being incubated in 1X PBS for approximately 2 h. The lengthy irradiation time is a considerably long period for cells to be in such a stressful environment. Work performed by Shorrocks *et al.* (2007) altered their UVA dose rate (between 1000-3000 J/cm^2) to ensure their irradiation time did not exceed 3 h, as they were concerned over a loss of viability due to prolonged periods in PBS [83]. They also kept their irradiation temperatures constant (either 4 or 37°C). Mahn *et al.* (2003) showed that it is more suitable to irradiate cells in 1X PBS than in medium such as DMEM which contains riboflavin and tryptophan/ HEPES, as these components led to an increase in hydrogen peroxide upon

exposure to UVA [278]. They also showed that phenol red acts as an UVA absorber rather than a photosensitizer, and this is also not optimal in irradiation experiments [278]. In conclusion, simple buffers such as PBS are ideal solutions for irradiation experiments, provided irradiation time is kept to a minimum.

3.2.2 Effects on Lipid Peroxidation

The generation of UVA-induced ROS in skin cells is well documented [83, 276, 277]. Reactive oxygen species produced as a result of UVA exposure results in an increase in lipid peroxidation in both human keratinocytes [83, 111] and fibroblasts [65, 112]. To study the effect of the FA vEC antioxidant combination on lipid peroxidation in HaCaTs and HFbs, levels of conjugated dienes and TBARS were assayed for, being indicators of mid and late stage peroxidation respectively (Chapter 1, figure 1.4).

In this study we found a negligible change in the levels of diene conjugation in HaCaTs exposed to 22.3 J/cm^2 UVA (UV-only vs. control, figure 3.5). These findings were similar to those established by Punnonen *et al.* (1991), who showed that when human keratinocytes were exposed to 2.5 and 15 J/cm^2 UVA there was little change in the amount of conjugated dienes [111]. Interestingly, in our study the trend observed in conjugated diene levels throughout all the treatment groups follows the trend established in the ROS assay (figure 3.4). Furthermore it is evident that pre-treatment of HaCaTs with vEC leads to a substantial decrease in the amount of conjugated dienes compared to UV-only cells (vEC: 1.09±0.03 μmol/mg lipid vs. UV-only: 1.77±0.66 μmol/mg lipid) (figure 3.5), which was in agreement with the effect of vEC pre-treatment on UVA-induced ROS production (figure 3.4). This illustrates that the vitamins may be protecting against increasing ROS levels, and subsequent lipid peroxidation. However, their involvement in the lipid peroxidation process still remains to be determined, as the TBARS assay showed the vitamins had little effect on the on the level of TBARS (figure 3.5). This was in contrast to the effect of FA on TBARS levels, which appeared to exacerbate the harmful effect of UVA (FA: 2.39±2.62 μmol/mg lipid vs. UV-only: 0.84±0.34 μmol/mg lipid). This detrimental effect displayed by FA pre-treatment was correlative to the ROS data (figure 3.5). It is

evident that the FA pre-treatment is having no photoprotective effect (when compared to the UV-only cells). One possibility may be that the FA is initially able to benefit the cells, yet the ferulate radicals generated through the antioxidant activity of FA may ultimately be having a negative effect. However this situation is unlikely as phenoxy radicals generated are highly stable as the unpaired electron may be positioned on the oxygen, or delocalized across the entire molecule [194]. Previous work has shown FA to exhibit antioxidant effects at concentrations of less than 50 µM, which is substantially lower than the 0.8 mM used in this study. This should be considered as although 0.8 mM FA displayed no cytotoxic effects in the HaCaTs (figure 3.1), the concentration may be too high in terms of antioxidant activities, as it is known that when the concentration of certain phenolic compounds is too high, a pro-oxidative effect is observed [279].

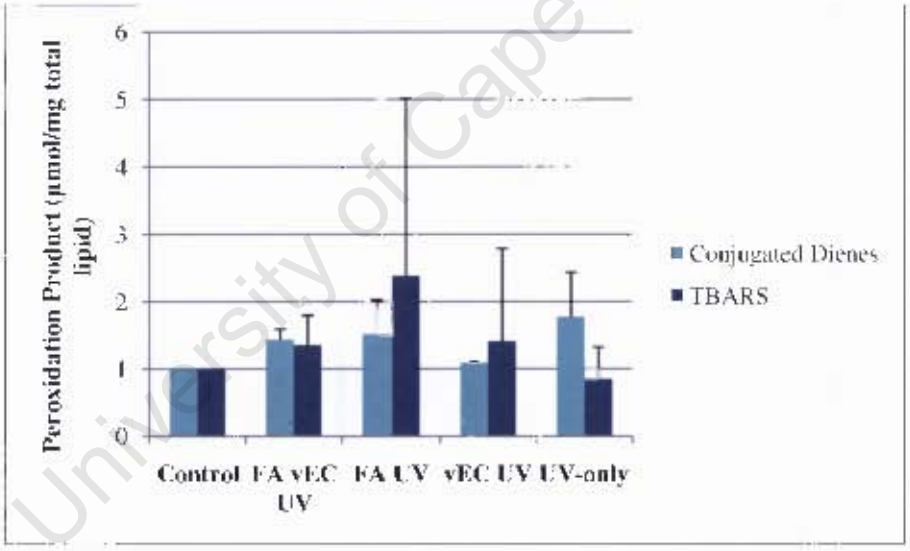

Figure 3.5 Quantification of the amount of conjugated dienes and TBARS in HaCaTs, expressed in µmol/mg lipid. Light blue: conjugated dienes, dark blue: TBARS. Values are relative to the control and data are presented as mean ± SD, n=2.

In addition to the FA pre-treated cells having the highest amount of TBARS compared to all groups, the UV-only cells displayed the lowest amount (figure 3.5), which was in direct contrast to the findings of Punnonen *et al.* (1991), who noted a significant increase in their

human keratinocyte cell line at UVA doses lower than that used in this study (2.5 and 15 J/cm^2 vs. 22.3 J/cm^2) [111]. This may be explained by the fact that their study utilised a different keratinocyte cell line (NCTC 2544), which may be more susceptible to UVA-induced peroxidation than the HaCaT keratinocytes used in this study.

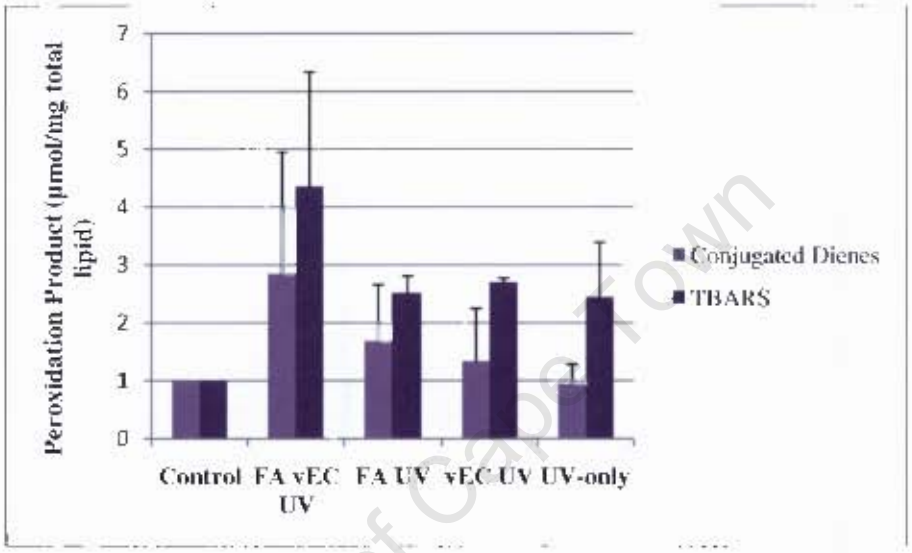

Figure 3.6 Quantification of the amount of conjugated dienes and TBARS in HFbs, expressed in µmol/mg lipid. Light purple: conjugated dienes, dark purple: TBARS. Values are relative to the control and data are presented as mean ± SD, n=2.

In HFbs, FA vEC pre-treated cells displayed a higher level of diene conjugation, whilst the lowest levels were observed in the UV-only group (figure 3.6). The addition of the FA vEC combination similarly led to the highest levels of TBARS compared to all other groups (figure 3.6). This illustrates that the antioxidant combination had no effect, possibly a detrimental one if any, on mid- and late-stage lipid peroxidation in the HFbs. The fact that there was no significant increase in TBARS in the UV-only cells was in contrast to work performed by Morliere *et al.* (1995), who demonstrated a dose-dependent increase in TBARS in human dermal fibroblasts exposed to 0-1440 J/cm^2 UVA [62]. Whilst no difference in TBARS levels was observed between the control, UV-only and FA-treated groups in this study, there was a significant increase in the amount of TBARS in cells pre-treated with

vEC compared to control cells (vEC: 2.7±0.07 μmol/mg lipid vs. Control: 1 μmol/mg lipid, $p<0.05$) (figure 3.6). This finding was in direct contrast to the effect of the vitamins in HaCaTs (Figure 3.5), indicating that the effects of antioxidant pre-treatment is cell type specific. Further lipid peroxidation analysis in both HaCaTs and HFbs is required to determine definitive results.

In previous studies, FA has been shown to lower the amount of conjugated dienes and reduce MDA formation induced by the pro-oxidants 2,2'-Azobis-(2-amidinopropane) (AAPH) and *tert*-butyl hydroperoxide (*tert*-BOOH) in rat liver microsomal membranes [197]. Although the conjugated diene and TBARS assays have been successfully employed in some studies looking at UV-induced lipid peroxidation in human keratinocytes and fibroblasts [65, 111, 112], these assays are more suitable for systems where large amounts of lipids are being analysed. The amount of total lipid obtained from a near confluent 10 cm^2 dish, which ranged between 0.2 and 2 mg (data not shown), was insufficient to provide a feasible trend in this particular study. This was most likely due to lipid lost during the extraction procedure. An alternate approach could be to detect lipid peroxidation end-products such as MDA by a more sensitive detection method such as high-performance liquid chromatography (HPLC) [197]. Shorrocks *et al.* (2007) made use of a colourimetric kit that reacted directly with lipid peroxidation end products MDA and 4-HNE [83] while Calabrese *et al.* (2008), who studied the effect of a naturally occurring ester of FA (ferulic acid ethyl ester) on lipid peroxidation in human dermal fibroblasts, analysed levels of 4-HNE by western blot analysis [156]. What these highlight is that there is no 'gold standard' method for measuring lipid peroxidation and for any study a combination of techniques would be needed to yield conclusive results.

Whilst ability of FA to inhibit lipid peroxidation is well documented [197, 198, 199, 280], the exact mechanism of action has yet to be elucidated. Castelluccio *et al.* (1996) examined whether FA exhibited its antioxidant activity from the aqueous or lipophilic phase by studying the preferential cellular localisation of a radiolabelled form of FA [280]. The majority associated with the albumin-rich fraction of plasma, whilst a portion also partitioned between the low-

density lipoprotein (LDL) and the aqueous phase. The FA isolated from the LDL-particle was shown not to associate with the lipid portion, indicating that FA exerts its antioxidant activity from the aqueous phase [280]. Trombino *et al.* (2004) demonstrated that whilst the combination of FA and vitamin C interact synergistically, the combination of FA and α-tocopherol appear to act antagonistically with regards to lipid peroxidation [197]. The combination of FA with vitamin C strongly inhibited MDA formation in rat liver microsomal membranes, as detected by HPLC. This combination was highly efficient and displayed activity at low concentrations of 5 μM for both antioxidants. Moreover, it was shown that while vitamin C protected FA from AAPH-induced depletion, vitamin E enhanced it [197]. Despite this discrepancy, the synergistic interaction between 15% vitamin C and 1% vitamin E has been shown to have a photoprotective effect against solar-stimulated radiation in porcine skin [213], and was further shown to be enhanced through the addition of 0.5% FA [208, 209]. This may be due to FA acting as a sacrificial substrate, or perhaps the amount of vitamin C is sufficient to simultaneously reduce the rate of FA consumption and recycle vitamin E. Although FA is able to absorb UV radiation [192], and this absorption is theoretically able to provide a sunscreen effect, work performed by Pinnell *et al.* (2005) shows that increasing the volume of antioxidant solution during treatment demonstrated no dose-response effect to support the sunscreen mechanism [209]. It is most likely having a photoprotective effect through its antioxidant activity.

3.3 Aim 3

The third aim of this study was to firstly establish whether pre-treatment could protect against cell death, and if not, determine the mode of death employed by human keratinocytes (HaCaTs) and fibroblasts (primary human dermal fibroblasts). Proteins specific to the mode of cell death in the HFbs would then be assessed by western blot analysis.

3.3.1 Effect of Treatments on Cell Viability

Zhong *et al.* (2004) found that HaCaTs exposed to 2500 and 5000 J/cm^2 UVA were extremely resistant to both apoptosis and necrosis [261]. This dose was substantially higher

than the 22.3 J/cm^2 UVA used in this study and expectedly there was no significant difference in cell viability between UV-only and control cells (figure 3.7). Furthermore, pre-treatment with FA or vEC, individually or in combination, did not have any effect on cell viability (figure 3.7). This result once again illustrated the refractory nature of the HaCaTs to UVA exposure. In 3T3s there was a significant decrease in viability in the UV-only cells compared to the control (UV-only: 50.02±1.78% vs. Control: 100%, $p<0.05$) (Figure 3.7). Pre-treatment of 3T3s with FA and vEC, individually or in combination, had no effect on cell viability compared to UV-only cells (figure 3.7).

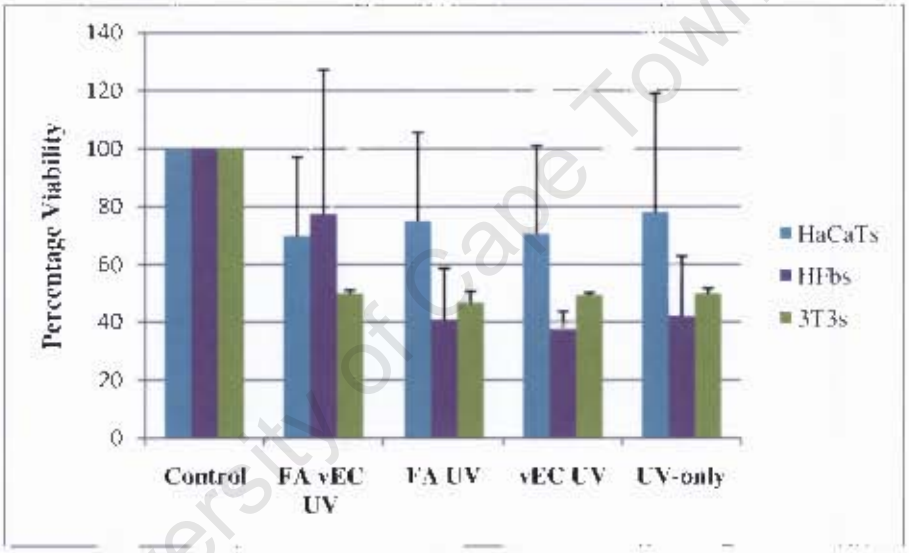

Figure 3.7 Cell viability following treatment in HaCaTs, 3T3s and HFbs. Values are expressed as a percentage of the control and data are presented as mean ± SD, n=3.

In contrast to the HaCaTs and 3T3s, the HFbs displayed a significant decrease in viability in the UV-only cells compared to the control (UV-only: 41.88±21.1% vs. Control: 100%, $p<0.05$) (Figure 3.7). Hazane *et al.* (2006) showed a decrease in human skin fibroblast viability following UVA exposure by means of the related MTT cell viability assay [275]. Their study correlated directly to the results currently observed, and reported a decrease in viability from 5 J/cm^2 UVA, with a viable population of approximately 50% at 10 J/cm^2 and 20% at 20 J/cm^2 [275]. The addition of FA or vEC had no effect on viability compared to the

UV-only cells; however, although cells treated with the FA vEC combination did not have a significantly larger viable population compared to UV-only, the combination pre-treatment was able to maintain a viable population comparable to that of control cells (FA vEC: 77.4±40.87% vs. Control: 100%) (figure 3.7). This result was in agreement with the data obtained in this study pertaining to UVA-induced ROS (figure 3.4), suggesting that in HFbs the reduction of intracellular ROS may protect against cell death. This conservation of cell viability was in line with previous studies performed on human fibroblasts transiently transfected with inducible thioredoxin [163]. These cells were subjected to the MTT cell viability assay, and showed that thioredoxin was able to decrease intracellular ROS levels (at 10 J/cm^2 UVA) and fully protect the cells from a decrease in viability (12 J/cm^2 UVA) [163]. These findings are encouraging, suggesting the possibility of supplementary antioxidants as feasible adjuvant photoprotective agents.

Unlike the protective effect demonstrated in HFbs, pre-treatment with FA vEC did not protect against cell death in the HaCaTs and 3T3s, illustrating that cellular response to treatment and UV exposure is cell type/ species specific. Keratinocytes are the most superficial cells of the human body, and are the first line of defence against environmental stressors such as UVA (Chapter 1, subsection 1.1.1). Bernerd *et al.* (1998) illustrated that UVA effects are targeted to the dermis [224]. They studied the effect of 25 and 30 J/cm^2 UVA on *in vitro* reconstructed skin. Regarding the induction of cell death, the keratinocytes were not affected by UVA, while the superficial dermal fibroblasts (obtained from a 16 yr old breast tissue donor) were drastically altered, suggesting a differential cell type sensitivity to UVA radiation [224]. Numerous studies concerned with the UVA-induced oxidative stress response have determined that fibroblasts offered less resistance than keratinocytes [281, 282]. In addition, keratinocytes express constitutively high levels of heme oxygenase-2 and ferritin [281, 283], which play a vital part in the defence response to oxidative stress [152] and may confer additional resistance to keratinocytes exposed to UVA. Furthermore, Zhong *et al.* (2004) demonstrated that the high levels of resistance against UVA-induced damage in human keratinocytes, including HaCaTs, may be due to low basal and UVA-inducible levels of labile iron [261]. They showed the free and UVA-induced labile iron pool in human keratinocytes is lower than that of human fibroblasts, and suggested this may

contribute to the resistance against cell death observed in keratinocytes. Intracellular ATP-depletion is considered a hallmark of necrotic cell death [262] and Zhong *et al.* (2004) further showed that there was no significant UVA-mediated ATP depletion in the keratinocytes, in contrast to the fibroblasts, which is hypothesised to further protect them from cell death [261].

3.3.2 The Mode of Cell Death

The results obtained from the XTT cell viability assay (figure 3.7) prompted the investigation into the mode of cell death by which the human keratinocytes and fibroblasts were dying. This was to be determined through Annexin V/ propidium iodide staining (figure 3.8).

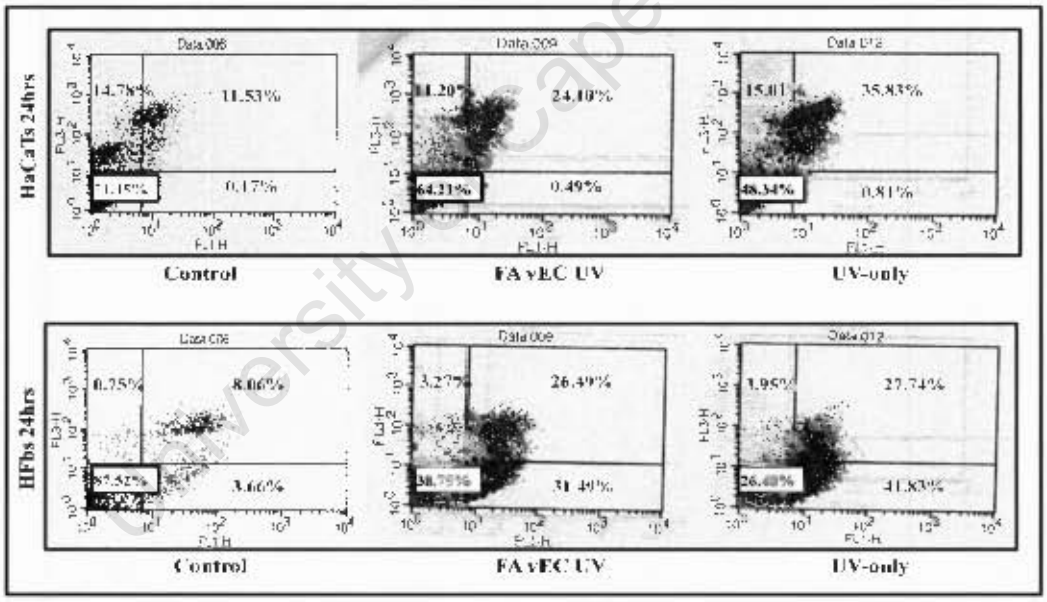

Figure 3.8 Representation of dot-plots generated from FACS analysis, using Annexin V/ propidium iodide staining to determine the mode of cell death. This figure represents HaCaTs and HFbs 24 h post-irradiation, sample groups shown include control, FA vEC treated and UV-only cells.

Two hours post-irradiation, HaCaTs pre-treated with FA alone or in combination with vEC had a significantly larger viable population than the control group (FA: 64.55±3.3% and FA vEC: 61.34±3.75% vs. Control: 44.25±5.96%, $p<0.05$) (figure 3.9). There was no difference between any of the early apoptotic populations between groups, however FA vEC pre-treated and UV-only cells had significantly larger populations of cells undergoing late apoptosis compared to control cells (FA vEC: 25.69±3.98% and UV-only: 26.82±1.71% vs. Control: 19.6±2.52%, $p<0.05$). The necrotic population of all UV-exposed cells was significantly smaller, than that of the control cells (UV-only: 10.39±3.99% vs. Control: 38.42±3.95%, $p<0.05$). The fact that the control HaCaTs, which are vehicle-only, sham irradiated cells, have a larger necrotic population than all UV-exposed groups may be due to the lengthy 2 h 12 min irradiation time. As indicated previously (Chapter 3, subsection 3.2.1) this is a long time for cells to be incubated in PBS. Although not addressed in this study, a suggestion to reduce irradiation time would relate to increasing the spectral power output, which would require a more powerful UV-emitting device than the one utilised in this study.

Despite all UV-exposed HaCaTs having a significantly smaller necrotic population than the control cells 2 h post-irradiation, at 4 h there was no variation in the any of the populations across all groups (figure 3.9). The protective effect of vEC in the HaCaTs that was previously observed to lower UVA-induced ROS (figure 3.4) and the amount of diene conjugation (figure 3.5) did not appear to have an effect on cell viability 4 h post-irradiation (figure 3.9).This indicates that the vEC may confer protection early on following UVA exposure, as ROS and conjugated diene are detected immediately post-irradiation. If the cells are continuously subjected to oxidative stress the vitamins may be depleted and cells may eventually die. The percentage of viable cells at the 4 h time point correlated to the XTT cell viability results (figure 3.7).

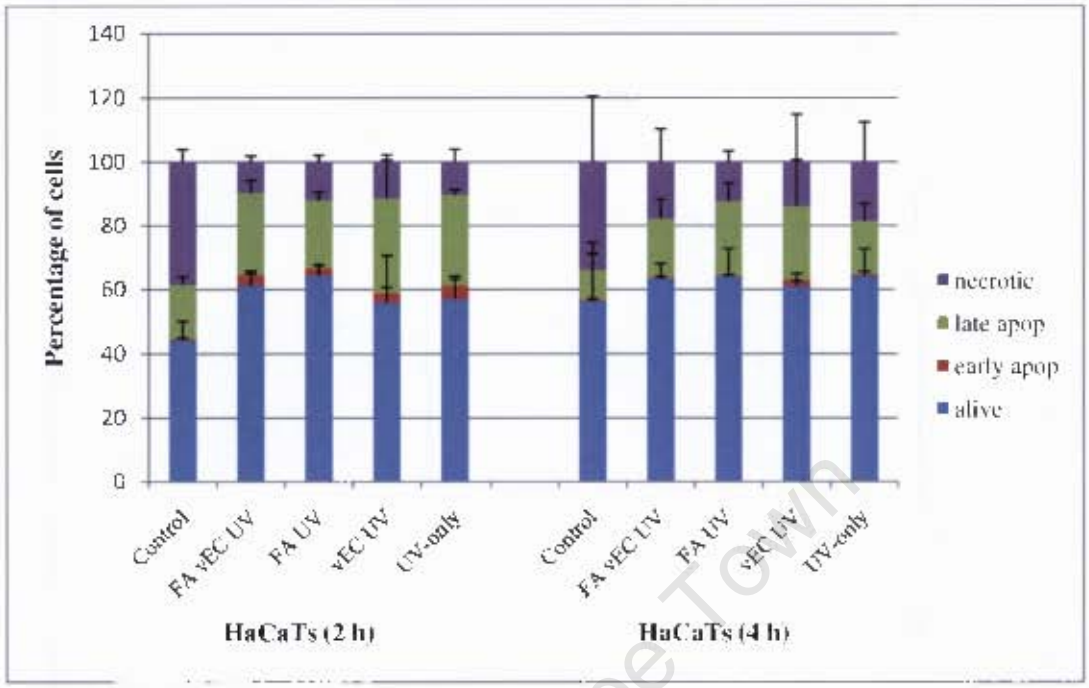

Figure 3.9 Graphic representation of the percentages of cells, sorted into the various modes of cell death, for HaCaTs at 2 h and 4 h post-irradiation as determined by Annexin V/ propidium iodide staining. Values are expressed as a percentage of the total cell population and data are presented as mean ± SD, n=3.

The same result determined at the 4 h time point was observed in HaCaTs at 12 h post-irradiation, in that there was no variation amongst populations in all groups (figure 3.10). In HaCaTs, 24 h post-irradiation, there was a significantly smaller viable population of UV-only cells than control cells (UV-only: 47.98±7.34% vs. Control: 73.11±1.71%, $p<0.05$) (figure 3.10), which was interesting considering Zhong *et al.* (2004) demonstrated that HaCaTs were extremely resistant to cell death at high doses of UVA (2500 and 5000 J/cm^2) [261]. Cells pre-treated with the FA vEC combination, as well as UV-only cells, had significantly higher populations of cells undergoing late apoptosis than the control cells (FA vEC: 32.96±8.08% and UV-only: 32.93±4.97% vs. Control: 14.95±3.39%, $p<0.05$). There was no significant difference between necrotic populations in the HaCaTs for all groups. Interestingly, control HaCaT cells significantly increased their viable population from 2 to 24 h (Control 2 h: 44.25±5.96% vs. Control 24 h: 73.11±1.71%, $p<0.05$), whilst

the viable population of the UV-only cells remained at a constant approximate 50%. The increase in the viable population of HaCaTs is interesting as their doubling time is approximately 42 h [265], yet the increase takes place within 24 h. One possibility that could explain this phenomenon may be that exposure to UVA may drive some cells into cell cycle arrest, as ROS are known to affect the cell cycle [284]. Whilst high doses of UVA (1500 J/cm^2) have been shown to have little effect on cell cycle progression [285], it can not be ruled out that a lower UVA dose (i.e. 22.3 J/cm^2) will have the same outcome. Treatment with FA or vEC, alone or in combination, did not affect cell viability from 2- 24 h. These data show the antioxidant treatments have no effect on cell viability, in accordance with the XTT cell viability data (figure 3.7), and the mode of cell death across 2- 24 h post-irradiation in human keratinocytes appears to be predominantly via apoptosis. Interestingly these results are in contrast to previous studies that have demonstrated the FA vEC combination is able to effectively reduce the number of sunburn cells (apoptotic keratinocytes) in porcine and human skin [208, 209, 210, 225, 286], as well as protect against caspase-3 and -7 activation in porcine skin [208, 209]. This discrepancy in results may be resolved by taking into account that our study was performed *in vitro*, whilst the experiments pertaining to porcine and human skin were *in vivo* studies. The fact that an immortalised keratinocyte cell line is utilised in this study must be considered, as cellular mechanisms may be slightly different to primary cells. Furthermore, cells *in vivo* are in contact with systems such as the neuro-endocrine and immune system [287] and these extrinsic factors must also be considered when comparing data.

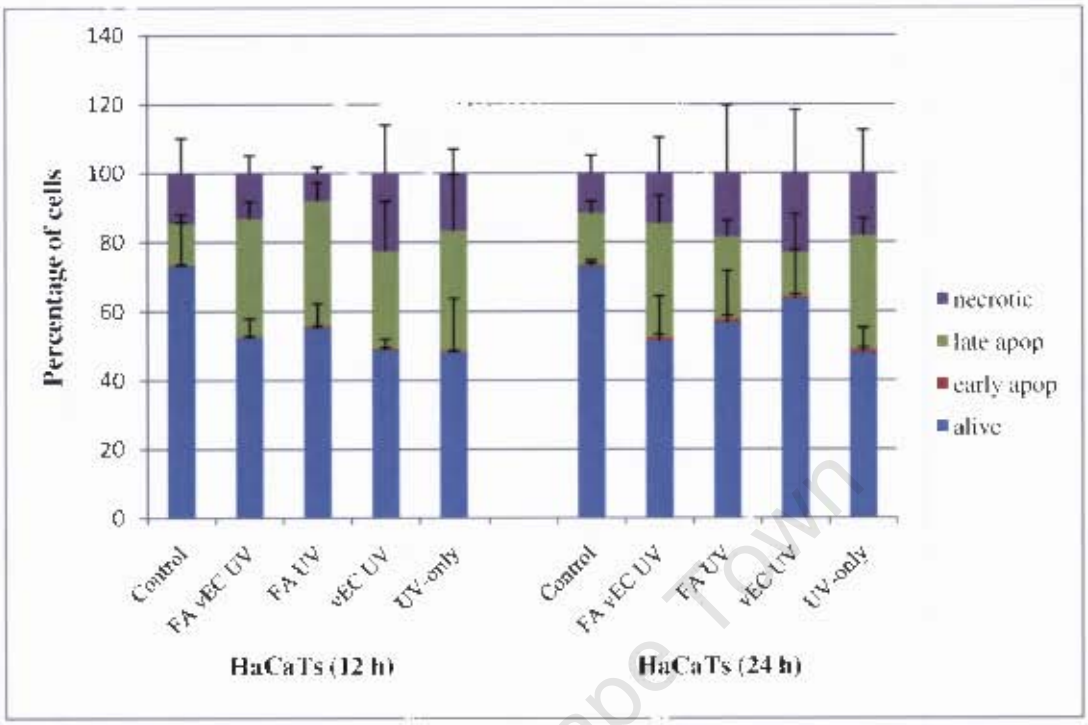

Figure 3.10 Graphic representation of the percentages of cells sorted into the various modes of cell death for HaCaTs 12 h and 24 h post-irradiation as determined by Annexin V/ propidium iodide staining. Values are expressed as a percentage of the total cell population and data are presented as mean ± SD, n=3.

In the HFbs, the 2 h time point showed no difference between viable, early apoptotic and late apoptotic populations in any of the groups of HFbs was observed (figure 3.11). It was observed that the UV-only necrotic population was significantly larger than the control cells (UV-only: 23.91±4.74% vs. Control: 5.14±2.22%, $p<0.05$). The same result was witnessed at 4 h post-irradiation, yet there was no difference between the necrotic populations of the control and UV-only cells (figure 3.11). Work performed by Didier *et al.* (2001) investigated the effect of UVA on normal human fibroblasts that were transiently transfected with an expression vector encoding human thioredoxin [163]. They found, through Annexin V/ propidium iodide staining, the thioredoxin was able to significantly reduce the number of Annexin V positive cells (apoptotic cells) 5 h post-irradiation with 5 and 10 J/cm^2 UVA. Furthermore, they noted that the mode of cell death shifted to necrosis at higher UVA

doses [163]. Zhong *et al.* (2004) demonstrated that necrosis was found to be the predominant mode of death in human dermal fibroblasts 4 h post irradiation[261]. However, the exceptionally high dose of UVA (1000, 2500 and 5000 J/cm^2) used in their study must be considered [261]. Bernerd *et al.* (1998) demonstrated the mode of cell death in human dermal fibroblasts, in *in vitro* reconstructed skin, that received 25 J/cm^2 UVA underwent apoptosis (6 h post-irradiation) [224]. In line with Bernerd *et al.* (1998), the dose of 22.3 J/cm^2 UVA used in this particular study clearly resulted in predominantly apoptotic cell death (figure 3.11). The XTT cell viability assay results (figure 3.7) were expected to correlate with the 4 h-post irradiation results obtained in this experiment, however the FA vEC combination failed to maintain the viable population at a level similar to that of the control (figure 3.11). This discrepancy emphasizes the importance of utilising multiple techniques to generate feasible results.

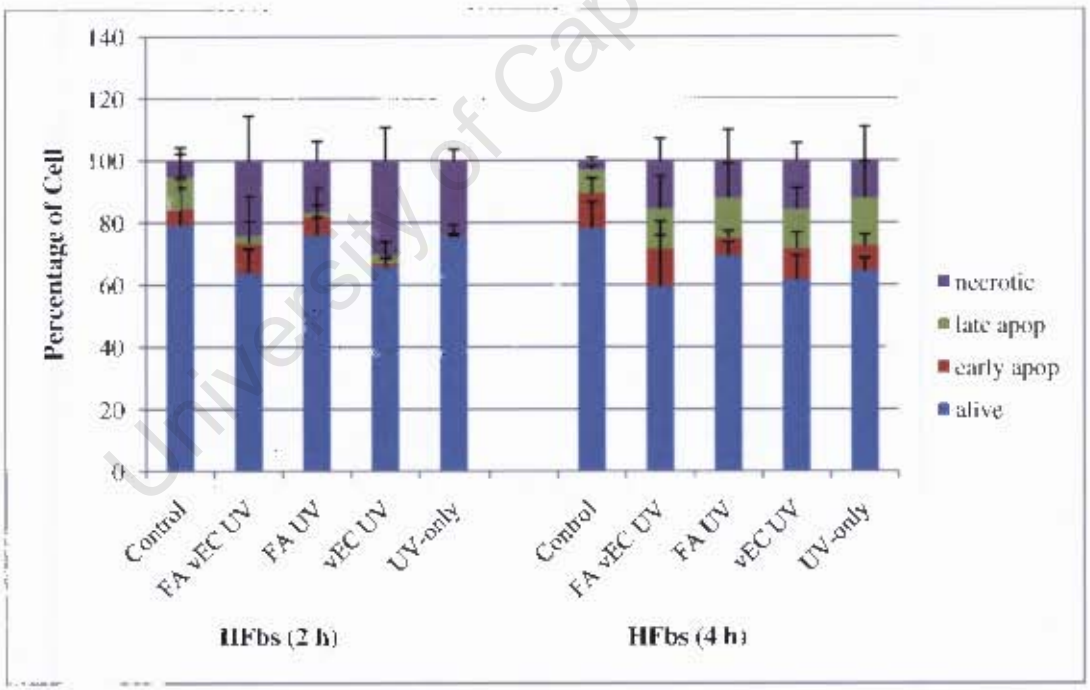

Figure 3.11 Graphic representation of the percentages of cells sorted into the various modes of cell death for HFbs at 2 h and 4 h post-irradiation as determined by Annexin V/ propidium iodide staining. Values are expressed as a percentage of the total cell population and data are presented as mean ± SD, n=3.

At the 12 h time point no variation in populations across all groups was detected, apart from the FA vEC, vEC and UV-only cells having significantly smaller viable populations than the control cells (FA vEC: 26.81±13.46%, vEC: 41.68±12.89%, UV-only: 42.12±16.28% vs. Control: 84.95±2.97%, $p<0.05$) (figure 3.12). This illustrates that the FA vEC and vEC pre-treatment is having no protective effect on cell viability at 12 h post-irradiation.

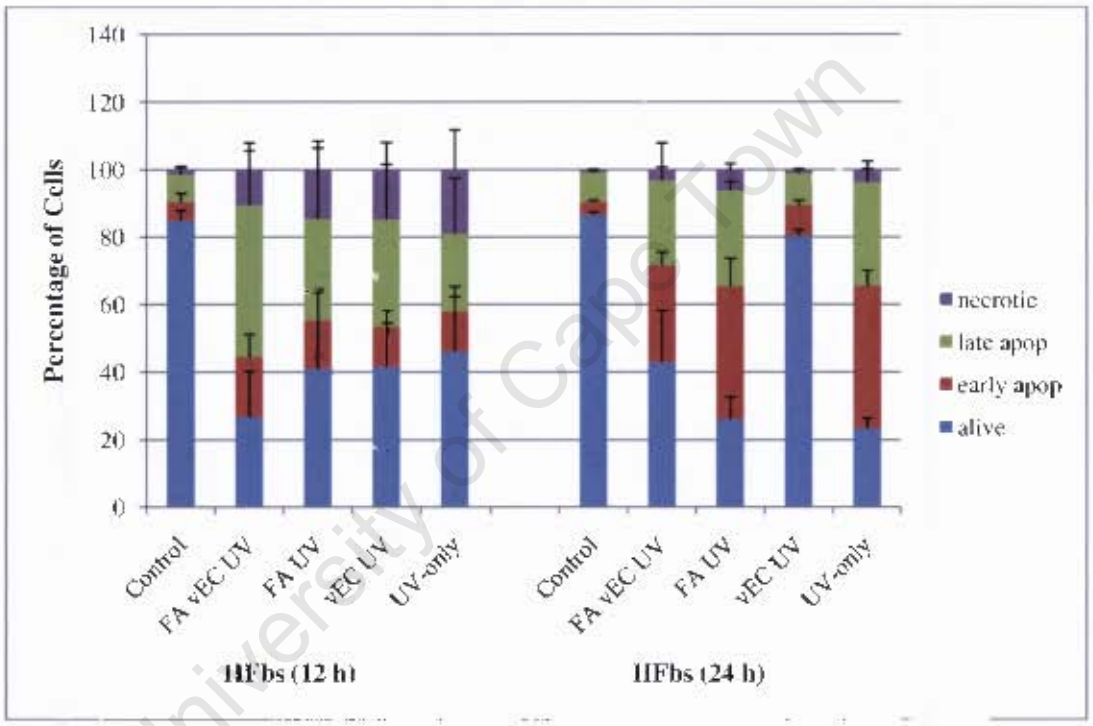

Figure 3.12 Graphic representation of the percentages of cells sorted into the various modes of cell death for HFbs at 12 h and 24 h post-irradiation as determined by Annexin V/ propidium iodide staining. Values are expressed as a percentage of the total cell population and data are presented as mean ± SD, n=3.

In the HFbs, all groups had significantly smaller viable populations than the control cells (UV-only: 23.37±3.02% vs. Control: 85.21±4.56%, $p<0.05$) at the 24 h time point (figure 3.12). Cells treated with FA, alone or in combination with vEC, as well as UV-only cells, had significantly smaller viable populations than cells pre-treated with vEC (UV-only:

23.37±3.02% vs. vEC: 80.38±1.83%, $p<0.05$). All UV-exposed groups had significantly larger populations of cells undergoing early apoptosis compared to control cells (UV-only: 42.2±4.5% vs. Control: 3.83±0.51%, $p<0.05$). Cells that received vEC pre-treatment had significantly less cells undergoing early apoptosis than FA pre-treated and UV-only cells (vEC: 9.07±1.47% vs. FA: 39.16±8.25% and UV-only: 42.2±4.5% $p<0.05$). The FA vEC combination treatment group also had significantly less cells undergoing early apoptosis than the UV-only cells (FA vEC: 28.59±3.97% vs. UV-only: 42.2±4.5%, $p<0.05$). HFbs that received FA pre-treatment, as well as the UV-only cells, had significantly higher populations of cells undergoing late apoptosis than all other groups (FA: 28.38±2.7% and UV-only: 30.73±6.25% vs. Control: 8.71±0.59%, $p<0.05$). All groups of HFbs had significantly higher numbers of cells undergoing necrosis than the control and vEC-pre-treated cells (UV-only: 3.71±0.26% vs. Control: 0.88±0.14% and vEC: 1.16±0.36%, $p<0.05$). Based on these results it appears that pre-treatment with vEC is able to afford some protection to HFbs against cell death at 24 h post-irradiation. At 2 h post-irradiation the mode of cell death in HFbs appears to be necrosis, however by 24 h post-irradiation the necrotic populations are negligible. At 24 h post-irradiation the necrotic fibroblast population observed at 2 h would no longer be detectable, and 24 h is sufficient to allow for the viable population to double [270, 271], which may explain the decrease in the necrotic population and increase in the viable population over 2-24 h. . It was determined that pre-treatment with FA vEC was able to decrease intracellular ROS (figure 3.4), which was detected immediately post-irradiation. This decrease in ROS did not correlate to any of the specified time points in the mode of death assay, showing that the FA vEC pre-treatment may afford initial antioxidant protection to HFbs, yet under conditions of persistent oxidative stress may not be sufficient to protect against UVA-induced cell death. However, the fact that the protective effect of the vitamins was observed 24 h post-irradiation shows that the beneficial effects of certain antioxidant pre-treatment may only be observed at later time point, and future studies should include an additional 48 h point to elucidate the true protective potential of the various treatments.

3.3.3 Apoptosis-Associated Protein Expression in HFbs

As it was clear that the HFbs displayed the most reactivity to UVA exposure and induction of cell death pathways after 24 h, a detailed analysis of the effect of treatments on cell death was undertaken. Furthermore, a time-dependent analysis (2-24 h) of apoptosis induced by UVA and subsequent protection by the addition of FA, individually and in combination with vEC, is lacking in literature. Two apoptosis-related proteins in HFbs were thus studied in an attempt to elucidate the cellular response to the various treatments in more detail. The Bcl-2 family of proteins, comprising both anti- and pro-apoptotic members, mediate the cellular 'life-or-death' switch by regulating MOMP [242, 243]. The family members Bcl-2 and Bax were selected as representatives of anti- and pro-apoptotic proteins respectively. The Bcl-2: Bax ratio is a well-known indicator of survival, with the value being inversely proportional to the level of apoptosis [288, 289, 290]. Amount of protein expression was determined by densitometry, and the ratio subsequently calculated (figure 3.13).

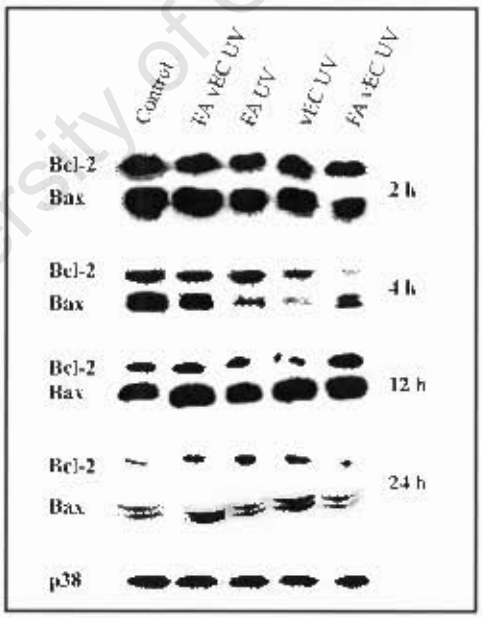

Figure 3.13 Panel of western blot analyses over 2-24 h of the apoptotic-associated proteins Bcl-2 and Bax. Bcl-2: 29 kDa, Bax: 23 kDa, p38: 38 kDa (n=2).

At the 2 h time point, there was no difference in the Bcl-2: Bax ratios in any of the treatment groups compared to the control cells (figure 3.14). Pre-treatment with FA and vEC, alone or in combination, appears to have no effect on the Bcl-2: Bax ratio, which may be explained by the fact that all UV-exposed groups are predominantly undergoing necrosis (figure 3.11), in which case the Bcl-2: Bax ratio would be rendered irrelevant.

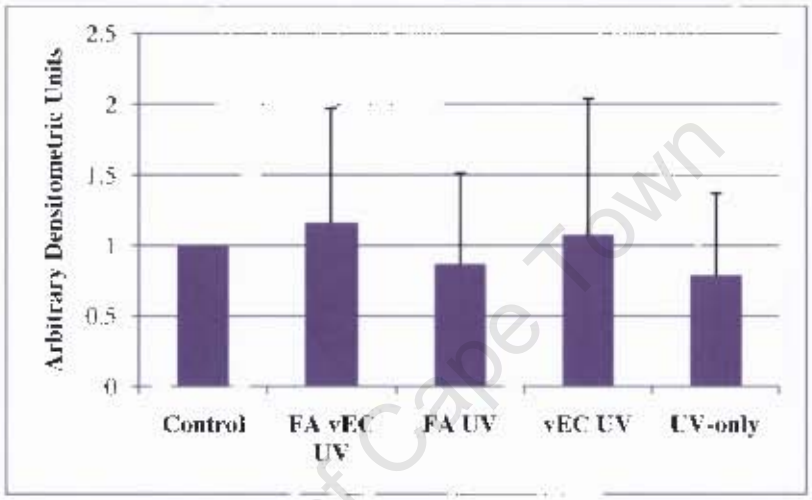

Figure 3.14 Bcl-2: Bax ratio determined in HFbs 2 h post-irradiation. Bcl-2 and Bax are anti- and pro-apoptotic proteins respectively. A ratio of >1 it is indicative of survival and <1 it is indicative of apoptosis. Values are relative to the control and data are presented as mean ± SD, n=2.

Following a 4 h recovery period there was a trend towards a lowered survival ratio in UV-only cells to the control (UV-only: 0.7±0.1 vs. Control: 1.14) (figure 3.14). This result correlates to the Annexin V/PI data that showed the UV-only cells had a smaller viable population compared to the control (figure 3.11), as well as the XTT viability assay performed 4 h post irradiation (figure 3.7). Interestingly the vEC pre-treated group had the highest Bcl-2: Bax ratio (vEC: 2.21±0.69), indicating the vitamins were working to prevent cell death. Although this effect did not correlate to the XTT assay (figure 3.7) or the FACS analysis of cell death (figure 3.11) at the 4 h time point , this effect was observed with the

FACS at 24 h post-irradiation (figure 3.12). Although the Bcl-2 was up-regulated around 4 h post-irradiation, its protective effect may have only been observed approximately 20 h later.

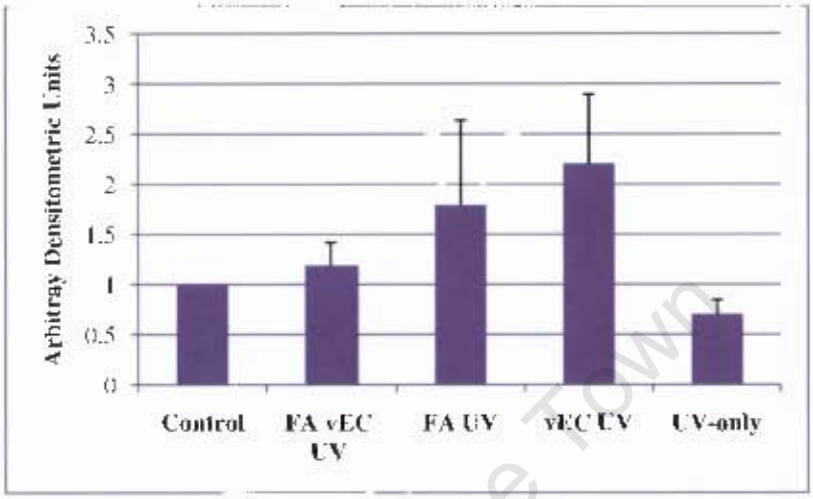

Figure 3.15 Bcl-2: Bax ratio determined in HFbs 4 h post-irradiation. Bcl-2 and Bax are anti- and pro-apoptotic proteins respectively. A ratio of >1 it is indicative of survival and <1 it is indicative of apoptosis. Values are relative to the control and data are presented as mean ± SD, n=2.

A study performed by Pourzand *et al.* (1997) demonstrated that at 4 h post-UVA exposure (2500 and 3000 J/cm^2), overexpression of Bcl-2 in R6 rat fibroblasts was able to inhibit apoptosis [291]. They further showed that Bcl-2 overexpression led to a significant decrease in HO-1 levels following 1000 J/cm^2 UVA exposure. They suggest that Bcl-2 prevents UVA-mediated apoptosis via suppression of the production or effects of ROS. They have further extrapolated that as the localisation of Bcl-2 is in the mitochondrial membrane, this may be the site of UVA-generated ROS involved in HO-1 activation and apoptosis [291]. These findings may indicate a dual purpose for the anti-apoptotic Bcl-2.

At the 12 h time point there was no significant difference in the Bcl-2: Bax ratio between any of the groups (figure 3.16). There did appear to be an increase in the ratio in the UV-only cells compared to all other groups, which was unexpected as a high value indicates a

high level of protection from apoptosis. At 12 h post-irradiation 30% of HFbs were undergoing apoptosis (figure 3.12) and although the Bcl-2: Bax ratio is indicating protection, it cannot be ignored that apoptosis is a multi-pathway process and an alternate pathway may have been initiated (Chapter 1, figure 1.13).

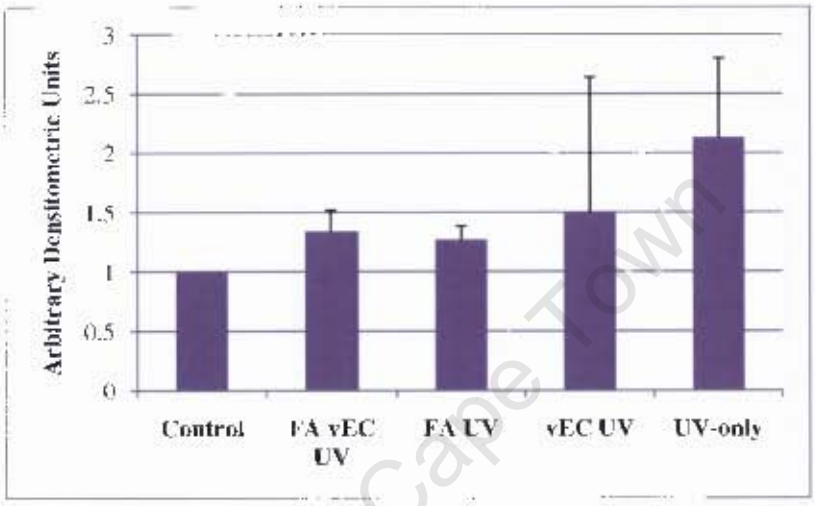

Figure 3.16 Bcl-2: Bax ratio determined in HFbs 12 h post-irradiation. Bcl-2 and Bax are anti- and pro-apoptotic proteins respectively. A ratio of >1 it is indicative of survival and <1 it is indicative of apoptosis. Values are relative to the control and data are presented as mean ± SD, n=2.

Twenty-four hours post-irradiation resulted in no variation between the ratios of any groups (figure 3.17). The higher ratio in the UV-only cells once again suggested that another apoptosis pathway may be activated following UVA-exposure. These results were in disagreement with the FACS data that showed pre-treatment with vEC was able to protect against cell death (figure 3.12). The UV-only cells exhibit a high survival ratio, which is in direct contrast to the large amount of apoptosis observed by Annexin V/ PI staining (figure 3.12), again indicating that an alternate pathway of apoptosis may have been initiated. Bcl-2 and Bax are relevant to this study as UVA is known to indirectly damage cells through ROS, which may target the mitochondrial membrane where Bcl-2 and Bax exert their effects. However, future protein expression studies should include an additional

protein, one that is activated by numerous apoptosis pathways, such as caspase-3, in order to draw a definitive conclusion. HFbs pre-treated with FA displayed the lowest survival ratio compared to all other groups (figure 3.17). The FA appears to be once again displaying a detrimental effect, as observed in the TBARS assay (figure 3.6). It may be exerting a pro-oxidative effect, or the ferulate radicals generated may condense with other ferulate radicals to give rise to the dimer curcumin [195, 292], which has well documented pro-apoptotic effects [293].

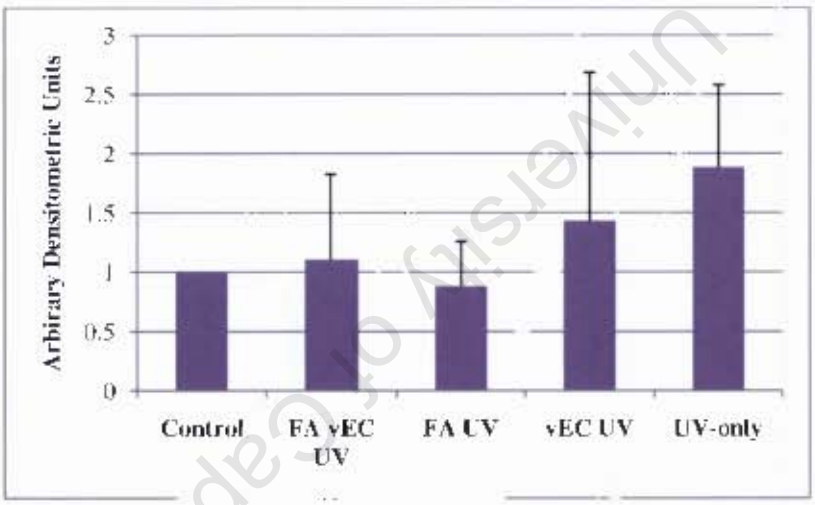

Figure 3.17 Bcl-2: Bax ratio determined in HFbs 24 h post-irradiation. Bcl-2 and Bax are anti- and pro-apoptotic proteins respectively. A ratio of >1 it is indicative of survival and <1 it is indicative of apoptosis. Values are relative to the control and data are presented as mean ± SD, n=2.

The process of apoptosis involves highly complex cell signalling, and a more definitive conclusion may be reached if for example, caspase-3 expression were examined, as the activation of this protein is the end-point of numerous pathways (Chapter 1, subsection 1.9.2). Numerous studies have incorporated the expression of caspase-3 when examining apoptosis [205, 208, 209]. Interestingly, Svobodova *et al.* (2007) showed that post-treatment of HaCaTs with a polyphenol derived from *Silybum marianum* (milk thistle) was able to attenuate intracellular ROS production (at 20 J/cm^2 UVA) and lipid peroxidation (at

30 J/cm^2), as well as a reduction in caspase-3 expression and enzymatic activity (at 20 J/cm^2) [205]. Whilst this study examined the antioxidant pre-treatment of skin cells, as numerous other studies have done[156, 209, 294] , it must be considered that post-treatment is potential option, or possible adjuvant therapy, to combating the harmful effects of UVA-induced photodamage.

3.4 Conclusions and Future Directions

3.4.1 Conclusions

This study aimed to elucidate the protective effects of the antioxidant combination of FA, vitamin C and vitamin E against UVA mediated photodamage in human epidermal keratinocytes and dermal fibroblasts. The first aim was to determine the optimal concentration of FA for human keratinocytes (HaCaTs) and fibroblasts (HFbs and 3T3s). An interesting dose-dependent proliferative effect was observed in HaCaTs, yet further studies are required to determine the mechanisms involved. The concentration of 0.8 mM FA was selected for all cell types, as this proved to be the highest concentration with the least amount of damage observed in all cell types.

The second aim studied the effects of the antioxidant combination on UVA-induced ROS generation and lipid peroxidation in HaCaTs and HFbs. Whilst no statistically significant effects were observed, it should be noted that pre-treatment of HFbs with FA vEC and HaCaTs with vEC resulted in lower amounts of intracellular ROS than cells that received no pre-treatment. Pre-treatment with the various treatments had little effect on the lipid peroxidation status of both cell types, as determined by the conjugated dienes and TBARS assay. Unexpectedly FA vEC pre-treatment of the HFbs appeared to have a detrimental effect on lipid peroxidation, as it led to higher levels of diene conjugation and TBARS compared to untreated cells. This result will need to be confirmed by additional experimental repetitions prior to any conclusions being made. HaCaTs pre-treated with vEC resulted in a reduced amount of conjugated dienes compared to cells that received no pre-treatment, illustrating that the role of the vitamins in reducing ROS may be directly related to their protective effect against mid-stage lipid peroxidation.

The final aim was to examine the effects of the various treatments on cell viability, and subsequently determine the mode of cell death elicited by UVA in HaCaTs and HFbs. The various treatments proved to have no significant effect on HaCaTs, HFbs and 3T3s, however the FA vEC combination did appear to be providing the HFbs some protection against cell death. The treatments did not protect HaCaTs from dying, and the predominant mode of cell death appeared to be apoptosis. The mode of cell death employed by the HFbs was apoptosis, and in contrast to the cell viability assay, pre-treatment with vEC displayed a significantly protective effect against UVA-induced apoptosis. This study was expanded to examine the expression of two apoptosis-associated proteins in the HFbs. The ratio provided by anti-apoptotic Bcl-2 and pro-apoptotic Bax served as an indicator of survival. The ratio was examined over a time course of 2-24 h, and although vEC pre-treated HFbs showed a high survival index, this series of experiments served as a reminder that apoptosis is a multi-pathway process, and other key proteins may need to be assessed in the future.

Overall, this study highlights that while intensive future work is required, there is enormous potential in the use of antioxidant combinations, like that of FA, vitamin C and vitamin E, as possible adjuvant therapies against UVA-mediated photodamage.

3.4.2 Future Directions

As with any research project, retrospect is often 20-20 vision, and this section aims to suggest improvements to benefit future studies. Firstly, there are many variations in current irradiation studies performed on human skin cells. Numerous variables are associated with irradiation conditions, including irradiation doses (5- 5000 J/cm^2), irradiation medium (PBS or colourless medium), irradiation time (0-3 h), wavelengths emitted (320-400 nm for UVA) and temperature at which the cells are maintained (4- 37°C). Primary cell cultures vary in the age of the donor (neonatal- 88 yrs), site of origin (e.g. foreskin, breast tissue), culture medium and passage number. All these factors need to be considered when comparing studies.

Whilst elucidating the optimal concentration of FA in HaCaTs, a dose-dependent proliferative effect was observed, which could be further examined by assessing cell numbers (manually counting cells using a Coulter counter), or by monitoring bromodeoxyuridine (BrdU) incorporation into the DNA. FACS analysis could also be performed to determine if FA lead to alterations in cell cycle arrest/ progression.

As previously mentioned the irradiation conditions in this study could be altered to ensure that cells undergo irradiation in the minimum amount of time possible. An improved light source with greater spectral power (to decrease the irradiation time), and a thermo-stabilizer plate to maintain a suitable temperature, should be used in future irradiation studies.

The phase contrast microscopy examining cell morphology post-irradiation allowed for the visual examination of the effects induced by UVA exposure. Cells could be further analysed using a nuclear dye such as 4',6-diamidino-2-phenylindole (DAPI) or Hoechst which would have enabled the visualisation of any UVA-induced DNA damage. In an attempt to correlate UVA-induced ROS formation and DNA damage cells could be co-stained with DHR 123, and visualised through fluorescent microscopy.

To determine whether the antioxidant treatments were able to attenuate UVA-induced lipid peroxidation, the conjugated dienes and TBARS assays were performed. No significant results were established, and this may be due to numerous reasons, one of the most likely being the extremely low amount of lipid obtained from near-confluent 10 cm^2 dishes (0.2-2 mg), some possibly lost through the extraction process. In addition, the number of biological and technical repeats needs to be increased to establish feasible trends. Other techniques may include detection of peroxidation products through HPLC or western blot analysis. These methods of lipid peroxidation analysis they may be superior to the TBARS and conjugated diene assays in cell culture systems.

In order to strengthen the western blot results, additional end-stage apoptotic markers, such as caspase-3, could have been included. Alternate options to determining cell death may also include caspase activity assays or lactate dehydrogenase (LDH) release assays to study apoptosis and necrosis respectively. What remains intriguing is that exposure to UVA undoubtedly leads to cell death, however the mode of cell death maybe be influenced by various antioxidant treatments.

Discrepancies between *in vivo* and *in vitro* studies point towards the need for a unified model. Organotypic cultures and 3D *in vitro* reconstructed skin models are ideal for studying the effects of antioxidant treatments. These systems allow neighbouring cells to interact, yet at the same time be isolated and studied individually. The encouraging findings of topical FA vEC pre-treatment witnessed in *in vivo* studies [208, 209, 210] still needs to be extrapolated to an *in vitro* environment in order to elucidate the cellular mechanisms at play in response to antioxidants such as FA. The *in vitro* examination of the FA vEC solution would be valuable in that the treatment appears to effect cells in a cell-type specific manner. Future work involving the FA vEC solution would be to first establish a 3D co-culture model before examining the effects on lipid, DNA and protein damage, as well as the effects on cell death.

Appendix A

A.1 Cell Culture Reagents

A.1.1 Dulbecco's Modified Eagle's Medium (DMEM)

DMEM- 2 l:

27.06 g DMEM powder medium (Highveld Biological Pty. Ltd., JHB, RSA)

7.4 g $NaHCO_3$

Adjust pH to 7.4

Make up to 2 l with autoclaved ddH_2O

Sterilise through a 0.2 µm filter and store in 400 ml aliquots at 4°C

A.1.2 Fetal calf serum (FCS)

Heat the bottle of FCS (Highveld Biological Pty. Ltd., JHB, RSA) once at 56°C for 20 min to inactivate complement factors.

Store in 50 ml aliquots at -20°C

A.1.3 Penicillin/ Streptomycin

Final concentration: Penicillin G sodium salt (Sigma-Aldrich, Schnelldorf, Germany) 100 U/ml; Streptomycin sulphate salt (Sigma-Aldrich, Schnelldorf, Germany) 100 µg/ml

100X penicillin/ streptomycin- 1 l:

Dissolve 6 g penicillin and 10 g streptomycin in 1 l autoclaved ddH_2O

Sterilise through a 0.2 µm filter and store in 50 ml aliquots at -20°C

A.1.4 10X Phosphate buffered saline (PBS)

10X PBS- 1 l:

80 g NaCl (1.37 M)

2 g KCl (0.03 M)

12.6 g Na_2HPO_4 anhydrous (0.09 M)

2 g KH_2PO_4 (0.01 M)

Make up to 1 l with ddH_2O and store at room temperature

Dilute to 1X with ddH_2O and autoclave before use

A.1.5 Trypsin/ ethylenediaminetetraacetic acid (EDTA)

0.05% Trypsin (Difco, Lawrence, USA)/ 0.02% EDTA (Sigma-Aldrich, Schnelldorf, Germany)

0.05% Trypsin/ 0.02% EDTA- 100 ml:

0.05 g Trypsin

0.02 g EDTA anhydrous

Dissolve trypsin in 100 ml autoclaved 1X PBS, then dissolve EDTA

Sterilise through a 0.2 µm filter and store in 20 ml aliquots at -20˚C

A.1.6 EDTA

0.05% EDTA- 100 ml:

0.05 g EDTA anhydrous

Dissolve in 80 ml autoclaved 1X PBS and adjust to pH8

Make up to 100 ml

Sterilise through a 0.2 µm filter and store in 20 ml aliquots at -20˚C

A.1.7 Cell Fixative

Glacial acetic acid (Associated Chemical Enterprises Pty. Ltd., JHB, RSA) and methanol (Saarchem (Merck), JHB, RSA) were prepared in a 1:3 ratio.

Fixative- 100 ml:

25 ml glacial acetic acid

75 ml methanol

A.1.8 Hoechst No. 33258

Hoechst No. 33258 trihydrochloride ((2'-[4-hydroxyphenyl]-5-[4-methyl-1-piperazinyl]-2,5'-bi-1H-benzimidazole) (Sigma-Aldrich, Schnelldorf, Germany)

Stock solution- 100 ml:

5 mg Hoechst No. 33258 trihydrochloride

100 ml 1X PBS

Stored (wrapped in aluminium foil) at 4°C

Working solution (final concentration 0.5 µg/ml)- 100 ml:

1 ml Hoechst stock solution

99 ml 1X PBS

Stored (wrapped in aluminium foil) at 4°C

A.1.9 Citric acid- disodium phosphate buffer (mounting fluid)

Mounting fluid- 100 ml:

22.2 ml 0.1M Citric acid (1.92 g citric acid made up to 100 ml with ddH_2O)

27.8 ml 0.2M $Na_2HPO_4.2H_2O$ (3.56 g $Na_2HPO_4.2H_2O$ made up to 100 ml with ddH_2O)

50 ml glycerol

Adjust to pH5.5 and store at 4°C

A.1.10 4% Paraformaldehyde (PFA)

4% PFA- 100 ml:

4 g PFA (Spi-Chem, Westchester, PA, USA)

Make up to 100 ml with 1X PBS and heat at 50°C to dissolve

Stored in 10 ml aliquots at -20°C

A.1.1.11 XTT Reagent

XTT Cell Proliferation Kit II (Roche, Germany)

Working Reagent- 5 ml:

4900 µl XTT labeling reagent

100 µl Electron coupling reagent

A.2 Antioxidants

A.2.1 Ferulic acid

Ferulic acid (Sigma-Aldrich, Schnelldorf, Germany) was made as a 10 mM stock solution.

Ferulic acid (10 mM) – 10 ml:

0.01942 g ferulic acid

400 µl absolute ethanol

9.6 ml sterile 1X PBS

Sterilise through a 0.2 µm filter and store in 1 ml aliquots at -20°C

A.2.2 Vitamin E

35 mM Vitamin E stock- 10 ml:

151,5 µl dl-α-Tocopheryl acetate (Vitamin E) (Roche- DSM Nutritional Products, Switzerland)

10 ml Absolute ethanol

Stored in 500 µl aliquots (wrapped in aluminium foil) at -20°C

Cells were exposed to a final concentration of 35 µM Vitamin E

A2.3 Vitamin C

5 mM Vitamin C stock- 10 ml:

0.0099 g Sodium l-ascorbate (Vitamin C) (Allied Drug Company, Pty. Ltd., Durban, RSA)

10 ml 1X PBS

Sterilise through a 0.2 µm filter and store in 1 ml aliquots (wrapped in aluminium foil) at -20°C

Cells were exposed to a final concentration of 50 µM Vitamin C

A.3 Flow Cytometry Reagents

A.3.2 Dihydrorhodamine 123 (DHR 123)

10 mg/ml (28.8 mM) DHR 123 stock solution- 1 ml:

Reconstitute 10 mg DHR 123 (Molecular Probes®, Invitrogen, Eugene, OR, USA)

1 ml DMSO

Store in 1 ml aliquots (wrapped in foil) at -80°C

1 mM DHR 123 working stock- 1 ml:

34.7 µl 10 mg/ml DHR 123

965.3 µl DMSO

Store in 1 ml aliquots (wrapped in foil) at -20°C

10 µM DHR 123 working solution -1 ml:

10 µl 10µM DHR 123

990 µl complete medium

To be made fresh before use

A.3.3 Annexin V

Fluorescein isothiocyanate conjugated Annexin V (Annexin V-FITC) requires a usage of 5 µl/ test (as per manufacturer's instructions).

A.3.4 Propidium Iodide

1 mg/ml Stock solution- 25 ml:

Reconstitute 25 mg stock powder (Sigma) in 25 ml ddH_2O

Store in 1 ml aliquots (wrapped in foil) at -20°C

50 µg/ml Working solution- 1 ml:

50 µl 1 mg PI stock solution

950 µl 1X PBS

Store (wrapped in foil) at -20°C

A.3.5 Annexin V binding buffer

1X Annexin V binding buffer- 100 ml:

0.2383 g 10 mM Hepes (pH7.4)

0.812 g 140 mM NaCl

0.037 g 2.5 mM $CaCl_2$

Make up to 100 ml with ddH_2O and store at 4°C

A.4 Lipid Peroxidation Reagents

A.4.1 Saline

0.9% Saline solution- 100 ml:

0.9 g NaCl

Make up to 100 ml with ddH_2O

A.4.2 $FeCl_3$

0.27% $FeCl_3$ solution- 100 ml:

0.27 g $FeCl_3.6H_2O$

Make up to 100 ml with ddH_2O

A.4.3 Butylated hydroxytoluene (BHT)

0.22% BHT solution- 100 ml:

0.22 g BHT

Make up to 100 ml with absolute ethanol; store (wrapped in aluminium foil) at 4°C

A.4.4 Glycine buffer

0.2 M Glycine.HCl buffer pH3.6- 1 l:

15 g Glycine

800 ml ddH_2O

Adjust to pH3.6 (HCl), make up to 1 l with ddH_2O and store at 4°C

A.4.5 Thiobarbituric acid (TBA)

0.5% TBA solution- 10 ml:

0.05 g TBA

0.03 g SDS

10 ml ddH_2O

To be made fresh before use

A.5 Protein Expression Reagents

A.5.1 Radio-Immunoprecipitation Assay (RIPA) buffer

Incomplete RIPA buffer:

150 mM NaCl

1% Triton X-100

0.1% SDS

20 mM Tris (pH7.5)

1% Deoxycholate

H_2O

Sterilise through a 0.45 µm filter and store in 5 ml aliquots at 4°C

Incomplete RIPA buffer stock- 50 ml:

1.5 ml 5 M NaCl

500 µl 100% Triton X-100

500 µl 10% SDS

1 ml 1 M Tris (pH7.5)

0.5 g Deoxycholate

46.5 ml H_2O

Sterilise through a 0.45 µm filter and store in 5 ml aliquots at 4˚C

A.5.2 Complete RIPA extraction buffer

Complete RIPA reagent- 3 ml:

120 µl Complete proteinase inhibitor cocktail

3 µl Aprotinin

15 µl PMSF

3 µl Pepstatin A

2859 µl RIPA buffer

Make fresh before use

Use 150 µl per 100 mm dish

A.5.3 Bovine serum albumin (BSA)

Bovine serum albumin fraction V (Roche, Mannheim, Germany)

2 mg BSA solution- 10 ml:

2 mg BSA powder

10 ml 0.9% NaCl (0.9 g NaCl and 99.1 ml ddH_2O); to be made fresh before use

A.5.4 Bicinchoninic acid (BCA) working reagent

BCA™ Protein Assay Kit (Thermo Scientific, Pierce, Rockford, IL, USA)

BCA working reagent- 10 ml:

9.8 ml Reagent A (supplied)

0.2 ml Reagent B (supplied)

To be made fresh before use

A.5.5 Resolving gel buffer

1.5 M Tris.HCl pH8.9/ 0.4% SDS- 200 ml:

36.2 g Tris

0.8 g SDS

Adjust to pH 8.9, make up to 200 ml with ddH_2O and store at 4°C

A.5.6 15% Resolving gel

1 x 1.5 mm 15% resolving gel:

3 ml Resolving buffer

4.5 ml Acrylamide/bis-acrylamide (30% solution) (Sigma-Aldrich, Schnelldorf, Germany)

1.5 ml ddH_2O

180 µl Fresh 10% ammonium persulphate

18 µl N,N,N',N'-Tetramethylrthylendiamin (TEMED)

Allow a minimum of 45 min for polymerisation before pouring the stacking gel

A.5.7 Stacking gel buffer

0.5 M Tric.HCl pH6.8/ 0.4% SDS- 100 ml:

5.9 g Tris

0.4 g SDS

Adjust to pH 6.8, make up to 100 ml with ddH_2O and store at 4°C

A.5.8 5% Stacking gel

1 x 1.5 mm 5% stacking gel:

1.5 ml Stacking buffer

1 ml Acrylamide/ bis-acrylamide (30% solution) (Sigma-Aldrich, Schnelldorf, Germany)

3.5 ml ddH_2O

60 µl fresh 10% Ammonium persulphate

6 µl N,N,N',N'-Tetramethylrthylendiamin (TEMED)

Insert comb immediately after pouring the gel (there should be 1 cm of stacking gel between the bottom of the comb and the resolving layer)

Allow a minimum of 1 hr for polymerisation before removing the comb

A.5.7 Loading dye

5X Stock loading dye- 50 ml:

1.75 g Tris

30 ml Glycerine

Make up to 40 ml with ddH_2O and adjust to pH 6.8

5 g SDS

Make up to a final volume of 50 ml with ddH_2O

Fresh loading dye- 200 µl:

100 µl 5X Loading dye

50 µl β-Mercaptoethanol

50 µl 0.025% Bromophenol blue

Diluted to 1X accordingly for individual protein samples

A.5.8 Tank buffer

10X Tank buffer stock- 1 l:

30.2 g Tris

144 g Glycine

10 g SDS

Make up to 1 l with ddH_2O and store at room temperature

1X Tank buffer working solution- 1 l:

100 ml 10X Tank buffer stock

900 ml ddH_2O

A.5.9 Transfer buffer

10X Transfer buffer stock- 1 l:

144 g Glycine

38 g Tris

Make up to 1 l with ddH_2O and store at 4°C

1X Transfer buffer working solution- 1 l:

100 ml 10X Transfer buffer

700 ml ddH_2O

200 ml Methanol

To be made fresh before use

Cool to 4°C before use

A.5.10 Tris-buffered saline with tween (TBS-T)

10X TBS-T stock- 1 l:

60.5 g Tris

87.6 g NaCl

Adjust to pH 7.4

Make up to 1 l with ddH_2O and store at room temperature

1X TBS-T working solution- 1 l:

100 ml 10X TBS-T stock

900 ml ddH_2O

1 ml Tween20

A.5.11 Fat-free milk

5% Fat-free milk solution- 10 ml:

0.5 g skim milk powder

Make up to 10 ml with TBS-T

To be made fresh before use

A.5.12 Chemiluminescent substrate

SuperSignal® West Pico Chemiluminescent Substrate (Thermo Scientific, Pierce, Rockford, IL, USA)

Chemiluminescent working reagent- 2 ml:

1 ml Stable peroxide solution (supplied)

1 ml Luminol/ enhancer solution (supplied)

To be made fresh before use

A.5.13 Developer

Developer working solution- 500 ml:

100 ml Developer (AGFA Healthcare, Belgium)

400 ml H_2O

Store in the dark at room temperature

A.5.14 Fixer

Fixer working solution- 500 ml:

100 ml Fixer (Illford Rapid Fixer, AGFA Healthcare, Belgium)

400 ml H_2O

Store in the dark at room temperature

Appendix B

B. 1 Mycoplasma Testing

Mycoplasma, a genus of bacteria that lack cell walls, are mostly unaffected by antibiotics such as penicillin [295]. Every alternate passage, cells were set aside for mycoplasma testing. Cells were grown on coverslips (22x22 mm, Marienfeld, Lauda-Konigshofen, Germany) in 35 mm^2 dishes for approximately 3 days. Medium was removed and cells were rinsed with 1X PBS before being placed in a fixative solution (Appendix A) for 5 min. Hoechst working stock (Appendix A) was added to the fixed cells for 6 min in the dark at room temperature. The coverslip was rinsed with 1X PBS and mounted onto a slide (Marienfeld, Lauda-Konigshofen, Germany) using mounting fluid (Appendix A). Slides were viewed using the DAPI filter (excitation: BP 365/12; emission: LP 397) on the fluorescent microscope (Zeiss Axiovert 200M).

B.2 Cell Counting

Trypsinized cells were re-suspended in 4 ml of complete medium in a 15 ml tube. A coverslip was placed onto the haemocytometer (Neubauer improved bright-line, Marienfeld, Lauda-Konigshofen, Germany) and 8 µl of suspended cells was placed on both halves of the haemocytometer. Cells in two quadrants on each half of the cytometer were counted and the average number of cells/ µl was calculated.

Bibliography

1. Tobin D. Biochemistry of human skin - our brain on the outside. *Chemical Society Reviews*. 2006;35:52-67.

2. Elias P. Stratum corneum defensive functions: An integrated view. *Journal of Investigative Dermatology*. 2005;125:183-200.

3. Slominski, A., Wortsman, J., Kuger, T., Paus, R., Solomon S. Corticotropin releasing hormone and proopiomelanocortin involvement in the cutaneous response to stress. *Physiological Reviews*. 2000;80(3):979-1020.

4. Errico MD, Lemma T, Calcagnile A, et al. Cell type and DNA damage specific response of human skin cells to environmental agents. *Mutation Research*. 2007;614:37-47.

5. Melanoma-skin cancer reviewed. *http://melanoma.blogsome.com/2006/03/22/skin-structure/*. 2006.

6. Koster M. Making an Epidermis. *Annals of the New York Academy of Sciences*. 2009;1170:7-10.

7. Truong AB, Kretz M, Ridky TW, Kimmel R, Khavari PA. p63 regulates proliferation and differentiation of developmentally mature keratinocytes. *Genes and Development*. 2006;20(22):3185-3197.

8. DermNet NZ. *http://www.dermnetnz.org/doctors/principles/images/epidermis.jpg*. 1996.

9. Nordlund JJ. The melanocyte and the epidermal melanin unit: an expanded concept. *Dermatologic Clinics*. 2007;25:271-281.

10. Quevedo WC. Epidermal melanin units: melanocyte-keratinocyte interactions. *American Zoologist*. 1972;12(1):35-41.

11. Hara M, Yaar M, Byers HR, et al. Kinesin participates in melanosomal movement along melanocyte dendrites. *Journal of Investigative Dermatology*. 2000;114(3):438-443.

12. Wu X, Hammer 3rd JA. Making sense of melanosome dynamics in mouse melanocytes. *Pigment Cell Research*. 2000;13(4):241-247.

13. Kobayashi N, Nakagawa A, Muramatsu T, et al. Supranuclear melanin caps reduce ultraviolet induced DNA photoproducts in human epidermis. *Journal of Investigative Dermatology*. 1998;110(5):806-810.

14. Gibbs S, Murli S, De Boer G, et al. Melanosome capping of keratinocytes in pigmented reconstructed epidermis-effect of ultraviolet radiation and 3-isobutyl-1-methyl-xanthine on melanogenesis. *Pigment Cell Research*. 2000;13(6):458-466.

15. Misery L. Langerhans cells in the neuro-immuno-cutaneous system. *Journal of Neuroimmunology*. 1998:83-87.

16. Misery L, Bourchanny D, Kanitakis J, Schmitt D, Claudy A. Modulation of substance P and somatostatin receptors in cutaneous lymphocytic inflammatory and tumoral infiltrates. *Dermatology*. 2001:238- 241.

17. Scholzen, T., Armstrong, C.A., Bunnett, N.W., Luger, T.A., Olerud, J.E., Ansel J. Neuropeptides in the skin: interactions between the neuroendocrine and the skin immune systems. *Experimental Dermatology*. 1998;7:81-96.

18. Bauer J, Bahmer FA, Worl J, et al. A strikingly constant ratio exists between Langerhans cells and other epidermal cells in human skin. A stereologic study using the optical disector method and the confocal laser scanning microscope. *Journal of Investigative Dermatology*. 2001;116(2):313-318.

19. Madison KC. Barrier function of the skin: "La Raison d'Etre" of the epidermis. *Journal of Investigative Dermatology*. 2003;121:231-241.

20. Burgeson RE, Christianot AM. The dermal-epidermal junction. *Current Opinion in Cell Biology*.:651-658.

21. Chang HY, Chi JT, Dudoit S, et al. Diversity, topographic differentiation, and positional memory in human fibroblasts. *Proceedings of the National Academy of Sciences of the United States of America*. 2002;99(20):12877-12882.

22. Postlewthwaite, A.E., Kang A. Fibroblasts and matrix proteins. In: *Gallin JI, Snyderman R, editors. Inflammation: basic principles and clinical correlates. Philadelphia: Lippincott Williams & Wilkins Philadelphia*.; 1999:227-257.

23. Smith RS, Smith TJ, Blieden TM, Phipps RP. Fibroblasts as sentinel cells. Synthesis of chemokines and regulation of inflammation. *American Journal of Pathology*. 1997;151(2):317-322.

24. Kahari, V-M., Saarialho-Kere U. Matrix metalloproteinases in skin. *Experimental Dermatology*. 1997;6:199-214.

25. Guo L, Yu QC, Fuchs E. Targeting expression of keratinocyte growth factor to keratinocytes elicits striking changes in epithelial differentiation in transgenic mice. *The EMBO journal*. 1993;12(3):973-986.

26. Smola H, Thiekotter G, Fusenig NE. Mutual induction of growth factor gene expression by epidermal-dermal cell interaction. *The Journal of Cell Biology*. 1993;122(2):417-429.

27. Werner S, Peters KG, Longaker MT, et al. Large induction of keratinocyte growth factor expression in the dermis during wound healing. *Proceedings of the National Academy of Sciences of the United States of America*. 1992;89(15):6896-6900.

28. Finch PW, Cunha GR, Rubin JS, Wong J, Ron D. Pattern of keratinocyte growth factor and keratinocyte growth factor receptor expression during mouse fetal development suggests a role in mediating morphogenetic mesenchymal-epithelial interactions. *American Journal of Anatomy*. 1995;203(2):223-240.

29. Maas-Szabowski N, Szabowski A, Stark HJ, et al. Organotypic cocultures with genetically modified mouse fibroblasts as a tool to dissect molecular mechanisms regulating keratinocyte growth and differentiation. *Journal of Investigative Dermatology*. 2001;116(5):816-820.

30. Maas-Szabowski N, Shimotoyodome A, Fusenig NE. Keratinocyte growth regulation in fibroblast cocultures via a double paracrine mechanism. *Journal of Cell Science*. 1999;112(12):1843-1853.

31. Maas-Szabowski N, Stark HJ, Fusenig NE. Keratinocyte growth regulation in defined organotypic cultures through IL-1-induced keratinocyte growth factor expression in resting fibroblasts. *Journal of Investigative Dermatology*. 2000;114(6):1075-1084.

32. Blomme EA, Sugimoto Y, Lin YC, Capen CC, Rosol TJ. Parathyroid hormone-related protein is a positive regulator of keratinocyte growth factor expression by normal dermal fibroblasts. *Molecular and Cellular Endocrinology*. 1999;152(1-2):189-197.

33. Rigel DS, Carucci JA. Malignant melanoma: prevention, early detection, and treatment in the 21st century. *CA: A Cancer Journal for Clinicians*. 2000;50(4):215-240.

34. Rigel D. Cutaneous ultraviolet exposure and its relationship to the development of skin cancer. *Journal of the American Academy of Dermatology*. 2008;58:129S-132S.

35. Cancer Association of South Africa (CANSA), Skin cancer 2009 fact sheet. *http://www.cansa.org.za*. 2009.

36. Einspahr JG, Stratton SP, Bowden GT, Alberts DS. Chemoprevention of human skin cancer. *Critical reviews in Oncology/Hematology*. 2002;41(3):269-285.

37. Buljan, M., Bulat, V., Situm, M., Mihic, L.L., Stanic-Duktaj S. Variations in clinical presentation of basal cell carcinoma. *Acta Clinica Croatica*. 2008;47:25-30.

38. Bowden GT. Prevention of non-melanoma skin cancer by targeting ultraviolet-B-light signalling. *Nature*. 2004;4:23-35.

39. Brash DE, Rudolph JA, Simon JA, et al. A role for sunlight in skin cancer: UV-induced p53 mutations in squamous cell carcinoma. *Proceedings of the National Academy of Sciences of the United States of America*. 1991;88:10124-10128.

40. Ichihashi M, Ueda M, Budiyanto A, et al. UV-induced skin damage. *Toxicology*. 2003;189(1-2):21-39.

41. He, Y., Pi, J., Huang, J-L., Diwan, B.A., Waalkes, M.P., Chignell C. Chronic UVA irradiation of human HaCaT keratinocytes induces malignant transformation associated with acquired apoptotic resistance Chronic UVA irradiation induces malignant transformation. *Oncogene*. 2006;25:3680-3688.

42. Eller MS, Gilchrest BA. Tanning as part of the eukaryotic SOS response. *Pigment Cell Research*. 2000;13 Suppl 8:94-97.

43. Gloster, H.M., Brodland D. The epidemiology of skin cancer. *Dermatologic Surgery*. 1996;22(3):217-226.

44. Matsumura Y, Ananthaswamy HN. Toxic effects of ultraviolet radiation on the skin. *Toxicology and Applied Pharmacology*. 2004;195:298 - 308.

45. Melnikova VO, Ananthaswamy HN. Cellular and molecular events leading to the development of skin cancer. *Mutation Research*. 2005;571:91-106.

46. Ravanat J, Douki T, Cadet J. Direct and indirect effects of UV radiation on DNA and its components. *Photochemistry and Photobiology*. 2001;63:88-102.

47. de Gruijl F. Photocarcinogenesis : UVA vs . UVB Radiation. *Skin Pharmacology and Applied Skin Physiology*. 2002;15:316-320.

48. Herrmann G, Wlaschek M, Lange TS, et al. UVA irradiation stimulates the synthesis of various matrix-metalloproteinases (MMPs) in cultured human fibroblasts. *Experimental Dermatology*. 1993;2(2):92-97.

49. Berneburg M, Gattermann N, Stege H, et al. Chronically ultraviolet-exposed human skin shows a higher mutation frequency of mitochondrial DNA as compared to unexposed skin and the hematopoietic system. *Photochemistry and Photobiology*. 1997;66(2):271-275.

50. Berneburg M, Grether-beck S, Ku V, et al. Singlet oxygen mediates the UVA-induced generation of the photoaging-associated mitochondrial common deletion. *The Journal of Biological Chemistry*. 1999;274(22):15345-15349.

51. Wlaschek M, Briviba K, Stricklin GP, Sies H, Scharffetter-Kochanek K. Singlet oxygen may mediate the ultraviolet A-induced synthesis of interstitial collagenase. *Journal of Investigative Dermatology*. 1995;104(2):194-198.

52. Svobodova A, Walterova D, Vostalova J. Ultraviolet light induced alteration to the skin. *Biomedical papers of the Medical Faculty of the University Palacky, Olomouc, Czechoslovakia*. 2006;150(1):25-38.

53. de Gruijl FR. Skin cancer and solar UV radiation. *European Journal of Cancer*. 1999;35(14):2003-2009.

54. Gruijl FR, Leun JC. Environment and health: 3. Ozone depletion and ultraviolet radiation. *Canadian Medical Association Journal*. 2000;163(7):851-855.

55. Duthie MS, Kimber I, Norval M. The effects of ultraviolet radiation on the human immune system. *British Journal of Dermatology*. 1999:995-1009.

56. Hussein MR. Ultraviolet radiation and skin cancer : molecular mechanisms. *Journal of Cutaneous Pathology*. 2005:191-205.

57. Ridley AJ, Whiteside JR, McMillan TJ, Allinson SL. Cellular and sub-cellular responses to UVA in relation to carcinogenesis. *International Journal of Radiation Biology*. 2009;85(3):177-195.

58. Calgary Optometrists. *http://www.eyeglasses-calgary-optometrists.com/images/solar%20light%20spectrum.gif*. 2010.

59. Runger TM, Kappes UP. Mechanisms of mutation formation with long-wave ultraviolet light (UVA). *Photodermatology, Photoimmunology & Photomedicine*. 2008;24(1):2-10.

60. Freeman, S.E., Gange, R.W., Sutherland, J.C., Matzinger, E.A., Sutherland B. Production of pyrimidine dimers in DNA of human skin exposed in situ to UVA radiation. *Journal of Investigative Dermatology*. 1987;88:430-433.

61. Ravanat, J-L., Douki,T., Cadet J. Direct and indirect effects of UV radiation on DNA and its components. *Journal of Photochemistry and Photobiology B: Biology*. 2001;63:88-102.

62. Cadet J, Sage E, Douki T. Ultraviolet radiation-mediated damage to cellular DNA. *Mutation Research*. 2005;571:3-17.

63. Drobetsky EA, Turcotte J, Chateauneuf A. A role for ultraviolet A in solar mutagenesis. *Proceedings of the National Academy of Sciences of the United States of America*. 1995;92(6):2350-2354.

64. Sander CS, Chang H, Salzmann S, et al. Photoaging is associated with protein oxidation in human skin in vivo. *The Journal of Investigative Dermatology*. 2002;118(4):618-625.

65. Morliere P, Moysan A, Tirache I. Action spectrum for UV-induced lipid peroxidation in cultured human skin fibroblasts. *Free Radical Biology and Medicine*. 1995;19(3):365-371.

66. Bachelor MA, Bowden GT. UVA-mediated activation of signaling pathways involved in skin tumor promotion and progression. *Seminars in Cancer Biology*. 2004;14(2):131-138.

67. Bruls, W.A.G, Slaper, H., Van Der Leun, J.C., Berrens L. Transmission of human epidermis and stratum corneum as a function of thickness in the ultraviolet and visible wavelengths. *Photochemistry and Photobiology*. 1984;40(4):485-494.

68. Svobodova, A., Psotova, J., Walterova D. Natural phenolics in the prevention of UV-induced skin damage. A review. *Biomedical papers of the Medical Faculty of the University Palacky, Olomouc, Czechoslovakia*. 2003;147(2):137-145.

69. Emri G, Wenczl E, Van Erp P, et al. Low doses of UVB or UVA induce chromosomal aberrations in cultured human skin cells. *Journal of Investigative Dermatology*. 2000;115(3):435-440.

70. Pastila R, Leszczynski D. Ultraviolet A exposure might increase metastasis of mouse melanoma: a pilot study. *Photodermatology, Photoimmunology and Photomedicine*. 2005;21(4):183-190.

71. de Laat A, van der Leun JC, de Gruijl FR. Carcinogenesis induced by UVA (365-nm) radiation: the dose-time dependence of tumor formation in hairless mice. *Carcinogenesis*. 1997;18(5):1013-1020.

72. Huang XX, Bernerd F, Halliday GM. Ultraviolet A within sunlight induces mutations in the epidermal basal layer of engineered human skin. *The American Journal of Pathology*. 2009;174(4):1534-1543.

73. Sutherland JC, Griffin KP. Absorption spectrum of DNA for wavelengths greater than 300 nm. *Radiation Research*. 1981;86(3):399-409.

74. Viteri G, Edwards AM, De La Fuente J, Silva E. Study of the interaction between triplet riboflavin and the alpha-, betaH- and betaL-crystallins of the eye lens. *Photochemistry and Photobiology*. 2003;77(5):535-540.

75. Albro PW, Bilski P, Corbett JT, Schroeder JL, Chignell CF. Photochemical reactions and phototoxicity of sterols: novel self-perpetuating mechanisms for lipid photooxidation. *Photochemistry and Photobiology*. 1997;66(3):316-325.

76. Young AR. Chromophores in human skin. *Physics in Medicine and Biology*. 1997;42:789-802.

77. Valencia A, Kochevar IE. Ultraviolet A induces apoptosis via reactive oxygen species in a model for Smith-Lemli-Opitz syndrome. *Free Radical Biology and Medicine*. 2006;40(4):641-650.

78. Hanson KM, Simon JD. Epidermal trans-urocanic acid and the UV-A-induced photoaging of the skin. *Proceedings of the National Academy of Sciences of the United States of America*. 1998;95(18):10576-10578.

79. Simon JD. Spectroscopic and dynamic studies of the epidermal chromophores trans-urocanic acid and eumelanin. *Accounts of Chemical Research*. 2000;33(5):307-313.

80. Darr, D., Fridovich I. Free radicals in cutaneous biology. *Journal of Investigative Dermatology*. 1994;102:671-675.

81. Rochette, P.J., Therrien, J-P., Drouin, R., Perdiz, D., Bastien, N., Drobetsky, E.A., Sage E. UVA-induced cyclobutane pyrimidine dimers form predominantly at thymine- thymine dipyrimidines and correlate with the mutation spectrum in rodent cells. *Nucleic Acids Research*. 2003;31(11):2786-2794.

82. Evans MD, Dizdaroglu M, Cooke MS. Oxidative DNA damage and disease: induction, repair and significance. *Mutation Research*. 2004;567(1):1-61.

83. Shorrocks, J., Paul, N.D., McMillan T. The dose rate of UVA treatment influences the cellular response of HaCaT keratinocytes. *Journal of Investigative Dermatology*. 2007:1-9.

84. Peak, J.G, Peak M. Comparison of initial yields of DNA-to-protein crosslinks and single-strand breaks induced in cultured human cells by far- and near-ultraviolet light, blue light and X-rays. *Mutation Research/ Fundamental and Molecular Mechanisms of Mutagenesis*. 1991;246(1):187-191.

85. Stary, A., Robert, C., Sarasin A. Deleterious effects of ultraviolet A radiation in human cells. *Mutation Research. DNA Repair*. 1997;383:1-9.

86. Cooke MS, Podmore ID, Mistry N, et al. Immunochemical detection of UV-induced DNA damage and repair. *Journal of Immunological Methods*. 2003;280(1-2):125-133.

87. Freeman SE, Hacham H, Gange RW, et al. Wavelength dependence of pyrimidine dimer formation in DNA of human skin irradiated in situ with ultraviolet light. *Proceedings of the National Academy of Sciences of the United States of America*. 1989;86(14):5605-5609.

88. Sage E, Lamolet B, Brulay E, et al. Mutagenic specificity of solar UV light in nucleotide excision repair-deficient rodent cells. *Proceedings of the National Academy of Sciences of the United States of America*. 1996;93(1):176-180.

89. Burren R, Scaletta C, Frenk E, Panizzon RG, Applegate LA. Sunlight and carcinogenesis: expression of p53 and pyrimidine dimers in human skin following UVA I, UVA I + II and solar simulating radiations. *International Journal of Cancer*. 1998;76(2):201-206.

90. Young AR, Potten CS, Nikaido O, et al. Human melanocytes and keratinocytes exposed to UVB or UVA in vivo show comparable levels of thymine dimers. *Journal of Investigative Dermatology*. 1998;111(6):936-940.

91. Douki T, Perdiz D, Grof P, et al. Oxidation of guanine in cellular DNA by solar UV radiation: biological role. *Photochemistry and Photobiology*. 1999;70(2):184-190.

92. Douki T, Reynaud-Angelin A, Cadet J, Sage E. Bipyrimidine photoproducts rather than oxidative lesions are the main type of DNA damage involved in the genotoxic effect of solar UVA radiation. *Biochemistry*. 2003;42(30):9221-9226.

93. Kuluncsics Z, Perdiz D, Brulay E, Muel B, Sage E. Wavelength dependence of ultraviolet-induced DNA damage distribution: involvement of direct or indirect mechanisms and possible artefacts. *Journal of Photochemistry and Photobiology B: Biology*. 1999;49(1):71-80.

94. Besaratinia A, Synold TW, Chen HH, et al. DNA lesions induced by UV A1 and B radiation in human cells: comparative analyses in the overall genome and in the p53 tumor suppressor gene. *Proceedings of the National Academy of Sciences of the United States of America*. 2005;102(29):10058-10063.

95. Mouret, S., Baudouin, C., Charveron, M., Favier, A., Cadet, J., Douki T. Cyclobutane pyrimidine dimers are predominant DNA lesions in whole human skin exposed to UVA radiation. *Proceedings of the National Academy of Sciences of the United States of America*. 2006;103(37):13765-13770.

96. Kappes UP, Luo D, Potter M, Schulmeister K, Runger TM. Short- and long-wave UV light (UVB and UVA) induce similar mutations in human skin cells. *The Journal of Investigative Dermatology*. 2006;126(3):667-675.

97. Davies MJ. Singlet oxygen-mediated damage to proteins and its consequences. *Biochemical and biophysical research communications*. 2003;305(3):761-770.

98. Stadtman ER. Protein oxidation and aging. *Science*. 1992;257(5074):1220-1224.

99. Au V, Madison SA. Effects of singlet oxygen on the extracellular matrix protein collagen: oxidation of the collagen crosslink histidinohydroxylysinonorleucine and histidine. *Archives of Biochemistry and Biophysics*. 2000;384(1):133-142.

100. Davies, K.J.A., Lin, S.W., Pacifici R. Protein damage and degradation by oxygen radicals. *The Journal of Biological Chemistry*. 1987;262(20):9914-9920.

101. Moskovitz J, Flescher E, Berlett BS, et al. Overexpression of peptide-methionine sulfoxide reductase in Saccharomyces cerevisiae and human T cells provides them with high resistance to oxidative stress. *Proceedings of the National Academy of Sciences of the United States of America*. 1998;95(24):14071-14075.

102. Ogawa F, Sander CS, Hansel A, et al. The repair enzyme peptide methionine-S-sulfoxide reductase is expressed in human epidermis and upregulated by UVA radiation. *Journal of Investigative Dermatology*. 2006;126:1128-1134.

103. Thiele JJ, Traber MG, Re R, et al. Macromolecular carbonyls in human stratum corneum: a biomarker for environmental oxidant exposure? *FEBS letters*. 1998;422(3):403-406.

104. Thiele JJ, Hsieh SN, Briviba K, Sies H. Protein oxidation in human stratum corneum: susceptibility of keratins to oxidation in vitro and presence of a keratin oxidation gradient in vivo. *Journal of Investigative Dermatology*. 1999;113(3):335-339.

105. Dimon-Gadal S, Gerbaud P, Therond P, et al. Increased oxidative damage to fibroblasts in skin with and without lesions in psoriasis. *Journal of Investigative Dermatology*. 2000;114(5):984-989.

106. Berlett BS, Stadtman ER. Protein oxidation in aging, disease, and oxidative stress. *The Journal of Biological Chemistry*. 1997;272(33):20313-20316.

107. Halliwell, B., Chirico S. Lipid peroxidation : its mechanism, measurement, and significance. *American Journal of Clinical Nutrition*. 1993;57 (suppl):71s5-725S.

108. Marnett LJ. Lipid peroxidation-DNA damage by malondialdehyde. *Mutation Research*. 1999;424(1-2):83-95.

109. Kuhn H, Borchert A. Regulation of enzymatic lipid peroxidation: the interplay of peroxidizing and peroxide reducing enzymes. *Free Radical Biology and Medicine*. 2002;33(2):154-172.

110. Kehrer JP. The Haber-Weiss reaction and mechanisms of toxicity. *Toxicology*. 2000;149(1):43-50.

111. Punnonen K, Jansen CT, Puntala A, Ahotupa M. Effects of in vitro UVA irradiation and PUVA treatment on membrane fatty acids and activities of antioxidant enzymes in human keratinocytes. *Journal of Investigative Dermatology*. 1991;96(2):255-259.

112. Vile, G.F., Tyrrell R. UVA radiation-induced oxidative damage to lipids and proteins in vitro and in human skin fibroblasts is dependent on iron and singlet oxygen. *Free Radical Biology and Medicine*. 1995;18(4):721-730.

113. Polte T, Tyrrell RM. Involvement of lipid peroxidation and organic peroxides in UVA-induced matrix metalloproteinase-1 expression. *Free Radical Biology and Medicine*. 2004;36(12):1566-1574.

114. Young, I.S., McEneny J. Lipoprotein oxidation and atherosclerosis. *Biochemical Society Transactions*. 2001;29(2):358-362.

115. Halliwell, B., Gutteridge J. Free radicals in biology and medicine, fourth edition. In: *Great Claredon Street, Oxford OX2 6DP, Oxford University Press.*; 2007.

116. Gerschman, R., Gilbert, D.L., Nye, S.W., Dwyer, P., Fenn W. Oxygen poisoning and X-irradiation: A mechanism in common. *Science*. 1954;119(3097):623-626.

117. Harman D. Aging: a theory based on free radical and radiation chemistry. *Biological Sciences and Clinical Medicine*. 1956;11(3):298-300.

118. Harman D. The aging process. *Proceedings of the National Academy of Sciences of the United States of America*. 1981;78(11):7124-7128.

119. McCord JM, Fridovich I. Superoxide dismutase. An enzymic function for erythrocuprein (hemocuprein). *The Journal of Biological Chemistry*. 1969;244(22):6049-6055.

120. Trachootham, D., Lu, W., Ogasawara, M.A., Valle, N.R-D., Huang P. Redox regulation of cell survival. *Antioxidants and Redox Signaling*. 2008;10(8):1343-1374.

121. Loschen G, Flohe L, Chance B. Respiratory chain linked H(2)O(2) production in pigeon heart mitochondria. *FEBS letters*. 1971;18(2):261-264.

122. Inoue M, Sato EF, Nishikawa M, et al. Mitochondrial generation of reactive oxygen species and its role in aerobic life. *Current Medicinal Chemistry*. 2003;10(23):2495-2505.

123. Conner EM, Grisham MB. Inflammation, free radicals, and antioxidants. *Nutrition*. 1996;12(4):274-277.

124. Gupta M, Dobashi K, Greene EL, Orak JK, Singh I. Studies on hepatic injury and antioxidant enzyme activities in rat subcellular organelles following in vivo ischemia and reperfusion. *Molecular and Cellular Biochemistry*. 1997;176(1-2):337-347.

125. Ames BN, Shigenaga MK, Hagen TM. Oxidants, antioxidants, and the degenerative diseases of aging. *Proceedings of the National Academy of Sciences of the United States of America*. 1993;90(17):7915-7922.

126. Valko M, Rhodes CJ, Moncol J, Izakovic M, Mazur M. Free radicals, metals and antioxidants in oxidative stress-induced cancer. *Chemico-Biological Interactions*. 2006;160:1-40.

127. Valko M, Izakovic M, Mazur M, Rhodes CJ, Telser J. Role of oxygen radicals in DNA damage and cancer incidence. *Molecular and Cellular Biochemistry*. 2004;266(1-2):37-56.

128. Li C, Jackson RM. Reactive species mechanisms of cellular hypoxia-reoxygenation injury. *American Journal of Physiology. Cell Physiology*. 2002;282(2):227-241.

129. Kamata H, Hirata H. Redox regulation of cellular signalling. *Cellular Signalling*. 1999;11:1-14.

130. Haber, F., Weiss J. The catalytic decomposition of hydrogen peroxide by iron salts. *Proceedings of the Royal Society of London. Series A, Mathematical and Physical Sciences*. 1934;147(861):332-351.

131. Petersen, A.B., Gniadecki, R., Vicanova, J., Thorn, T., Wulf H. Hydrogen peroxide is responsible for UVA-induced DNA damage measured by alkaline comet assay in HaCaT keratinocytes. *Journal of Photochemistry and Photobiology B: Biology*. 2000;59:123-131.

132. Droge W. Free radicals in the physiological control of cell function. *Physiological Reviews*. 2002;82(1):47-95.

133. Mahadev K, Wu X, Zilbering A, et al. Hydrogen peroxide generated during cellular insulin stimulation is integral to activation of the distal insulin signaling cascade in 3T3-L1 adipocytes. *The Journal of Biological Chemistry*. 2001;276(52):48662-48669.

134. Colavitti R, Pani G, Bedogni B, et al. Reactive oxygen species as downstream mediators of angiogenic signaling by vascular endothelial growth factor receptor-2/KDR. *The Journal of Biological Chemistry*. 2002;277(5):3101-3108.

135. Kuwabara, M., Asanuma, T., Niwa, K., Inanami O. Regulation of cell survival and death signals induced by oxidative stress. *Journal of Clinical Nutrition*. 2008;43:51-57.

136. Sies H. Oxidative stress: From basic research to clinical application. *The American Journal of Medicine*. 1991;91(3):S31-S38.

137. Faraci FM, Didion SP. Vascular protection: superoxide dismutase isoforms in the vessel wall. *Arteriosclerosis, Thrombosis, and Vascular Biology*. 2004;24(8):1367-1373.

138. Shindo Y, Witt E, Han D, Epstein W, Packer L. Enzymic and non-enzymic antioxidants in epidermis and dermis of human skin. *Journal of Investigative Dermatology*. 1994;102(1):122-124.

139. Pigeolet, E., Corbisier, P., Houbion, A., Lambert, D., Michiels, C., Raes, M., Zachary, M.D., Remacle J. Glutathione peroxidase, superoxide dismutase, and catalase inactivation by peroxides and oxygen derived free radicals. *Mechanisms of Aging and Development*. 1990;51(3):283-97.

140. Shindo Y, Hashimoto T. Time course of changes in antioxidant enzymes in human skin fibroblasts after UVA irradiation. *Journal of Dermatological Science*. 1997;14(3):225-232.

141. Keyse SM, Tyrrell RM. Heme oxygenase is the major 32-kDa stress protein induced in human skin fibroblasts by UVA radiation, hydrogen peroxide, and sodium arsenite. *Proceedings of the National Academy of Sciences of the United States of America*. 1989;86(1):99-103.

142. Basu-Modak S, Tyrrell RM. Singlet oxygen: a primary effector in the ultraviolet A/near-visible light induction of the human heme oxygenase gene. *Cancer Research*. 1993;53(19):4505-4510.

143. Kikuchi G, Yoshida T, Noguchi M. Heme oxygenase and heme degradation. *Biochemical and Biophysical Research Communications*. 2005;338(1):558-567.

144. Stocker R. Antioxidant activities of bile pigments. *Antioxidants and Redox Signaling*. 2004;6(5):841-849.

145. Mancuso C, Bonsignore A, Di Stasio E, Mordente A, Motterlini R. Bilirubin and S-nitrosothiols interaction: evidence for a possible role of bilirubin as a scavenger of nitric oxide. *Biochemical Pharmacology*. 2003;66(12):2355-2363.

146. Mancuso C, Pani G, Calabrese V. Bilirubin: an endogenous scavenger of nitric oxide and reactive nitrogen species. *Communications in Free Radical Research*. 2006;11(5):207-213.

147. Mancuso C, Bonsignore A, Capone C, Di Stasio E, Pani G. Albumin-bound bilirubin interacts with nitric oxide by a redox mechanism. *Antioxidants and Redox Signaling*. 2006;8(3-4):487-494.

148. Tyrrell RM, Reeve VE. Potential protection of skin by acute UVA irradiation-from cellular to animal models. *Progress in Biophysics and Molecular Biology*. 2006;92(1):86-91.

149. Allanson M, Reeve VE. Ultraviolet A (320-400 nm) modulation of ultraviolet B (290-320 nm)-induced immune suppression is mediated by carbon monoxide. *Journal of Investigative Dermatology*. 2005;124(3):644-650.

150. Allanson M, Domanski D, Reeve VE. Photoimmunoprotection by UVA (320-400 nm) radiation is determined by UVA dose and is associated with cutaneous cyclic guanosine monophosphate. *Journal of Investigative Dermatology*. 2006;126:191-197.

151. Allanson M, Reeve VE. Carbon monoxide signalling reduces photocarcinogenesis in the hairless mouse. *Cancer Immunology, Immunotherapy*. 2007;56:1807-1815.

152. Vile GF, Tyrrell RM. Oxidative stress resulting from ultraviolet A irradiation of human skin fibroblasts leads to a heme oxygenase-dependent increase in ferritin. *The Journal of Biological Chemistry*. 1993;268(20):14678-14681.

153. Vile GF, Basu-Modak S, Waltner C, Tyrrell RM. Heme oxygenase 1 mediates an adaptive response to oxidative stress in human skin fibroblasts. *Proceedings of the National Academy of Sciences of the United States of America*. 1994;91(7):2607-2610.

154. Pourzand C, Watkin RD, Brown JE, Tyrrell RM. Ultraviolet A radiation induces immediate release of iron in human primary skin fibroblasts: the role of ferritin. *Proceedings of the National Academy of Sciences of the United States of America*. 1999;96(12):6751-6756.

155. Reelfs, O., Tyrrell, R.M., Pourzand C. Ultraviolet A radiation-induced immediate iron release is a key modulator of the activation of NF-kB in human skin fibroblasts. *Journal of Investigative Dermatology*. 2004;122:1440-1447.

156. Calabrese, V., Calafato, S., Puleo, E., Cornelius, C., Sapienza, M., Morganti, P., Mancuso C. Redox regulation of cellular stress response by ferulic acid ethyl ester in human dermal fibroblasts : role of vitagenes ☆. *Clinics in Dermatology*. 2008;26:358-363.

157. Prestera, T., Talalay, P., Alam, J., Ahn, Y.I., Lee, P.J., Choi A. Parallel induction of heme oxygenase-I and chemoprotective phase 2 enzymes by electrophiles and antioxidants : Regulation by upstream antioxidant-responsive elements (ARE). *Molecular Medicine*. 1995;1(7):827-837.

158. Alam J, Stewart D, Touchard C, et al. Nrf2, a Cap'n'Collar transcription factor, regulates induction of the heme oxygenase-1 gene. *The Journal of Biological Chemistry*. 1999;274(37):26071-26078.

159. Li, N., Venkatesan, M.I., Miguel, A., Kaplan, R., Gujuluva, C., Alam, J., Nel A. Induction of heme-oxygenase-1 expression in macrophages by diesel exhaust particle chemicals and quinones via the antioxidant-responsive element. *Journal Immunology*. 2000;165:3393-3401.

160. Scapagnini G, Colombrita C, Amadio M, et al. Curcumin activates defensive genes and protects neurons against oxidative stress. *Antioxidants and Redox Signaling*. 2006;8(3-4):395-403.

161. Nakamura, H., Nakamura, K., Yodoi J. Redox regulation of cellular activation. *Annual Reviews of Immunology*. 1997;15:351-369.

162. Bourdon E, Blache D. The importance of proteins in defense against oxidation. *Antioxidants and Redox Signaling*. 2001;3(2):293-311.

163. Didier C, Kerblat I, Drouet C, et al. Induction of thioredoxin by ultraviolet-A radiation prevents oxidative-mediated cell death in human skin fibroblasts. *Free Radical Biology and Medicine*. 2001;31(5):585-598.

164. Colven RM, Pinnell SR. Topical vitamin C in aging. *Clinics in Dermatology*. 1996;14(2):227-234.

165. Pinnell S. Cutaneous photodamage, oxidative stress and topical antioxidant protection. *Journal of the American Academy of Dermatolgy*. 2003;48:1-19.

166. Bates C. Bioavailability of vitamin C. *European Journal of Clinical Nutrition*. 1997;51:S28-S33.

167. Ou-Yang H, Stamatas G, Saliou C, Kollias N. A chemiluminescence study of UVA-induced oxidative stress in human skin in vivo. *Journal of Investigative Dermatology*. 2004;122(4):1020-1029.

168. Fuchs, J., Packer L. Oxidative stress in dermatology. In: *Marcel Decker Inc.*; 1993.

169. Thiele, J.J., Dreher, F., Packer L. Antioxidant defense systems in skin. *Journal of Cutaneous and Ocular Toxicology*. 2002;21(1&2):119-160.

170. Hoppe U, Bergemann J, Diembeck W, et al. Coenzyme Q10, a cutaneous antioxidant and energizer. *BioFactors*. 1999;9(2-4):371-378.

171. Cohn W. Bioavailability of vitamin E. *European Journal of Clinical Nutrition*. 1997;51 Suppl 1:80S-85S.

172. Wang X, Quinn PJ. The location and function of vitamin E in membranes (review). *Molecular Membrane Biology*. 2000;17(3):143-156.

173. Fukuzawa K, Matsuura K, Tokumura A, Suzuki A, Terao J. Kinetics and dynamics of singlet oxygen scavenging by alpha-tocopherol in phospholipid model membranes. *Free Radical Biology and Medicine*. 1997;22(5):923-930.

174. Thiele JJ, Traber MG, Packer L. Depletion of human stratum corneum vitamin E: an early and sensitive in vivo marker of UV induced photo-oxidation. *Journal of Investigative Dermatology*. 1998;110(5):756-761.

175. Podda M, Grundmann-Kollmann M. Low molecular weight antioxidants and their role in skin ageing. *Clinical and Experimental Dermatology*. 2001;26(7):578-582.

176. Cross, C.E., Halliwell, B., Borish, E.T., Pryor, W.A. Ames, B.N., Saul, R.L., McChord J. Oxygen radicals and human disease. *Annals of Internal Medicine*. 1987;107:526-545.

177. Soobrattee MA, Neergheen VS, Luximon-Ramma A, Aruoma OI, Bahorun T. Phenolics as potential antioxidant therapeutic agents: mechanism and actions. *Mutation Research*. 2005;579(1-2):200-213.

178. Saulnier, L., Thibault J. Ferulic acid and diferulic acids as components of sugar-beet pectins and maize bran heteroxylans. *Journal of the Science of Food and Agriculture*. 1999;79:396-402.

179. Brakenhielm E, Cao R, Cao Y. Suppression of angiogenesis, tumor growth, and wound healing by resveratrol, a natural compound in red wine and grapes. *The FASEB Journal.* 2001;15(10):1798-1800.

180. Hodgson JM, Chan SY, Puddey IB, et al. Phenolic acid metabolites as biomarkers for tea- and coffee-derived polyphenol exposure in human subjects. *The British Journal of Nutrition.* 2004;91(2):301-306.

181. Rangkadilok N, Worasuttayangkurn L, Bennett RN, Satayavivad J. Identification and quantification of polyphenolic compounds in Longan (Euphoria longana Lam.) fruit. *Journal of Agricultural and Food Chemistry.* 2005;53(5):1387-1392.

182. Yao L, Caffin N, D'Arcy B, et al. Seasonal variations of phenolic compounds in Australia-grown tea (Camellia sinensis). *Journal of Agricultural and Food Chemistry.* 2005;53(16):6477-6483.

183. Faulds CB, Williams G. Review The role of hydroxycinnamates in the plant cell. *Critical Reviews in Food Science and Nutrition.* 1999;395(July 1998):393-395.

184. Graf E. Antioxidant potential of ferulic acid. *Free Radical Biology and Medicine.* 1992;13:435-448.

185. Manach C, Scalbert A, Morand C, Remesy C, Jimenez L. Polyphenols: food sources and bioavailability. *The American Journal of Clinical Nutrition.* 2004;79(5):727-747.

186. Rice-Evans, C.A., Miller, N.J., Paganga G. Structure-antioxidant activity relationships of flavonoids and phenolic acids. *Free Radical Biology and Medicine.* 1996;20(7):933-956.

187. Marques, M., Paula, M., Borges, F., Sousa, J., Calheiros, R., Garrido, J., Gaspas, A., Diniz, C., Fresco P. Cytotoxic and COX-2 inhibition properties of hydroxycinnamic derivatives. *Letters in Drug Design and Discovery.* 2006;3(5):316-320.

188. Perez-Alvarez V, Bobadilla RA, Muriel P. Structure-hepatoprotective activity relationship of 3,4-dihydroxycinnamic acid (caffeic acid) derivatives. *Journal of Applied Toxicology*. 2001;21(6):527-531.

189. Natella F, Nardini M, Di Felice M, Scaccini C. Benzoic and cinnamic acid derivatives as antioxidants: structure-activity relation. *Journal of Agricultural and Food Chemistry*. 1999;47(4):1453-1459.

190. Shahidi, F., Wanasundara P. Phenolic antioxidants. *Critical Reviews in Food Science and Nutrition*. 1992;32:67-103.

191. Lempereur, I., Rouau, X., Abecassiss J. Genetic and agronomic variation in arabinoxylan and ferulic acid contents of durum wheat (Triticum durum L.) grain and its milling fractions. *Journal of Cereal Science*. 1997;25:103-110.

192. Pan GX, Spencer L, Leary GJ. Reactivity of ferulic acid and its derivatives toward hydrogen peroxide and peracetic acid. *Journal of Agricultural and Food Chemistry*. 1999;47(8):3325-3331.

193. Nenadis, N., Zhang, H., Tsimidou M. Structure-Antioxidant Activity Relationship of Ferulic Acid Derivatives: Effect of Carbon Side Chain Characteristic Groups. *Journal of Agriculture and Food Chemistry*. 2003;51(7):1874-1879.

194. Srinivasan, M., Sudheer, A.R., Menon V. Ferulic acid : Therapeutic potential through its antioxidant property. *Journal of Clinical Biochemistry and Medicine*. 2007;40:92-100.

195. Adhami, V.M., Syed, D.N., Khan, N., Afaq F. Phytochemicals for prevention of solar ultraviolet radiation-induced damages. *Photochemistry and Photobiology*. 2008;84:489-500.

196. Kanski J, Aksenova M, Stoyanova A, Butterfield DA. Ferulic acid antioxidant protection against hydroxyl and peroxyl radical oxidation in synaptosomal and neuronal cell culture systems in vitro: structure-activity studies. *The Journal of Nutritional Biochemistry*. 2002;13(5):273-281.

197. Trombino, S., Serini, S., Di Nicuolo, F., Celleno, L., Ando, S., Picci, N., Calviello, G., Palozza P. Antioxidant effect of ferulic acid in isolated membranes and intact cells : Synergistic interactions with alpha-tocopherol , beta-carotene , and ascorbic acid. *Journal of Agriculture and Food Chemistry*. 2004;52:2411-2420.

198. Saija, A., Tomaino, A., Lo Cascio, R., Trombetta, D., Proteggente, A., De Pasquale, A., Uccella, N., Bonina F. Ferulic and caffeic acids as potential protective agents against photooxidative skin damage. *Journal of the Science of Food and Agriculture*. 1999;79:476-480.

199. Kikuzaki H, Hisamoto M, Hirose K, Akiyama K, Taniguchi H. Antioxidant properties of ferulic acid and its related compounds. *Journal of Agricultural and Food Chemistry*. 2002;50(7):2161-2168.

200. Chen, J.H., Ho C. Antioxidant activities of caffeic acid and its related hydroxycinnamic acid compounds. *Journal of Agricultural and Food Science*. 1997;45:2374-2378.

201. Psotova, J., Lasovsky, J., Vicar J. Metal-chelating properties, electrochemical behavior, scavenging and cytoprotective activities of six natural phenolics. *Biomedical Papers*. 2003;147(2):147-153.

202. Choi, S.W., Lee, S.K., Kim, E.O., Oh, J.H., Yoon, K.S., Parris, N., Hicks, K.B., Moreau R. Antioxidant and antimelanogenic activities of polyamine conjugates from corn bran and related hydroxycinnamic acids. *Journal of Agricultural and Food Chemistry*. 2007;55:3920-3925.

203. Agar NS, Halliday GM, Barnetson RS, et al. The basal layer in human squamous tumors harbors more UVA than UVB fingerprint mutations: a role for UVA in human skin carcinogenesis. *Proceedings of the National Academy of Sciences of the United States of America*. 2004;101(14):4954-4959.

204. Gasparro FP, Mitchnick M, Nash JF. A review of sunscreen safety and efficacy. *Photochemistry and Photobiology*. 1998;68(3):243-256.

205. Svobodova, A., Zdarilova, A., Walterova, D., Vostalova J. Flavonolignans from Silybum marianum moderate UVA-induced oxidative damage to HaCaT keratinocytes. *Journal of Dermatological Science*. 2007;48:213-224.

206. Fuhrman B, Volkova N, Rosenblat M, Aviram M. Lycopene synergistically inhibits LDL oxidation in combination with vitamin E, glabridin, rosmarinic acid, carnosic acid, or garlic. *Antioxidants and Redox Signaling*. 2000;2(3):491-506.

207. Dai F, Chen WF, Zhou B. Antioxidant synergism of green tea polyphenols with alpha-tocopherol and L-ascorbic acid in SDS micelles. *Biochimie*. 2008;90(10):1499-1505.

208. Lin, F-Y., Monteiro-Riviere, N.A., Grichnik, J.M., Zielinski, J.E., Pinnell S. A topical antioxidant solution containing vitamin C, vitamin E, and ferulic acid prevents ultraviolet radiation-induced caspase-3 induction in skin. In: *Dermatology European Academy of Dermatology and Venereology, Florence, Italy.*; 2004:7-20.

209. Lin, F-H., Lin, J-Y., Gupta, R.D., Tournas, J.A., Burch, J.A., Selim, M.A., Monteiro-Riviere, N.A., Grichnik, J.M., Zielinski, J., Pinnell S. Ferulic acid stabilizes a solution of vitamins C and E and doubles its photoprotection of skin. *Journal of Investigative Dermatology*. 2005;125:826-832.

210. Murray, J.C., Burch, J.A., Streilein, R.D., Innacchione, M.A., Hall, R.P., Pinnell S. A topical antioxidant solution containing vitamins C and E stabilized by ferulic acid provides protection for human skin against damage caused by ultraviolet irradiation. *Journal of the American Academy of Dermatology*. 2008;59:418-425.

211. Niki E. Interaction of ascorbate and alpha-tocopherol. *Annals New York Academy of Sciences*. 1987:186-199.

212. Burke K. Interaction of vitamins C and E as better cosmeceuticals. *Dermatologic Therapy*. 2007;20:314-321.

213. Lin, J-Y., Selim, M.A., Shea, C.R., Grichnik, J.M., Omar, M.M., Monteiro-Riviere, N.A., Pinnell S. UV photoprotection by combination topical antioxidants vitamin C and vitamin E. *Journal of the Academy of American Dermatology*. 2003;48(6):866-874.

214. Kiffin R, Christian C, Knecht E, Cuervo AM. Activation of chaperone-mediated autophagy during oxidative stress. *Molecular Biology of the Cell*. 2004;15:4829-4840.

215. Kiffin R, Bandyopadhyay U, Cuervo AM. Oxidative stress and autophagy. *Antioxidants and Redox Signaling*. 2006;8(1-2):152-162.

216. Kaushik S, Cuervo AM. Autophagy as a cell-repair mechanism: activation of chaperone-mediated autophagy during oxidative stress. *Molecular Aspects of Medicine*. 2006;27(5-6):444-454.

217. Kerr JF, Wyllie AH, Currie AR. Apoptosis: a basic biological phenomenon with wide-ranging implications in tissue kinetics. *British Journal of Cancer*. 1972;26(4):239-257.

218. Horvitz HR. Genetic control of programmed cell death in the nematode Caenorhabditis elegans. *Cancer Research*. 1999;59(Suppl 7):1701S-1706S.

219. Bratton DL, Fadok VA, Richter DA, et al. Appearance of phosphatidylserine on apoptotic cells requires calcium-mediated nonspecific flip-flop and is enhanced by loss of the aminophospholipid translocase. *The Journal of Biological Chemistry*. 1997;272(42):26159-26165.

220. Savill J, Fadok V. Corpse clearance defines the meaning of cell death. *Nature*. 2000;407:784-788.

221. Savill J. Apoptosis. Phagocytic docking without shocking. *Nature*. 1998;392(6675):442-443.

222. Platt N, da Silva RP, Gordon S. Recognizing death: the phagocytosis of apoptotic cells. *Trends in Cell Biology*. 1998;8(9):365-372.

223. Elmore S. Apoptosis : A review of programmed cell death. *Toxicologic Pathology*. 2007;35:495-516.

224. Bernerd F, Asselineau D. UVA exposure of human skin reconstructed in vitro induces apoptosis of dermal fibroblasts: subsequent connective tissue repair and implications in photoaging. *Cell Death and Differentiation*. 1998;5(9):792-802.

225. Tournas, J.A., Lin, F-H., Burch, J.A., Selim, M.A., Monteiro-Riviere, N.A., Zielinski, J.E., Pinnell S. Ubiquinone, idebenone and kinetin provide ineffective photoprotection to skin when compared to a topical antioxidant combination of vitamins C and E with ferulic acid. *The Journal of Investigative Dermatology*. 2006;126:1185-1188.

226. Hu S, Snipas SJ, Vincenz C, Salvesen G, Dixit VM. Caspase-14 is a novel developmentally regulated protease. *The Journal of Biological Chemistry*. 1998;273(45):29648-29653.

227. Nakagawa T, Zhu H, Morishima N, et al. Caspase-12 mediates endoplasmic-reticulum-specific apoptosis and cytotoxicity by amyloid-beta. *Nature*. 2000;403(6765):98-103.

228. Koenig, U., Eckhart, L., Tschachler E. Evidence that caspase-13 is not a human but a bovine gene. *Biochemical and Biophysical Research Communications*. 2001;285:1150-1154.

229. Kang SJ, Wang S, Kuida K, Yuan J. Distinct downstream pathways of caspase-11 in regulating apoptosis and cytokine maturation during septic shock response. *Cell Death and Differentiation*. 2002;9(10):1115-1125.

230. Jin Z, El-deiry WS. Overview of cell death signaling pathways. *Cancer Biology and Therapy*. 2005;4(2):139-163.

231. Degterev A, Boyce M, Yuan J. A decade of caspases. *Oncogene*. 2003;22:8543-8567.

232. Locksley RM, Killeen N, Lenardo MJ. The TNF and TNF receptor superfamilies: integrating mammalian biology. *Cell*. 2001;104(4):487-501.

233. Ashkenazi A, Dixit VM. Death receptors: signaling and modulation. *Science*. 1998;281(5381):1305-1308.

234. Hsu H, Xiong J, Goeddel DV. The TNF receptor 1-associated protein TRADD signals cell death and NF-kappa B activation. *Cell*. 1995;81(4):495-504.

235. Wajant H. The Fas signaling pathway: more than a paradigm. *Science*. 2002;296(5573):1635-1636.

236. Kischkel FC, Hellbardt S, Behrmann I, et al. Cytotoxicity-dependent APO-1 (Fas / CD95) - associated proteins form a death-inducing signaling complex (DISC) with the receptor. *The EMBO Journal*. 1995;14(22):5579-5588.

237. Walczak H, Krammer PH. The CD95 (APO-1/Fas) and the TRAIL (APO-2L) apoptosis systems. *Experimental Cell Research*. 2000;256:58-66.

238. Kataoka T, Schroter M, Hahne M, et al. FLIP prevents apoptosis induced by death receptors but not by perforin/granzyme B, chemotherapeutic drugs, and gamma irradiation. *Journal of Immunology*. 1998;161(8):3936-3942.

239. Hengartner MO. The biochemistry of apoptosis. *Nature*. 2000;407:770-776.

240. Chipuk JE, Green DR. Do inducers of apoptosis trigger caspase-independent cell death? *Nature Reviews*. 2005;6(3):268-275.

241. Ricci JE, Waterhouse N, Green DR. Mitochondrial functions during cell death, a complex (I-V) dilemma. *Cell Death and Differentiation*. 2003;10(5):488-492.

242. Chipuk JE, Bouchier-Hayes L, Green DR. Mitochondrial outer membrane permeabilization during apoptosis: the innocent bystander scenario. *Cell Death and Differentiation*. 2006;13(8):1396-1402.

243. Chipuk JE, Green DR. How do BCL-2 proteins induce mitochondrial outer membrane permeabilization? *Trends in Cell Biology*. 2008;18(4):157-164.

244. Vaux, D.L., Cory, S., Adams J. Bcl-2 gene promotes haemopoietic cell survival and cooperates with c-myc to immortalize pre-B cells. *Nature*. 1988;335:440-442.

245. Youle RJ, Strasser A. The BCL-2 protein family: opposing activities that mediate cell death. *Nature Reviews*. 2008;9(1):47-59.

246. Zong WX, Lindsten T, Ross AJ, MacGregor GR, Thompson CB. BH3-only proteins that bind pro-survival Bcl-2 family members fail to induce apoptosis in the absence of Bax and Bak. *Genes and Development*. 2001;15(12):1481-1486.

247. Cheng EH, Wei MC, Weiler S, et al. BCL-2, BCL-X(L) sequester BH3 domain-only molecules preventing BAX- and BAK-mediated mitochondrial apoptosis. *Molecular Cell*. 2001;8(3):705-711.

248. Li LY, Luo X, Wang X. Endonuclease G is an apoptotic DNase when released from mitochondria. *Nature*. 2001;412(6842):95-99.

249. Joza N, Susin SA, Daugas E, et al. Essential role of the mitochondrial apoptosis-inducing factor in programmed cell death. *Nature*. 2001;410(6828):549-554.

250. Saelens X, Festjens N, Vande Walle L, et al. Toxic proteins released from mitochondria in cell death. *Oncogene*. 2004;23(16):2861-2874.

251. Salvesen GS, Duckett CS. IAP proteins: blocking the road to death's door. *Nature Reviews*. 2002;3(6):401-410.

252. Cain K, Bratton SB, Langlais C, et al. Apaf-1 oligomerizes into biologically active approximately 700-kDa and inactive approximately 1.4-MDa apoptosome complexes. *The Journal of Biological Chemistry*. 2000;275(9):6067-6070.

253. Bratton SB, Walker G, Srinivasula SM, et al. Recruitment, activation and retention of caspases-9 and -3 by Apaf-1 apoptosome and associated XIAP complexes. *The EMBO Journal*. 2001;20(5):998-1009.

254. Gross A, Yin XM, Wang K, et al. Caspase cleaved BID targets mitochondria and is required for cytochrome c release, while BCL-XL prevents this release but not tumor necrosis factor-R1/Fas death. *The Journal of Biological Chemistry*. 1999;274(2):1156-1163.

255. Yin XM, Wang K, Gross A, et al. Bid-deficient mice are resistant to Fas-induced hepatocellular apoptosis. *Nature*. 1999;400(6747):886-891.

256. Zeiss CJ. The apoptosis-necrosis continuum: insights from genetically altered mice. *Veterinary Pathology*. 2003;40(5):481-495.

257. Leist M, Single B, Castoldi AF, Kuhnle S, Nicotera P. Intracellular adenosine triphosphate (ATP) concentration: a switch in the decision between apoptosis and necrosis. *The Journal of Experimental Medicine*. 1997;185(8):1481-1486.

258. Denecker G, Vercammen D, Steemans M, et al. Death receptor-induced apoptotic and necrotic cell death: differential role of caspases and mitochondria. *Cell Death and Differentiation*. 2001;8(8):829-840.

259. Fiers W, Beyaert R, Declercq W, Vandenabeele P. More than one way to die: apoptosis, necrosis and reactive oxygen damage. *Oncogene*. 1999;18(54):7719-7730.

260. Majno G, Joris I. Apoptosis, oncosis, and necrosis. An overview of cell death. *The American Journal of Pathology*. 1995;146:3-15.

261. Zhong JL, Yiakouvaki A, Holley P, Tyrrell RM, Pourzand C. Susceptibility of skin cells to UVA-induced necrotic cell death reflects the intracellular level of labile iron. *Journal of Investigative Dermatology*. 2004;123(4):771-780.

262. Eguchi, Y., Shimizu, S., Tsujimoto Y. Intracellular ATP levels determine cell death fate by apoptosis or necrosis. *Cancer Research*. 1997;57:1835-1840.

263. Folch, J., Lees, M., Sloan-Stanley G. A simple method for the isolation and purification of total lipides from animal tissues. *The Journal of Biological Chemistry*. 1957;226(1):497-509.

264. Asakawa, T., Matsushita S. Coloring conditions of thiobarbituric acid test for detecting lipid hydroperoxides. *Lipids*. 1980;15:137-1140.

265. Benavente CA, Jacobson EL. Niacin restriction upregulates NADPH oxidase and reactive oxygen species (ROS) in human keratinocytes. *Free Radical Biology and Medicine*. 2008;44(4):527-537.

266. Balasubramanian S, Efimova T, Eckert RL. Green tea polyphenol stimulates a Ras, MEKK1, MEK3, and p38 cascade to increase activator protein 1 factor-dependent involucrin gene expression in normal human keratinocytes. *The Journal of Biological Chemistry*. 2002;277(3):1828-1836.

267. Balasubramanian S, Zhu L, Eckert RL. Apigenin inhibition of involucrin gene expression is associated with a specific reduction in phosphorylation of protein kinase Cdelta Tyr311. *The Journal of Biological Chemistry*. 2006;281(47):36162-36172.

268. Balasubramanian S, Eckert RL. Curcumin suppresses AP1 transcription factor-dependent differentiation and activates apoptosis in human epidermal keratinocytes. *The Journal of Biological Chemistry*. 2007;282(9):6707-6715.

269. Balasubramanian S, Eckert RL. Keratinocyte proliferation, differentiation, and apoptosis-differential mechanisms of regulation by curcumin, EGCG and apigenin. *Toxicology and Applied Pharmacology*. 2007;224(3):214-219.

270. Kyoung Kim H, Kyoung Kim Y, Song IH, et al. Down-regulation of a forkhead transcription factor, FOXO3a, accelerates cellular senescence in human dermal fibroblasts. *The Journal of Gerontology*. 2005;60(1):4-9.

271. Yang EK, Seo YK, Youn HH, et al. Tissue engineered artificial skin composed of dermis and epidermis. *Artificial Organs*. 2000;24(1):7-17.

272. Phillips CL, Combs SB, Pinnell SR. Effects of ascorbic acid on proliferation and collagen synthesis in relation to the donor age of human dermal fibroblasts. *Journal of Investigative Dermatology*. 1994;103(2):228-232.

273. Lu C, Liu Y. Interactions of lipoic acid radical cations with vitamins C and E analogue and hydroxycinnamic acid derivatives. *Archives of Biochemistry and Biophysics*. 2002;406(1):78-84.

274. Boukamp, P., Petrussevska, R.T., Breitkreutz, D., Hornung, J., Markham, A., Fusenig N. Normal eratinization in a spontaneously immortalized aneuploid human keratinocyte cell line. *The Journal of Cell Biology*. 1988;106:761-771.

275. Hazane, F., Sauvaigo, S., Douki, T., Favier, A., Beani J. Age-dependent DNA repair and cell cycle distribution of human skin fibroblasts in response to UVA irradiation. *Journal of Photochemistry and Photobiology B: Biology*. 2006;82:214-223.

276. Naru, E., Suzuki, T., Moriyama, M., Inomata, K., Hayashi, A., Arakane, K., Kaji K. Functional changes induced by chronic UVA irradiation to cultured human dermal fibroblasts. *British Journal of Dermatology*. 2005;153:6-12.

277. Opländer C, Cortese MM, Korth H, et al. The impact of nitrite and antioxidants on ultraviolet-A-induced cell death of human skin fibroblasts. *Free Radical Biology and Medicine*. 2007;43:818 - 829.

278. Mahns, A., Melchheier, I., Suschek, C.V., Sies, H., Klotz L. Irradiation of cells with ultraviolet-A (320-400 nm) in the presence of cell culture medium elicits biological effects due to extracellular generation of hydrogen peroxide. *Free Radical Research*. 2003;37(4):391-397.

279. Stadler, R.H., Markovic, J., Turesky R. In vitro anti- and pro-oxidative effects of natural polyphenols. *Biological Trace Elements*. 1995;47(1-3):299-305.

280. Castelluccio C, Bolwell GP, Gerrish C, Rice-Evans C. Differential distribution of ferulic acid to the major plasma constituents in relation to its potential as an antioxidant. *The Biochemical Journal*. 1996;316 (Pt 2(Pt 2):691-694.

281. Applegate, L.A., Noel, A., Vile, G., Frenk, E., Tyrrell R. Two genes contribute to different extents to the heme oxygenase enzyme activity measured in cultured human skin

fibroblasts and keratinocytes: implications for protection against oxidative stress. *Photochemistry and Photobiology*. 1994;61(3):285-291.

282. Niggli, H.J., Applegate LA. Glutathione response after UVA irradiation in mitotic and postmitotic human skin fibroblasts and keratinocytes. *Photochemistry and Photobiology*. 1997;65(4):680-684.

283. Applegate, L.A., Frenk E. Oxidative defense in cultured human skin fibroblasts and keratinocytes from sun-exposed and non-exposed skin. *Photodermatology Photoimmunology and Photomedicine*. 1995;11(3):95-101.

284. Boostra, J. Post J. Molecular events associated with reactive oxygen species and cell cycle progression in mammalian cells. *Gene*. 2004;337:1-13.

285. Thorn, T., Gniadecki, R., Petersen, A.B., Vicanova, J., Wulf H. Differences in activation of G2/M checkpoint in keratinocytes after genotoxic stress induced by hydrogen peroxide and ultraviolet a radiation. *Free Radical Research*. 2001;35(4):405-416.

286. Lin J, Tournas JA, Burch JA, Monteiro-riviere NA, Zielinski J. Topical isoflavones provide effective photoprotection to skin. *Solutions*. 2008:61-66.

287. Boulais N, Misery L. The epidermis: a sensory tissue. *European Journal of Dermatology*. 2008;18(2):119-127.

288. Pepper C, Hoy T, Bentley DP. Bcl-2 / Bax ratios in chronic lymphocytic leukaemia and their correlation with in vitro apoptosis and clinical resistance. *British Journal of Cancer*. 1997;76(7):935-938.

289. Oltval, Z. N., Milliman, C. L., Korsmeyer S. Bcl-2 heterodimerizes in vivo with a conserved homolog, Bax, that accelaerates programed cell death. *Cell*. 1993;74(4):609-619.

290. Loro, L.L., Vintermyr, O.K., Liavaag, P.G., Jonsson, R., Johannessen A. Oral squamous cell carcinoma is associated with decreased bcl-2/bax expression ratio and increased apoptosis. *Human Pathology*. 1999;30(9):1097-1105.

291. Pourzand C, Rossier G, Reelfs O, Bonier C, Tyrrell RM. The overexpression of Bcl-2 inhibits UVA-mediated immediate apoptosis in rat 6 fibroblasts: Evidence for the involvement of Bcl-2 as an antioxidant. *Cancer Research*. 1997;57:1405-1411.

292. Liu R. Potential synergy of phytochemicals in cancer prevention: mechanism of action. *The Journal of Nutrition*. 2004;134(12 (supp):3479S-3485S.

293. Reuter, S., Eifes, S., Dicato, M., Aggarwal, B.B., Diederich M. Modulation of anti-apoptotic and survival pathways by curcumin as a strategy to induce apoptosis in cancer cells. *Biochemical Pharmacology*. 2008;76(11):1340-1351.

294. Wondrak GT, Cabello CM, Villeneuve NF, et al. Cinnamoyl-based Nrf2-activators targeting human skin cell photo-oxidative stress. *Free Radical Biology and Medicine*. 2008;45:385-395.

295. Ryan, K.J., Ray C. Sherris Medical Microbiology. In: *4th Ed. McGraw Hill.*; 2004:409-412.